



universität
wien

Diplomarbeit

Titel der Arbeit

Reliability and Validity Assessment of Independent
Components in Replicated Visual Attention Task

Verfasser

Bernhard Meyer

Angestrebter akademischer Grad

Magister der Naturwissenschaften (Mag. rer. nat.)

Wien, im April 2010

Studienkennzahl: 298

Studienrichtung: Psychologie

Betreuerin: PD Dr. Uta Sailer

Danksagung

Zunächst gilt großer Dank meinen Eltern für Ihre Unterstützung. Ihre Betrachtung von Bildung als beste Investition in die Zukunft haben Sie mir nicht nur in finanzieller Hinsicht weitergegeben. Meiner Schwester danke ich als Wegbereiterin, als Erstgeborene hat Sie viele Möglichkeiten für mich erarbeitet. Meinem Bruder gilt Dank für seine Ideale die mir immer wieder ein motivierender Rückenwind waren.

Für die Ermöglichung dieser sehr methodischen Arbeit danke ich meiner Betreuerin PD Dr. Uta Sailer. Sie gab mir die Freiheit eigene Wege und auch Irrwege anzugehen um doch in vielen Diskussionen entscheidende Aspekte anzuregen und auch sachlich zu beurteilen. Überhaupt möchte ich mich bei allen Mitstudierenden am Institut für die vielen Handgriffe, von A wie Ableiten bis mindestens M wie Matlab Schulungen, bedanken.

Bei meinen VersuchsteilnehmerInnen möchte ich mich einerseits für die wenig unterhaltsame Aufgabe entschuldigen und Ihnen gleichzeitig versichern, dass diese inhaltlich begründbar ist. Ich danke jedenfalls für die Bereitschaft zum und die Geduld beim Mitmachen.

Bei meiner Freundin bedanke ich mich fürs Zuhören, Einbringen und Begeistern weit über die Psychologie hinaus.

Viele nicht genannte WegbegleiterInnen haben sich als wahre Energiequellen erwiesen, Ihnen möchte ich an dieser Stelle danken.

Table of Contents

Abstract.....	7
Abstract in German.....	8
Theoretical Part.....	9
1 Independent Component Analysis and Quality.....	11
1.1 Method and Introduction.....	11
1.2 Algorithm Infomax.....	12
1.3 Assumptions.....	13
1.4 Quality of Independent Components.....	14
1.5 Reliability of Independent Components.....	15
1.6 Reliability and Baseline Correction	20
1.7 Artifacts - Good and Bad.....	21
1.8 Artifact vs. Cortical Components.....	22
1.9 Event Related Potentials.....	25
2 Independent Component Analysis and Visual Attention Task	27
2.1 Historical Perspective.....	27
2.2 Methodical Perspective.....	29
2.3 Event Related Potential - P300.....	32
2.4 Independent Components P3b and P3f.....	35
2.5 P3b and P3f – Other Reports.....	41
3 Research Question.....	43
Empirical Part.....	45
4 Materials and Methods.....	47
4.1 Subjects.....	47
4.2 Visual Attention Task.....	47
4.3 EEG-recordings.....	48
5 Analysis.....	51

5.1 Behavioral data.....	51
5.2 Preprocessing.....	51
5.2.1 EOG-correction.....	51
5.2.2 Low-pass filtering and epochs.....	52
5.2.3 Baseline Correction.....	53
5.2.4 30 vs. 59 channels setting.....	53
5.2.5 Artifacts.....	55
5.3 Reliability and ICA Calculation.....	56
5.4 Preprocessing Proceedings - Overview.....	57
5.5 Event Related Potentials.....	58
5.6 Independent Components – Reports and Plots.....	58
5.7 Preprocessing Influence on P3fs.....	60
6 Results.....	61
6.1 Behavioral Data and Artifact Rejection.....	61
6.2 Reliability Results.....	64
6.3 Event Related Potential - P300.....	67
6.4 Independent Components Results – P3b and P3f.....	67
6.5 Preprocessing Influence on Components.....	77
Discussion.....	83
References:.....	89
Appendix.....	93
Screenshots of Instruction.....	93
Screenshot of Pause between Blocks.....	93
Scalp Maps of all Components and Reliability Information.....	93
'L'-shaped Critical Regions for nine Proceedings.....	98
Reliable Components.....	100
Lebenslauf.....	103

Abstract

Independent component analysis (ICA) is a promising tool to find maximally independent electroencephalographic (EEG) sources. The experiment which is used here is based on the visual 'oddball' paradigm and is historically remarkable as it serves as dominant reference for ICA application on EEG. The major benefit of this task is the large number of a maximum of 600 target trials and the resulting P300 event related potential (ERP). Basic elements replicated in this thesis are two postulated independent components response locked before (P3f) and after (P3b) button press in target conditions explaining major variance of P300 deflection. Due to no commonly accepted preprocessing guideline the main focus of the present work was to provide methodical recommendations based on split-half reliability assessment and additional validity considerations. Therefore a total of nine different preprocessing proceedings was calculated to get systematic reliability and validity estimations. Six major approaches in which three baseline correction methods were varied combined with 30 and 58/59 channels settings. At first a inspection for P3b and P3f components was conducted for the baseline proceeding with the best reliability outcome and 30 channels due to the challenging number of 4783 calculated components for all nine full datasets. Finally, content based comparison to other proceedings was made to estimate impact of baseline correction methods and other preprocessing steps.

Given results show that the number of components assessed as reliable is mainly dependent on the chosen baseline correction method. Removing the epoch mean results in a significantly better reliability compared to the traditional approach of removing the baseline mean and to the most recent recommendation to totally skip this step prior to ICA calculations. Furthermore no dependency of reliability on the number of channels could be found for this dataset if optimum baseline method was chosen. Components with P3b characteristics were available in the decomposition of each of the fifteen subjects calculated with the epoch mean baseline correction method. Regarding P3f, five subjects showed a independent component with distinct characteristic and four more subjects had such component contaminated with P3b or other parietal activation. The comparison with other proceedings for two selected subjects could find a corresponding component for two P3f findings for the prestimulus baseline method but not after skipping baseline correction prior to ICA. Therefore, this work provides empirical evidence about epoch mean baseline correction method considering reliability and validity of calculated components.

Abstract in German

Die Analyse unabhängiger Komponenten (ICA) gilt als aussichtsreiche Möglichkeit, maximal unabhängige Quellen für elektroencephalographische (EEG) Daten zu errechnen. Das Experiment dieser Arbeit basiert auf einem visuellen 'oddball' Paradigma, welches als Hauptreferenz für die Anwendung des ICA-Verfahrens bezüglich EEG Daten historisch bedeutsam ist. Der Hauptvorteil dieser Aufgabe ist die große Anzahl an bearbeiteten Epochen und dem damit resultierenden ereigniskorrelierten Potential (EKP) P300. Die wesentlichen Elemente, welche in dieser Arbeit repliziert werden sollen, sind die postulierten unabhängige Komponenten vor (P3f) und nach (P3b) einem Tastendruck. Diese P3f und P3b Komponenten sind in Phase mit der Reaktion und sollen wesentliche Varianzanteile der P300 erklären. Der methodische Schwerpunkt dieser Arbeit erklärt sich aus einem Mangel an allgemein anerkannten Leitlinien für die Vorbereitung der Daten bis zur eigentlichen ICA-Berechnung. Daher wurden mittels einer „split-half“-Reliabilitätsberechnung und unter Berücksichtigung von Validitätsüberlegungen neun verschiedene Rechenverfahren beurteilt, um methodische Empfehlungen anzubieten. Die sechs Hauptverfahren variieren drei „baseline“-Korrekturen kombiniert mit 30 bzw. 58/59 Kanalkonfiguration. Zunächst wurde die Methode mit dem besten Reliabilitätsergebnis und 30 Kanälen nach P3b und P3f Komponenten durchsucht, da insgesamt die herausfordernde Zahl von 4783 Komponenten für neun Gesamtdatensätze berechnet wurden. Schlussendlich wurden inhaltsbezogene Vergleiche mit anderen Methoden durchgeführt um den jeweiligen Einfluss abschätzen zu können.

Die Ergebnisse zeigen, dass das Ausmaß an reliabel eingeschätzten Komponenten hauptsächlich von der „baseline“-Korrektur und weniger von Kanalkonfigurationen abhängt. Die Entfernung des Mittelwerts der Gesamtepoche erzielte eine höhere Reliabilität als der traditionelle Ansatz des „Baseline“-Mittelwertes und auch besser, als jüngste Empfehlungen diesen Schritt vor der ICA-Berechnung ganz auszulassen. Auch wurde keine Abhängigkeit der Reliabilität von der Kanalanzahl bei dieser Datenmenge gefunden wenn optimale „Baseline“-Korrektur gewählt wurde. P3b Komponenten wurden bei allen fünfzehn Versuchspersonen der „Epochenmittelwert“-Korrektur gefunden. Bezüglich P3f zeigten fünf Personen eine deutliche Charakteristik und weitere vier P3f-Merkmale kontaminiert mit P3b- oder anderer parietaler Aktivität. Der Vergleich mit anderen Methoden für zwei Versuchspersonen zeigte auch zugehörige P3f-Komponenten, wenn die „Baseline“-Mittelwerte abgezogen wurden, jedoch nicht, wenn dieser Schritt ausgelassen wurde. Daher bietet diese Arbeit die empirische Bestätigung einer erhöhten Reliabilität und Validität berechneter Komponenten bei Korrektur durch den Mittelwert der Gesamtepoche.

Theoretical Part

1 Independent Component Analysis and Quality

1.1 Method and Introduction

Independent Component Analysis (ICA) as a solution for Blind Source Separation (BSS) is frequently illustrated by the cocktail party-effect (figure 1). People are able to distinguish between two or even more voices in one room at the same time. To enable such a separation of recorded voices by two or more microphones needs a sophisticated mathematical solution, which ICA provides.

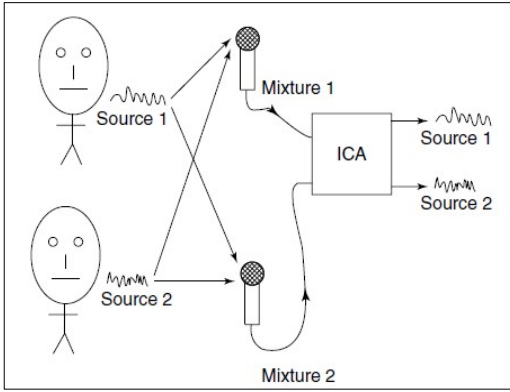


Figure 1: Simple illustration of the cocktail party-effect. Two people speaking recorded by two microphones. ICA provides separation of mixed sources.

(Stone, 2005, p. 907)

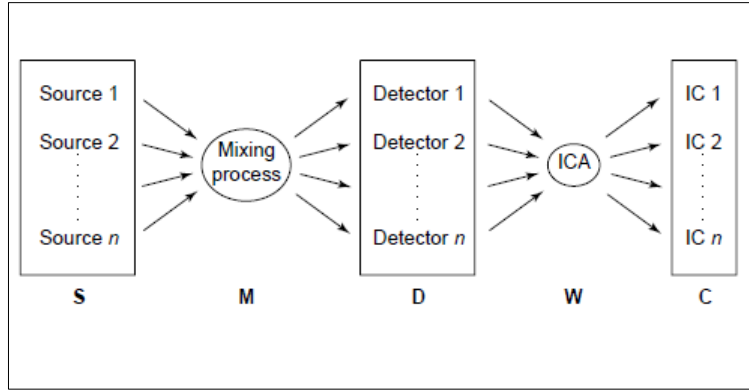


Figure 2: ICA model explaining all steps from n sources (S) measured with n detectors (D) leading to n independent components (C). See description in text particularly regarding mixing (M) and unmixing (W) step.

(Brown, Yamada & Sejnowski, 2001, p. 55)

It is important to note that we face different cortical or artifact sources instead of different people's voices in our context. Additionally, the measurement is provided by scalp electrodes instead of microphones as in the mentioned image. Electroencephalography (EEG) measures electrical potentials at the scalp which are commonly digitized and written into a matrix with one row for each channel (electrode) and one column for each samplingpoint. ICA estimates a matrix (W) which enables to unmix the measured data (D) leading to a matrix of independent components (C). This linear transformation could be mathematically described by a matrix multiplication $WD = C$ or for backward calculation for instance after artifact removal $W^{-1}C = D$ (Brown, Yamada & Sejnowski, 2001, p. 57). Therefore the activity of each independent component (IC) at one specific channel can

be calculated as well.

1.2 Algorithm Infomax

Different solutions are available to calculate an unmixing-matrix and the resulting independent components (ICs). The algorithms Jade (Cardoso & Souloumiac, 1993) and Infomax (Nadal & Parga, 1994; Bell & Sejnowski, 1995) had and still have an important historical impact on the application of ICA in a neurophysiological setting (Hyvärinen, Karhunen & Oja, 2001, p. 11). To focus on the analytical part of that thesis the following description will be constrained to the latter, although dozens of alternatives are discussed and still developed.

Infomax and many other ICA-learning-algorithms are based on artificial neuronal networks to minimize or maximize different kind of cost functions. The input of that network in our context is EEG-data (D), the output reflects ICs (C) and complementary synaptic weights (W), introduced as unmixing matrix in recent chapter. Each possible cost function represents the obtained independency of a given output. In case of Infomax, that function tries to maximize mutual information between input and output and consequently maximizes the output entropy. Mutual information and entropy are higher-order generalizations of correlation and variance and lead to the conclusion that independent is a stronger assumption than uncorrelated (Brown, Yamada & Sejnowski, 2001, p. 61). Further explanations regarding mathematics, mutual information, entropy and embedding of that algorithm into other maximum likelihood estimations are available in Hyvärinen & Oja (2000, p. 9ff) and at full length in Hyvärinen, Karhunen and Oja (2001, p. 211ff).

Regarding application of Infomax and other learning-algorithms several parameters determine the exact performance as for instance learning rate or various stopping conditions. Repeated testings showed that the exact values of these parameters have little effect on the results, at least in the context of questions that are of interest within that thesis and hence no extensive discussion is done in here (Makeig, Westerfield, Jung, Covington, Townsend, Sejnowski & Courchesne, 1999b, p. 2678; Jung, Makeig, McKeown, Bell, Lee & Sejnowski, 2001a, p. 1116).

1.3 Assumptions

Opposed to principal component analysis (PCA) and also to factor analysis (FA) intending to explain as much data as possible with a limited number of components or factors, ICA tries to find statistically independent components (Hyvärinen, Karhunen & Oja, 2001, p. 2f). The fact that two variables are uncorrelated does not mean that they are also independent. Independency is a stronger criterion and to provide that, ICA estimates local maxima of nongaussianity. The idea supporting that procedure is based upon the central limit theorem saying that any sum of nongaussian random variables is closer to gaussian than each original variable (Hyvärinen, Karhunen & Oja, 2001, p. 9). Note that in comparison to PCA an ICA decomposition does not offer just an orthogonal solution (Figure 3) even though such uncorrelated principle components are part of an initial preprocessing step for ICA algorithms as e.g. Infomax (Brown et al., 2001, p. 61).

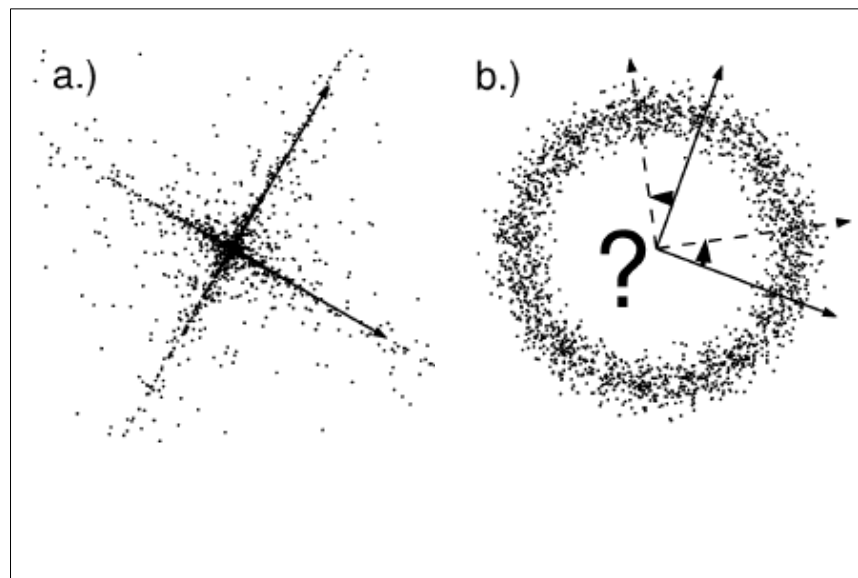
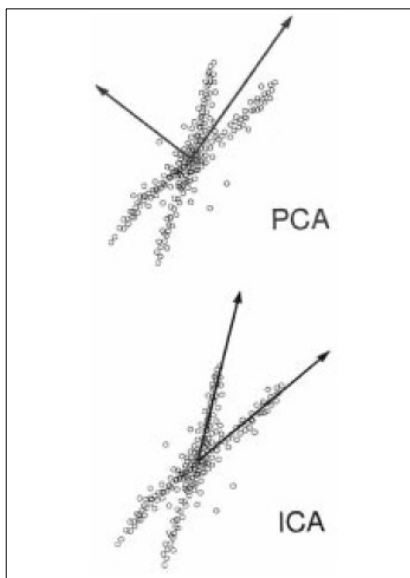


Figure 3: Orthogonal PCA vs. ICA **Figure 4:** Distribution of two independent supergaussian a) vs. two independent gaussian b) variables. The axes illustrate that it is quite easy to find a base for two independent time series in the first case compared to the latter one. (Meinecke, Ziehe, Kawanabe & Müller, 2002, p. 1516)

Considerations regarding nongaussian maxima leads us to a key assumption for ICA in general, gaussian variables are not allowed because they cannot be separated from each other and would be combined in one or more components. Figure 4 shows that two distributions do not offer any information regarding directions for the mixing matrix because they are rotationally symmetric.

(Hyvärinen, Karhunen & Oja, 2001, p. 161-63). In the context of EEG-data that topic is mainly discussed regarding technical artifacts of recording procedures due to the fact that artifacts like eye-movements are typically nongaussian.

Focusing on brain-signals we need to assume that the scalp electrodes measure linearly summed projections of near instantly and independently projecting sources. Next, ICA requires spatially fixed sources for the duration of the input data. In fact, spatiotemporal dynamics as associated e.g. with epileptic and migraine phenomena or with sleep spindles could seriously violate that assumption (Onton, Westerfield, Townsend & Makeig, 2006, p. 811).

1.4 Quality of Independent Components

The more channels included in the input matrix for an ICA-calculation, the more data are required to get a good quality of the resulting components. Practically recommended is a minimum number of data points calculated by the square of channels² multiplied by factor k . That factor increases also with the number of channels and goes up to 20 for 256 channels (Onton, Westerfield, Townsend & Makeig, 2006, p. 813). An example of 59 channels with 20 as highly generous dimensioned factor k would equal 69620 datapoints. If you have epochs of one second with a sampling rate of 250Hz and consequently 250 datapoints for each epoch we would need 279 epochs to assure that we have a high quality decomposition according to that guideline.

An approach to increase the quality with a limited number of data would be to reduce the number of channels or to conduct preprocessing via PCA to reduce the dimension of given data. The latter is able to face overlearning and reduces noise even though it is difficult to estimate the optimum number of desired components (Hyvärinen, Karhunen & Oja, 2001, p. 267ff). Overlearning happens if the dimension of data is less than the dimension of the ICA solution as discussed in other terms below. Applied to EEG data, Onton et al. (2006, p. 814) recommend PCA as efficient data compression but also to consider if a reduced number of channels is the preferable choice, especially if some channels have noisy periods.

At that point it is necessary to emphasize once more that the number of channels usually equals the number of resulting ICs. If there are more sources than channels respectively ICs we could talk about overcompleteness (Brown, Yamada & Sejnowski, 2001, p. 60) leading to the result that we would lose information. As another term Mouraux and Jannetti (2008, p. 1051) would evaluate this situation as underfitting model. Hence a bad approach would be to simply add as much of any available data into the decomposition. An example in the context of artifact-rejection would be to add data contaminated with a kind of artifact that appears just during a short period of all data. Furthermore if cortical sources of no interest are likely contributing to that data and accordingly occupy ICs. The opposite case of overfitting is caused by more channels than sources. That results in spurious activity because there is a lack of information for the spared components. As mentioned regarding PCA we face the problem that we do not know the real number of cortical and artifact sources, respectively the best number of components.

A possible reason why one decomposition results in less components than channels is that two channels contain the same information e.g. due to a short circuit. Another reason for such a loss of information-variability could be the interpolation of one channel. Currently any interpolation prior to ICA-decomposition is not recommended to prevent the introduction of non-linearity and noisy ICA-solutions. Next it is questionable what to win with such an interpolation. If you are interested in component-results without clustering or back calculation to relevant channel you do not gain information by interpolation because no independent data are generated and the here discussed interpolation-algorithm would not even influence a given weight-matrix (EEGLABlist: <http://scn.ucsd.edu/pipermail/eeglablist/>, Interpolation and ICA, [04.-05.01.10]).

A brief and vivid illustration of the introduced assumptions and quality-criteria is given in Brown, Yamada & Sejnowski (2001, p. 60).

1.5 Reliability of Independent Components

A reasonable next step after talking about the quality of resulting ICs would be to ask for any kind of assessment or quality criteria. Confirming that, efforts for the implementation of such an evaluation came up soon (e.g. Makeig, Westerfield, Townsend, Jung, Chourchesne & Sejnowski,

1999a, p. 1140f.; Makeig et al., 1999b, p. 2673f.). One motivation to calculate such a value could be to get some further insights regarding data-processing steps, for instance which ICA-algorithm or which baseline correction method to use. On the other hand it would be useful to control the reliability of individual ICs to focus on trustworthy results (Groppe, Makeig & Kutas, 2009). Both intentions will be a major topic of that thesis and initially treated in this chapter after the introduction of how to establish such a reliability-criteria. Reliability as a concept discussed in classical psychometrics intends to describe the accuracy of the measurement of a certain feature, for example of the questioned personality. Different approaches to determine that value in that discipline and also in context of physical measurements have in common that they try to replicate the results of interest (e.g. Kubinger, 2006, p. 45ff.).

As it was done in the context of test-constructions, various viable solutions for reliability assessment of ICs were developed and e.g. summarized in Groppe et al. (2009). The possibly most intuitive opportunity is to upgrade reliability evaluation for ICs which are frequently and similarly identified in the data of different subjects, even though we do not know if the differences or similarities should be attributed to the reliability of the calculated components or to inter-participant effects. Hence, methods to calculate the reliability of individual independent components are necessary to seriously answer that question. First we have approaches using bootstrap resampling running ICA for large number of times (Meinecke, Ziehe, Kawanabe & Müller, 2002; Himberg, Hyvärinen & Esposito, 2004; Harmeling, Meinecke & Müller, 2004)). For example, Makeig et al. (1999a, p.1140f.) used 200 randomly chosen subgroups of four subjects to build such samples. Furthermore Makeig et al. (1999b, p. 2673) calculated ICA several times within and across different task conditions using all and also subsets of channels. The resulting scalp map data were correlated with the original ICA-solution to get a reliability estimation. Obviously such a calculation is limited by the available computation resources. That should be considered especially while using quite time-consuming ICA-algorithms such as Infomax. Finally other information than topographic distribution like the activation-characteristic is ignored by that approach. That means that the variability in the course of time is not included in such calculations. For example, it is not important whether ICs are contributing to a ERP of interest or not.

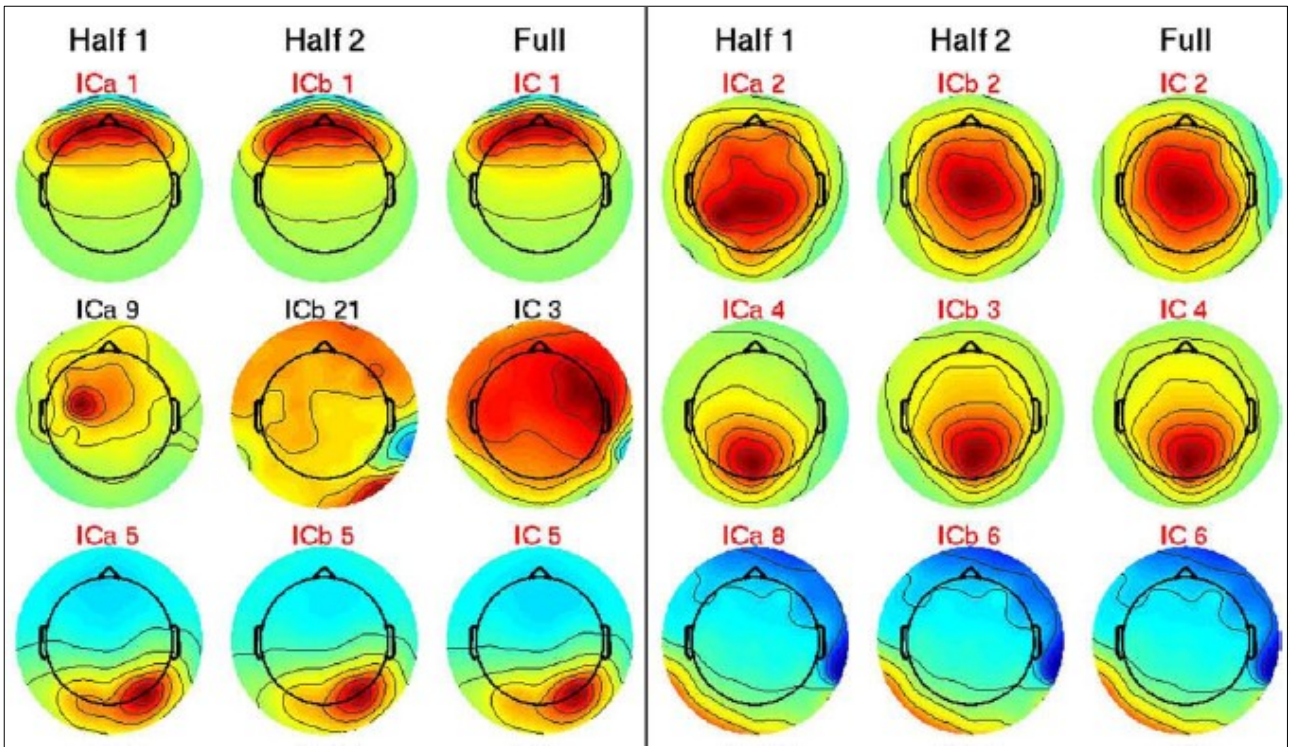


Figure 5: Topographies of top six IC-triplets of one subject (both sides). ICs highlighted red are assessed as reliable. Weights were normalized for easier comparison. For further information see Groppe et al. (2009, p. 1205).

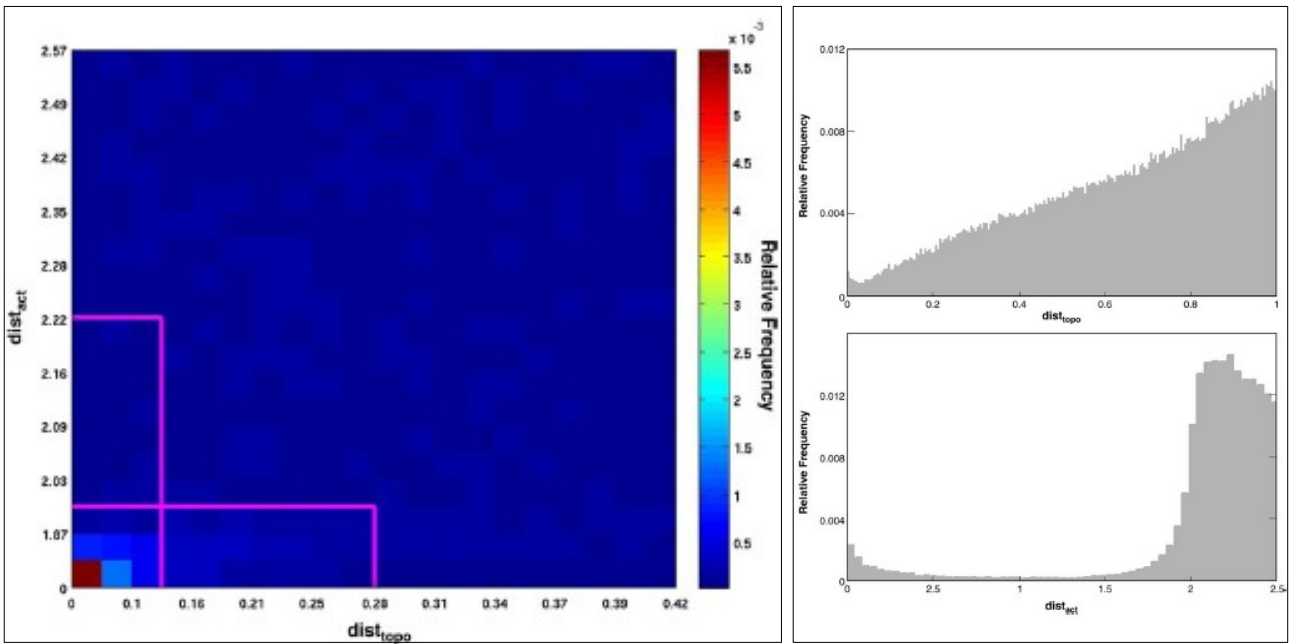


Figure 6: 'L'-shaped critical region for testing the similarity-hypothesis (see text) and containing $1/n$ (n = number of components) (left) of total empirical distribution (right). To enable comparison every box of that plot includes one percentile increment on each dimension (e.g. 2% of calculated IC pairs are within the topographic-distance range of 0.1). The very top and right border is constrained by the topographic-distance (right top) and activation-distance (right bottom) distribution calculated including each possible IC pair of all triplets. For further information see text and Groppe et al. (2009, 1203-04)

The most recently published method to assess reliability is a split-half comparison (Groppe et al., 2009). To start that calculation we need ICA decompositions of one full dataset and two comparable halves of the same data. Each half should represent the full dataset as much as possible, e.g. including all experimental conditions. Mostly, the best way is to separate odd and even epochs. Next, homologous triplets of ICs from every dataset are formed using a measure of topographic similarity, hence the scalp topographies of that triplet look similar as we can see in selection of figure 5. The activation of the ICs is not accounted for that step.

Next, the introduced topographic-distance metric and a complementary activation-distance metric for all three possible comparisons of each given triplet are tested against a null hypothesis that says that the tested pair is no more similar than a randomly chosen pair of ICs. The topographic-distance value is calculated with one minus a cosine-similarity measure and it equals zero for identical scalp maps. Note that the polarity with minimal distance is used and that the calculation is based on normalized scalp topographies. The activation-distance value is calculated by the maximum normalized sum squared difference between the IC-pair and it equals zero for identical activations. To test the similarity-hypothesis it is necessary to calculate an 'L'-shaped critical region favoring high similarities in one feature (figure 6). Note that for example a box-shaped critical region would favor two quite similar features. The outer right boarder of the lower rectangle is defined using the 90th percentile of the introduced topographic-distance distribution visible at the right upper corner in figure 6. The definition of the top of the other rectangle uses the 90th percentile of the activation-distance distribution situated at the right bottom of figure 6. To ensure that every IC of one decomposition could be similar to exactly one IC of the corresponding decomposition, the other side of both rectangles is chosen in a way that the combined area includes $1/n$ of the empirical distribution, considering that n equals the number of components in each decomposition. Using that definition, an assessment of all ICs for a full dataset is available. For further explanations see Groppe et al. (2009).

As technical guideline we can summarize that we first start with three ICA-decompositions. All following calculations described above were conducted using EEGLAB compatible Matlab-scripts (Delorme & Makeig, 2004; The MathWorks: <http://www.mathworks.com/>, [last 26.03.10]). The algorithm and EEGLAB are freely available for download (EEGLAB: <http://scn.ucsd.edu/eeglab/>; Algorithm Reliability: <http://www.cogsci.ucsd.edu/~dgroppe/eeglab.html/>, [last 26.03.10])

The advantage of the split-half method (Groppe et al., 2009) in comparison to other approaches is that it offers a statistical hypothesis test taking scalp topography and activation into account. Please note that just topography distance is used for building triplets to prevent large computational efforts. This assessment is provided using moderate computational resources mainly because it needs just three ICA-decompositions. And finally we obtain a reliability-assessment of all individual ICs.

The main disadvantage of this evaluation is that the test power is low compared to e.g. bootstrap due to two facts. The first reason is that mistakes during the pairing of ICs lower the chance to find similar pairs and the chance to reject the null hypothesis and hence increases the Type I error. Secondly, to reduce the amount of data by the split-half has a critical influence on the test power and on the minimum amount of data necessary for ICA-decomposition as discussed in the previous chapter. Experiment 1 and 2 analyzed by Groppe et al. (2009) were recorded with 64 channels and had a mean number of 643 and 844 epochs (minimum of 548 and 660 epochs). Experiment 3 and 4 had just 30 channels but contained even more epochs with mean number of 1641 and 2185 (minimum of 1197 and 1765 epochs). Estimations of minimum number of epochs needed are discussed in the previous chapter even though the double amount of data is necessary because of splitting. Less data would likely affect the number of reliable components. Finally tricky situations could require the analysis of multiple ICs as done by Meinecke et al. (2002) and Harmeling et al. (2004). Such tricky situations could otherwise be assessed as unreliable as Groppe et al. (2009) emphasized.

In general, the accuracy of every assessment regarding the reliability of ICs has to be further discussed, because we simply do not know the exact number of mistakes. Even two ICAs of the same dataset could differ slightly and so ICA of ERP data still has an exploratory character (Makeig et al., 1999b, p. 1667). That example illustrates the importance of such a reliability-value and asks for a quality assessment. Next, such a single value is not able to evaluate the quality and assumptions of a given ICA solution as chapters above partly outlined. The mentioned psychometric (e.g. Kubinger, 2006) established different quality-criteria which are also interesting in context of ICA. The validity-term is one illustrative example as it describes if we actually measure what we intent to measure. A high reliability value is not useful if we measure something of no interest, as for example artifacts. Still, such an assessment provides an empirical base for decisions in ICA research as the following example demonstrates.

1.6 Reliability and Baseline Correction

As previously explained reliability is not one single value that is able to guarantee the quality of a given decomposition. Even though it is not a sufficient criterion we are able to improve the quality of our analysis by benefiting from that information. One possibility to achieve this goal is to find the optimum method of preprocessing for decomposing data. The following example also demonstrates one application of the introduced split-half method and was published together with the introduction of the procedure (Groppe et al., 2009, p. 1208). As shown in figure 7, removing the mean of the complete epoch increases the calculated reliability dramatically in comparison to removing the mean of the baseline period. Please note that the removal of the prestimulus baseline is necessary after ICA decomposition to enable an interpretation of ERP or scalp map plots. Even though it is not yet clear why that happens, this result is important because it is contradictory to the traditional recommendation. In the past, most researchers removed the prestimulus baseline before applying ICA to that data (e.g. Makeig et al., 1999a; Makeig et al., 1999b) which is still recommend in the tutorial of the EEGLAB-toolbox as e.g. in chapter 12, multiple datasets (EEGLAB Tutorial: http://sccn.ucsd.edu/wiki/eeglab_tutorial_online/, [last 26.03.10]).

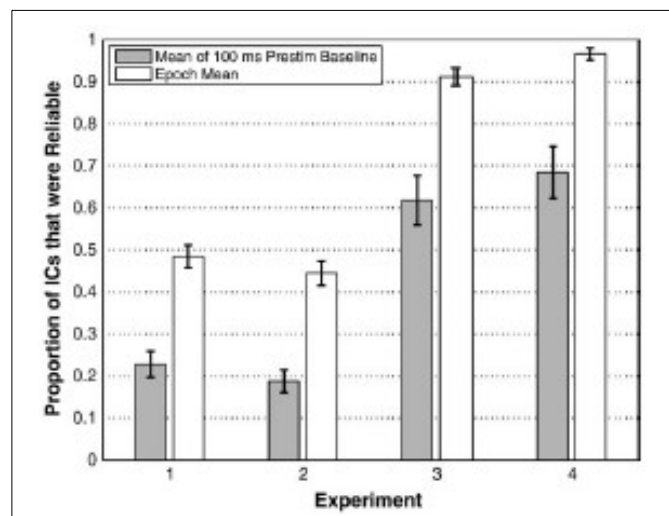


Figure 7: Percentage of ICs assessed as reliable per subject with standard error of the mean. Experiment 1 and 2 were conducted with 64 channels, 3 and 4 with 30 channels. For baseline-correction prestimulus period (grey bar) or total epoch mean (white bar) was used. (Groppe et al., 2009, p. 1208)

Recent discussions regarding that topic favor none of these two possibilities but recommended to completely skip any kind of baseline removal before ICA-decomposition (e.g. EEGLABlist: <http://sccn.ucsd.edu/pipermail/eeglablist/>, A quick question about baseline correction after ICA, [05.01.10]). Groppe et al. (2009) offered two possible interpretations for the effect shown in figure

7. On the one hand, removing the mean of each epoch may work as leaky high-pass filter and the removed low frequency variance lead to more variable ICA solutions. On the other hand, possibly all baseline correction methods do affect ICA decompositions, but the epoch mean approach to a lesser extent. The latter would explain the recommendation to skip that step even though no empirical evidence is given for its superiority. Still, that preprocessing-step is under ongoing discussion and all three mentioned possibilities are calculated in that thesis to get further insights. Please note that experiments with more channels and less data have a lower percentage of reliable components as mentioned in the recent chapter. That is likely because more channels require more datapoints (Onton et al., 2006) but we do not know if more trials, less channels or both determine this higher reliability.

1.7 Artifacts - Good and Bad

Considerations regarding the quality of ICs already illustrated that too many ICs could be occupied by artifacts in general and especially, sequences of rare artifacts could lead to overcompleteness (Brown et al., 2001, p. 60) or in other terms underfitting (Mouraux & Jannetti, 2008, p. 1051). Based on this fact, one recommendation should be to conventionally prune such exceptional periods of data.

In addition to the elaborated difference between rare and constantly appearing artifacts, one further and major differentiation is between stereotyped and non-stereotyped artifacts. The first type commonly includes eye-blinks and -movements, various distinct muscle tensions and heart-activity with a relatively fixed spatial and temporal pattern which is attributed to only a few components. In contrast, non-stereotyped artifacts such as movements of electrodes or cables could result in dozens of ICs. One approach to handle this problem could be to prune artifacts, calculate ICA and then prune artifacts producing such artificial components again before calculating a second ICA (Onton et al, 2006, p. 814).

Even if we would have ICs with data containing just stereotyped artifacts and cortical sources our identification and removal of components is constrained by probably mixed components. As already said, we do not know the exact number of sources of a given EEG and we do not have a situation

that n independent sources result in n ICs. It is important to emphasize that one component could be mixed, for example, data may contain blink artifacts and additionally cortical sources as shown by Li and Principe (2006, p. 5274f.). That case should be considered if ICs have to be identified and is therefore discussed after the characterization of ICs related to artifacts and cortical sources in the following chapter.

For the sake of completeness one should note that removing artifacts via ICA is a promising field of research offering also semi-automatic (e.g. Viola, Thorne, Edmonds, Schneider, Eichele & Debener, 2009) and automatic approaches (e.g. Gao, Yang, Lin, Wang & Zheng, 2010). Even so the ICA-artifact-discussion of this thesis focuses mainly on conventionally removing of artifact contaminated epochs and following identification of artifact and cortical ICs to prevent going astray.

1.8 Artifact vs. Cortical Components

The idea to handle artifacts using ICA soon came up (e.g. Jung, Humphries, Lee, Makeig, McKeown, Iragui & Sejnowski, 1998) and was developed in parallel to ERP-research. In addition to explanations regarding the quality of ICs, the previous chapters already provided some insights regarding the topic of ICA and artifacts. In contrast to that, this chapter intends to offer some guidelines within a practical scope for the identification of such components.

Due to the fact that only stereotyped artifacts can be successfully decomposed and treated by ICA (Onton et al, 2006, p. 814), we can focus on five classes of artifacts with specific characteristics as the examples in the center of figure 8 show. Next, figures 8-12 show various features of these artifacts in contrast to cortical components. The latter do have general properties discussed in this chapter and specific ones as discussed for the components P3b and P3f in the next chapter.

Jung, Makeig, Westerfield, Townsend, Courchesne & Sejnowski (2000a, p. 1749) recommend to show each component activity in time as shown in figure 8 (center) for that five artifact examples. Obviously, this provides more information for clearly visible artifacts as electrocardiac spikes or

eye blinks and in that case it offers a intuitive and powerful solution. If available, recordings of EOG or electrocardiogram (ECG) could support finding of significant periods.

Next and frequently discussed is to plot the topographic distributions of given ICs as done in the center of figure 8 and in the added examples of figure 9. Please note that the polarities of ICs are not necessarily equal to the polarity of projections to any electrode of interest. The IC4 in figure 9 is an example for such a paradox polarity because the shown distribution is typical for a cortical component contributing to the P300 ERP. Moreover orthogonal projections of cortical sources oriented parallel to a virtual tangent at the scalp surface can be distinguished from radial projections as IC19 and IC7 point out. Remarkably, both components seem to have similar source dipoles but singular electrodes would show different activations. Intersubject variability could also lead to such differences because a cortical source of one person could be in a sulcus and a different source projects from the top of a gyrus directly to the electrode above (Onton et al., 2006, p. 814f.). The distribution of blinks and eye-movements is expected frontally due to the given location of the eye dipole. Of course a muscle causing an artifact component could be situated in different regions causing various topographic patterns and could be quite similar to ECG-ICs as IC31 and IC10 in figure 9 show. In contrast the muscle-component IC2 in figure 8 reveals that such an artifact-component does not always build a partial corona at the margin. All these considerations emphasize the problem of the interpretation of voltages at selected electrodes or scalp maps solely, especially for ambiguous components.

The ERP-plot of each component as in figures 11 and 12 could provide information about the activation in each single trial and their average. If an IC has different activations in certain trials further investigations could follow based on that hint. For instance, these trials could contain overseen drifts or increases of eye-blinks as the EEG timeline may show. Furthermore, a separation of data prior to ICA could follow up that analysis. An approach used in this thesis is to distinguish between targets on the left and the right side to see which components are related to eye movements because ICA should deliver similar cortical components which should not be related to that systematic side difference (Jung et al., 2000a, p. 1749f.). Furthermore, a cortical component should have similar deflections as the ERP of interest. Calculations to find ICs contributing most strongly to the ERP could be a useful support to conduct that step. Please see the demonstration in the context of P300 related components P3b and P3f below for further explanation.

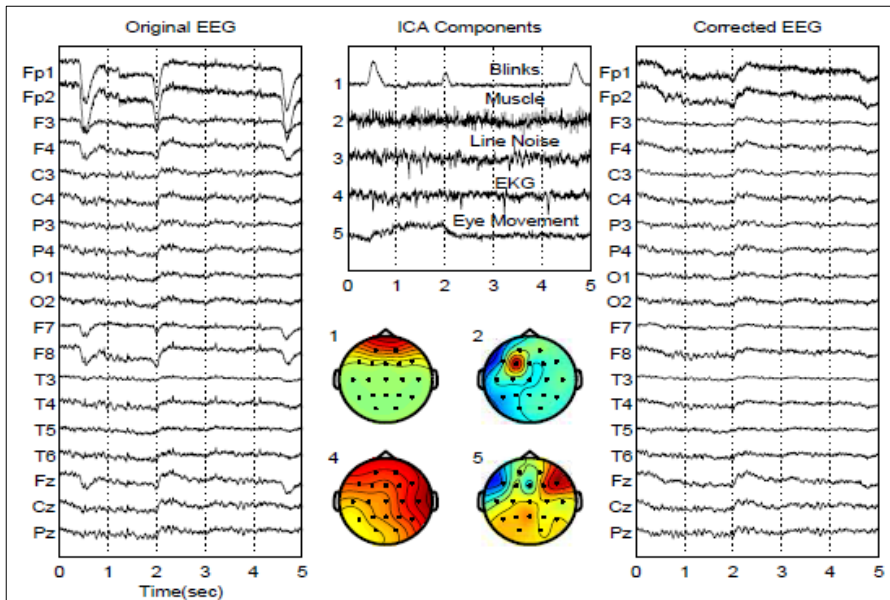


Figure 8: Five-second timeline and topography of five stereotyped artifact-ICs (center) and the effect of rejecting these components on EEG time series (left to right). (Jung et al., 1998, p. 900)

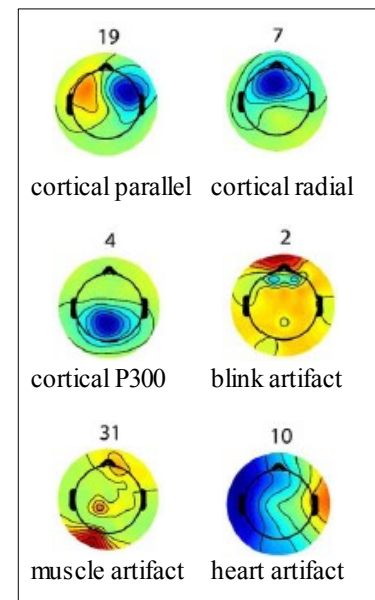


Figure 9: Topography of selected ICs related to various cortical sources and artifacts. (Onton et al., 2006, p. 816)

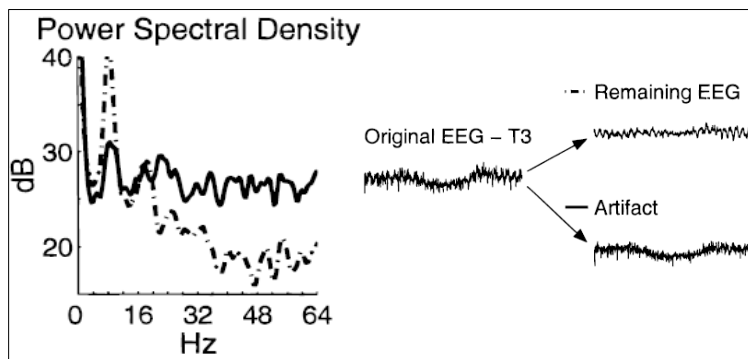


Figure 10: Typical power spectra (left) of artifact-ICs (thick line) vs. remaining EEG (dash-dotted line) and the effect of artifact in schematic time course (right). (Jung, Makeig, Humphries, Lee, McKeown, Iragui & Sejnowski, 2000b, p. 168)

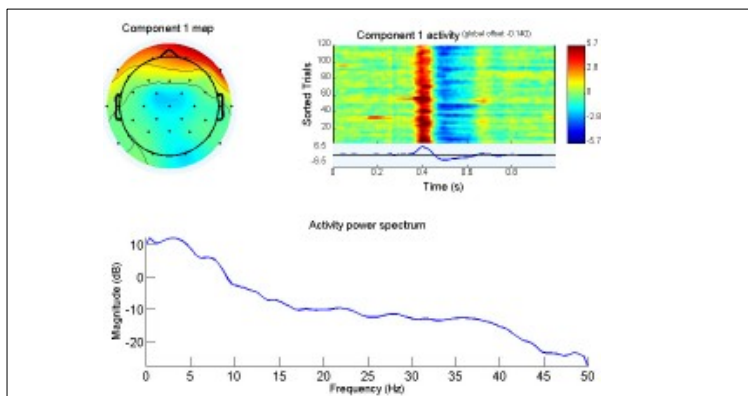


Figure 11: Topography (top left), ERP with single trial visualization above (top right) and frequency spectrum (bottom) of IC1, a component mixed by blink-artifacts and P300-variance. (Li & Principe, 1998, p. 5274)

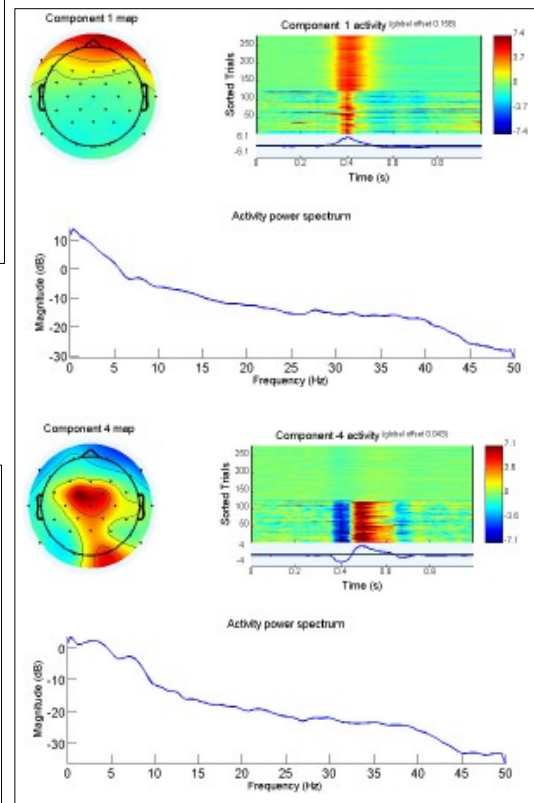


Figure 12: Topography, ERPs and frequency spectra of original IC1 (top) and IC4 (bottom) containing additional trials with spontaneous blinks. See text for explanation. (Li & Principe, 1998, p. 5275)

Maybe less obviously, all components have their frequency spectra (figures 10 to 12). Please note calculations to find ICs contributing most strongly to certain frequencies. Generally, there are spectra most likely related to artifacts, especially when power does not decrease or even increase with higher frequencies as the thick line in figure 10 illustrates, whereas ICs of cortical sources should be similar to the thin line. For further specification, theories regarding the frequency of the phenomena of interest have to be taken into account.

Finally there are different solutions to localize the sources available. LORETA (Pascual-Marqui, Michel & Lehmann, 1994) and BESA (Scherg, 1990) are two examples to meet such a request that could be applied also to single ICs. Of course, computing dipole estimations is resource-consuming if applied to many components. Generally such visualizations offer a very intuitive idea of a given source, but e.g. mixed ICs would not be resolved just by source localization. It is strongly recommended to combine visualizations of different aspects to identify ICs. The following considerations should illustrate why using multiple approaches.

To prevent a premature identification and removal of a certain component one should be aware that there is a possibility of mixed components as discussed e.g. in Li and Principe (2006, p. 5274f.). This could be the case if an artifact and a cortical component always appear together as in IC1 (figure 11) in which a P300-deflection and a blink-artifact are combined. Adding trials with spontaneous blinks led to the separate components IC1 and IC4 in figure 12. That demonstration provides a practical evidence that ICA is not always able to unmix different sources. Furthermore, we should be cautious regarding the identification and removal of components. In the above example, we could suggest IC1 to be a blink artifact and consequently prune that component, but for that given case a loss of ERP-data could be demonstrated (Li and Principe, 2006, p. 5275f.). This should also be considered in other circumstances.

1.9 Event Related Potentials

Before digital computers found their way into EEG labs, a trial-by-trial averaging of event-related-activity could be accomplished by simpler hardware solutions. The success of event-related-potentials (ERPs) is partly traceable to these technical constraints. Recent developments still use

that technique to determine whether an ERP is locked to various kinds of events (Delorme & Makeig, 2004, p. 9f). It is well known that the EEG measures the sum of post-synaptic potentials of quite a large population of synchronously active cortical neurons. Next, it is evident that ERPs are generated in similarly oriented cortical pyramidal neurons firing in phase. Therefore, event-related synchronization (ERS) increases and event-related desynchronization (ERD) decreases the measured power. Changes in power could also be a consequence of reorganization or 'resetting' triggered by the event, a so called event-related phase resetting (ERPR). In addition to these considerations, we have to assume that especially the late ERPs are generated by a couple of sources and that they can only be spatially distinguished on a very coarse level due to the fact that the scalp and other anatomical influences disperse the electrical fields of interest. If we want to distinguish these sources temporally we face overlapping and jitter phenomena. One important approach to handle this issue is to recover independent sources via ICA (Mouraux & Iannetti, 2008). The following description will use a visual attention task to provide further insights regarding the application of ICA in ERP-research as explained in the next chapters.

2 Independent Component Analysis and Visual Attention Task

2.1 Historical Perspective

The first developments of the ICA-technique also in context of neurophysiological settings were made in France in the 1980s (Hyvärinen, Karhunen & Oja, 2001, p. 11). The biggest breakthrough was the first international workshop in the end of that decade leading to historic descriptions of that concept (e.g. Common, 1989; Cardoso, 1989). Soon after the idea spread internationally, the algorithm Infomax was developed in France and Spain (Nadal & Parga, 1994) and finally in California, USA (Bell & Sejnowski, 1995). The authors of the latter paper are members of the Salk Center, a institute highly related to the Swartz Center both situated in a suburb of San Diego. Their work initiated further efforts in this topic focusing mainly on the application of ICA to EEG-data.

For the first paper beyond methodical considerations an experiment required ten subjects to push a button after detecting an auditory target stimulus. The ICA of the measured EEG firstly focused on the methodical refinement using continuous data (Makeig, Bell, Jung & Sejnowski, 1996). The following report of ICA application on ERP used data of obviously selected participants of the same experiment (Makeig, Jung, Bell, Ghahremani & Sejnowski, 1997).

Even though an auditory 'oddball' task marked the beginning most applications of ICA on ERPs explored in San Diego were executed using a visual 'oddball' paradigm or more precisely a visual selective attention task originally developed for research about different attention abnormalities (Townsend & Courchesne, 1994; Townsend, Harris & Courchesne, 1996). Details of that task will be further explained in the empirical part of this thesis while introducing my method for replication. The first two papers using experiments with that visual 'oddball' paradigm are frequently quoted milestones for application of ICA in ERP research, twenty (Makeig et al., 1999a) respectively ten (Makeig et al., 1999b) participants were measured using 31 EEG-channels. The major insights were two ICs called P3b and P3f associated with the P300 ERP which will be further discussed in

the so chapters below. The two experimental settings led to papers not explicitly reporting these ICs (e.g. Makeig, Westerfield, Jung, Enghoff, Townsend, Courchesne & Sejnowski, 2002; Anemüller, Sejnowski & Makeig, 2003) and three additional publications with a major focus on these P3b and P3f components (Jung et al., 2001a, Makeig, Delorme, Westerfield, Jung, Townsend, Courchesne and Sejnowski, 2004 and Delorme, Westerfield and Makeig, 2007). Please also note that data gathered with this visual attention task was additionally used for a method for artifact rejection via ICA (e.g. Jung, Makeig, Westerfield, Townsend, Courchesne & Sejnowski, 2001b). According to Delorme et al. (2007, p. 11950) all of these five papers discussing the P3b and P3f ICs use the same dataset. Ten participants were recorded in the an experiment with the 'discrimination' task and twelve additional subjects and therefore a total of 22 subjects with the 'detection' task. Both conditions are 'oddball' variants explained in the chapters below. Please note that one report (Delorme et al. 2007) includes additionally two more subjects recorded with 256 channels for source localization. The two initial papers included only two hints regarding solely one referenced experiment:

Subsequent to this analysis, detection-task data were collected from 12 more normal subjects. [...] Further results of the enlarged subject group comparisons will be reported elsewhere.

(Makeig et al., 1999b, p. 2675)

Results shown [...] replicate our earlier observations, which were based on the decomposition of 1s epochs (-100 to 900 ms) for ten of these subjects [...] (Makeig et al, 1999).

(Makeig et al, 1999a, p. 1143)

To summarize the available information on the 'detection' task all five publications used subsets of twenty (Makeig et al., 1999a, p. 1136), ten (Makeig et al., 1999b, p. 2666; Jung et al. 2001a) and fifteen subjects (Makeig et al., 2004; Delorme et al. 2007) of the original 'detection'-task dataset. Details of the insights gained in these papers are introduced below. Concerning a historical description, it is important to be aware that the word 'replicate' in the second quote refers to a similar result with a different time window or subsets of subjects, but is based on the same dataset or subjects measured at two separate days for 'detection' and 'discrimination' task (Makeig et al., 1999b, p. 2669). The only additional experiment was conducted with two subjects for source localization. To recognize the significance of P3b and P3f ICs in the introduced history of ICA and due to ongoing discussions about ICA, a basic intention of this thesis is the replication of these aspects in a new experiment using the mentioned visual 'oddball' paradigm as further explained in the following chapters.

2.2 Methodical Perspective

The **visual attention task** (Townsend & Courchesne, 1994; Townsend et al., 1996) used for the empirical work of this thesis and for the recording of the referenced original dataset continuously displays one green and four blue squares. Subjects are required to press a key whenever a white circle appears inside of the target location or in the green square but to ignore circles in blue squares (figures 13 and 25). Finally this procedure collects a relatively large number of 600 target and 2400 non-target trials at five different locations. For a detailed description of this procedure see the empirical part below and various papers using the same dataset recorded in such an experimental setting (Makeig et al., 1999a, p.1136; Makeig et al., 1999b, p. 2666; Jung et al., 2001b; Makeig et al., 2004, p. 759; Delorme et al., 2007, p. 11950). The selected publications focus on the same aspects as major parts of the replication in this work. Regarding motivations and historical background see the previous chapter. Please note that Makeig et al. (1999b, p. 2666) used a 'detection' and a 'discrimination' condition even though this replication takes only the first one into account. The 'detection'-task simply consisted of circles as targets. In comparison to that condition, the 'discrimination'-task uses filled squares as targets and additionally circles as nogo-distractors. The effect of such a nogo-distractor on P300 will mainly be discussed in chapter 2.3. All conditions required pressing a key with the right thumb in target trials. Moreover one subject was asked to just mentally note targets in a second 'detection' session for control purposes (Makeig et al., 1999b, p. 2670). Corresponding effects are further discussed below.

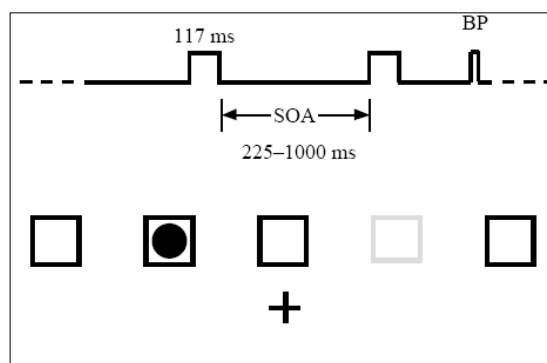


Figure 13: Timeline and example of a non-target stimuli on screen as presented in the detection condition of the original experiment (e.g. Makeig et al., 1999a, p. 1136).

On closer examination there are two inconsistent values in Makeig et al. (1999a, p. 1136) and Makeig et al. (1999b, p. 2666). First the schematic (figure 13) shows a lower interstimulus-value. Same has to be 250 ms and not 225 ms in order to get a sequence of 250, 500, 750 and 1000 ms as

written in the description. Second the average interstimulus interval is 625 ms. As a consequence the calculated total duration of each block is $(625 + 117) \text{ ms} (80 + 20) \text{ trials} = 74.2 \text{ s}$ and not 76 s as claimed in these papers.

The reported number of **subjects** for the 'detection' condition of these five papers are twenty (six women, 14 men) (Makeig et al., 1999a, p.1136), fifteen (unknown distribution) (Delorme et al., 2007, p. 11950), fifteen (three women, twelve men) (Makeig et al., 2004, p. 759) and a minimum of ten (two women, eight men) (Makeig et al., 1999b, p. 2666; Jung et al., 2001b, p. 1111). We have to assume that the same dataset was used for all of these papers and that it was measured in more than one session (Delorme et al., 2007, p. 11950; Makeig et al., 1999b, p. 2675). This dataset likely contains data from a 'detection'-experiment with 22 subjects and data from a 'discrimination'-experiment with ten subjects. A further indication for this is the similar age distribution of these participants. The reported ages range from 16 to 53 years with 20 subjects, 19 to 53 years with fifteen subjects and 22 to 40 years with 10 subjects. Finally we can consider a selection of subjects most probably depending on the phenomena of interest, as for example the ICs P3b and P3f. Because no alternative explanation is offered by the authors we have to be cautious regarding the representativeness of each used dataset. All participants were right-handed and had normal or corrected to normal vision. Additionally, one recording with two subjects was conducted for source localization in Delorme et al. (2007).

Behavioral: Only target responses between 150 and 1000 ms were accepted, however no responses shorter than 200 ms were recorded (Makeig et al., 1999a, p. 1136). Considering this constraint, 94.8 % of targets for the 'detection' task and 91.4 % for the 'discrimination' task were answered with a button press. The mean subject-median reaction time reported were 353 ms and 455 ms for the 'detection' and the 'discrimination' condition respectively (Makeig et al., 1999b, p. 2669). To prevent possible effects related with extreme reaction times, solely Delorme et al. (2007, p. 11950) removed trials including the fastest and the slowest 5 % of all reactions.

Recordings of the main original dataset were conducted by using 29 scalp electrodes. Their position was based on a modified international 10-20 system and two periocular electrodes all referenced on the right mastoid with an input impedance below 5 k Ω . Those data were digitized using a 512 Hz sampling rate and an analog pass band of 0.01-50 Hz.

Preprocessing included a downsampling to 256 Hz and a low-pass filtering with a cut-off frequency of 40 Hz. In addition to the main experiment Delorme et al. (2007) recorded two further subjects, thus providing an enhanced source-localization by using 253 channels and 256 Hz. Prior to ICA calculations, **epochs** from -100 prestimulus to 400 ms after stimulus onset (Makeig et al., 1999a, p. 1137), -100 to 900 ms (Makeig et al., 1999b, p. 2669, Jung et al., 2001b) and from -200 to 800 ms (Makeig et al., 2004, p. 759f.; Delorme et al., 2007, p. 11951) were extracted. Please note that Delorme et al. (2007, p. 11950) additionally used 4 s epochs for some frequency analysis. Regarding the extraction of two different epochs no explanation is available in these papers even though it would be reasonable to associate a longer baseline with an extensive frequency analysis conducted in latter studies. In all five studies the prestimulus **baseline** was removed before ICA decomposition as e.g. discussed in Delorme et al. (2009, p. 1208) and in related chapters above. Finally these authors pruned trials with potentials over 70 μ V but no rejection of trials with extreme tendencies and no visual inspection of **artifacts** were reported. Finally 400 to 600 target trials were left for the following analysis (e.g. Makeig et al., 1999b, p. 2666).

ICA was conducted to sets of 25 (Makeig et al., 1999a, p. 1137) or 25-75 averaged ERP epochs (Makeig et al., 1999b, p. 2669; Jung et al., 2001b, p. 1113f.) of the concatenated dataset of target and nontarget conditions and of all and subsets of all subjects. Furthermore a decomposition of individual data of each subject was conducted (Makeig et al., 1999b, p. 2671). In the last two studies the total dataset of 400 to 600 target epochs of each subject (Makeig et al., 2004, p. 760; Makeig et al., 2007, p. 11951) was decomposed separately. That proceeding serves as reference for the ICA-decomposition of this thesis. The problem of small subsets and different conditions is discussed on Jung et al. (2001b, p. 1113f.). Each mentioned ICA used Infomax (Nadal & Parga, 1994; Bell & Sejnowski, 1995) with an initial learning rate of about $\epsilon = 0.004$ and a batch size of 65-110 (Makeig et al., 1999b, p. 2669), 50 (Makeig et al., 2004, p. 760; Delorme et al., 2007, p. 11951) and 65 (Makeig et al., 1999a, p. 1137). The training stopped when the learning rate decreased below a value between 10^{-6} and 10^{-7} . Please note that ICA was conducted with specific Matlab-routines implemented into the EEGLAB-toolbox since 2004 (Delorme & Makeig, 2004; The MathWorks: <http://www.mathworks.com/>; EEGLAB: <http://sccn.ucsd.edu/eeglab/>, [last 26.03.10]). Further information regarding ICA, Infomax and the quality of these calculations are available in the first part of this thesis. The results of these decompositions are discussed in the following chapters.

2.3 Event Related Potential - P300

The P300 ERP is a relatively large positive deflection with a latency at about 300 ms after the stimulus onset and was first reported in 1965. The amplitude is defined as the difference between the mean prestimulus baseline voltage and the largest peak within a time window of about 250 to 500 ms. That ERP is typically measured at the midline electrodes Fz, Cz and Pz with an increasing value from frontal to parietal (Polich, 2007, p. 2). To evoke such a potential one can use infrequent target stimuli or infrequent targets embedded in frequent standard stimuli. The third possibility is to add an infrequent nogo-distractor which requires no answer but looks similar to the target stimuli. All of these experiments (figure 14) are different versions of the so-called 'oddball' paradigm and they require participants to mentally or physically respond to rare stimuli. Usually sounds or visualizations are presented, where in young adults the typical latency of a visual evoked P300 is about 400 ms and therefore slower than an auditory evoked potential at about 300 ms. Generally, the P300 is associated with orienting and updating the memory representation of a given environment, for example if a new or a infrequent stimulus is attended. Conventionally we mainly distinguish between the components P3a and P3b discussed as follows (Polich & Cirado, 2006, p. 172f.).

To prevent any misconceptions the ERP-components P3a and P3b are no ICs calculated via ICA. The main features of the P3b are that it is evoked by rare target stimuli and that it has its maximum over parietal regions. In comparison to that the P3a is elicited by infrequent easy or difficult to discriminate nogo-distractors asking for no response as for example implemented in the 3-stimulus experiment in figure 14. In comparison to the P3b the component P3a is more anterior and likely has other generators. Depth recordings pointed out that the P3a is generated in the anterior cingulate and the fronto-parietal cortex and that generators of the P3b are likely situated in superior temporal, posterior parietal, hippocampal, cingulate and frontal structures. Studies using fMRI were able to partially confirm most of these regions except for the temporal and hippocampal ones. EEG source localization via LORETA (Pascual-Marqui, Michel & Lehmann, 1994) was able to confirm cingulate, frontal and right parietal areas for P3a and quite distributed activations of bilateral frontal, parietal, hippocampal, cingulate and temporo-occipital regions for P3b. Even though these localizations are quite unspecific, they could point out that the P3a is associated with the orientation of attention and the P3b with the demanding attention allocation and the evaluation of task relevant stimuli (Volpe, Mucci, Bucci, Merlotti, Galderisi & Maj, 2007).

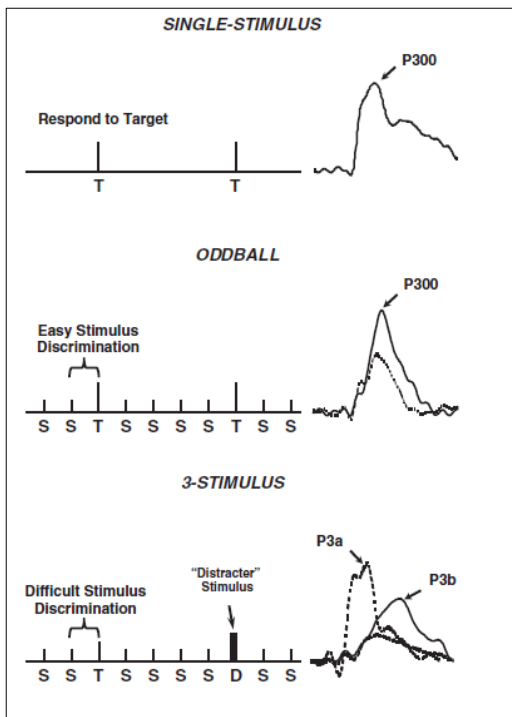


Figure 14: Schematic of three experiments (left) and ERPs (right). The timeline contains just one infrequent stimulus (top), a frequent and an infrequent stimulus (middle) and an additional nogo distractor stimulus (bottom). Subjects respond solely to infrequent targets (Polich & Criado, 2006, p. 173)

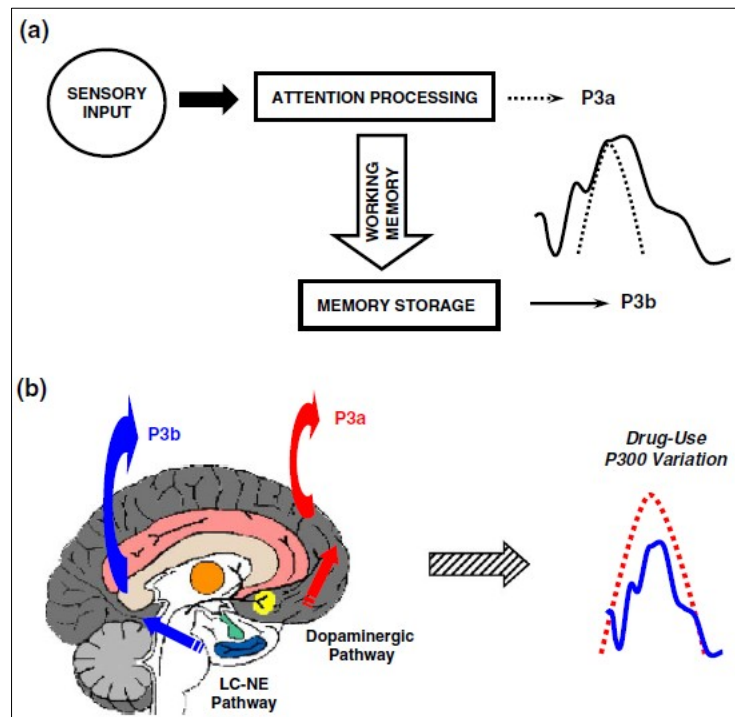


Figure 15: The components P3a and P3b and their associated cognitive processes in a schematic model. The P3a is related to the focal attention on a demanding stimulus and the P3b is produced by storage operations of the working memory (top). The P3a is associated with dopaminergic (DA) variability and the P3b with locus-coeruleus-norepinephrine (LC-NE) pathways and related drug use (bottom). (Polich & Criado, 2006, p. 175)

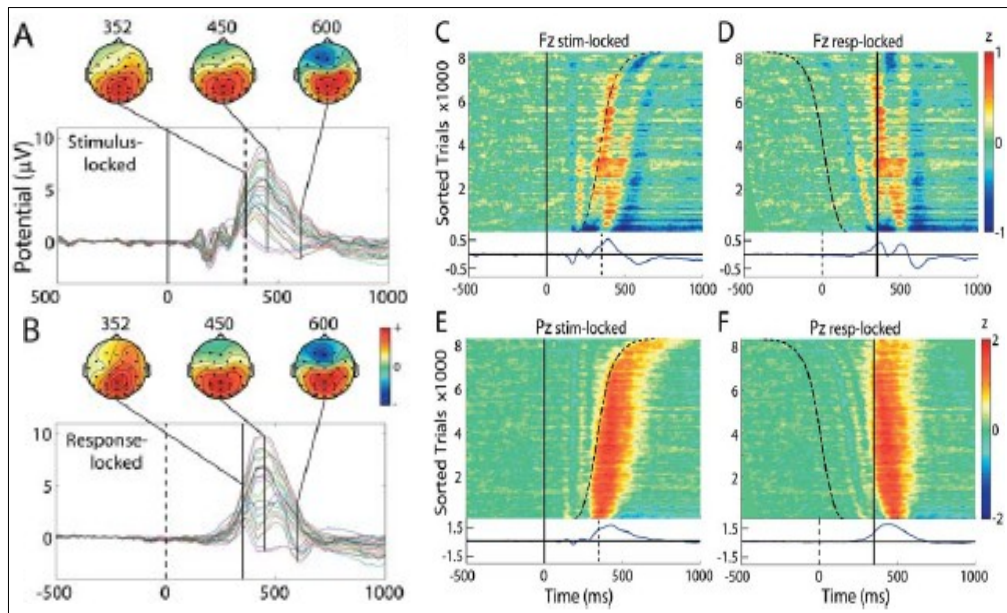


Figure 16: The stimulus-locked and response-locked grand mean calculated for 15 subjects and all 29 electrodes with related topographies (A, B) or just Fz and Pz (C-F). The latter pictures include all trials sorted by the response time with a smoothing window of 300 trials. The subject-median response time of 352 ms and the stimulus onsets are also available. (Makeig et al., 2004, p. 749)

Even though we do not know the exact generators of the P300 ERP, the quite integral model of figure 15 shows two different pathways with the corresponding function. According to that, the P3a is connected with activity in the anterior cingulate cortex due to a replacement of contents in working memory, whereas the P3b reflects a memory storage initiated in the hippocampus and transmitted to the parietal cortex. Confirming that theory fMRI studies revealed that the frontal lobe area's size is correlated with the P3a amplitude and the parietal area's size with the P3b amplitude. According to the P300 topographic distribution and to findings regarding the size of the corpus callosum, the initial processing of the incoming stimuli is likely to take place in right frontal areas and that information is then further transmitted between the hemispheres. An important support for two different pathways of the P3a and the P3b is that both have distinct neurotransmitter systems as it is implemented in the illustration of figure 15. Various modulations of these component amplitudes related to drug abuse suggest that the P3a is related to a dopaminergic and the P3b to a locus-coeruleus norepinephrine pathway (Polich & Criado, 2006). In addition to the research about neurotransmitters there are neuroelectrical descriptions of the P3a and the P3b (Polich, 2007, p. 12f.) as for example the explanation via event-related desynchronization already mentioned in previous chapters.

In the case of the previously introduced visual attention task (Townsend et al., 1996) the visual stimuli are displayed at five locations and one location serves as an infrequent target vs. frequent standard stimuli (figures 13 and 25). This situation is similar to the 'oddball'-case in figure 14. The 'discrimination' condition, also introduced but not replicated in the empirical part of this thesis, has an additional nogo-distractor and is another version of the '3-stimulus' task in figure 14. Please note the description of that task in the methodical chapter above. Participants of the 'detection' task are required to respond to targets by pressing a key, whereby these target trials evoke an ERP as shown in figure 16. The plots A and B of figure 16 show the grand mean of fifteen subjects at all 29 electrodes and the topographic distributions with an expected parietal activation of the P300 peak. The pictures C to F of figure 16 illustrate all single trials sorted by the response times with a vertical smoothing window of 300 trials, measured at the electrodes Fz and Pz. These plots illustrate the response locked character of the ERP P300. The following chapter introduces ICA decompositions of that P300 and the major ICs P3b and P3f. After that the relationship of these components with the mentioned P3b and P3a deflections will be discussed.

2.4 Independent Components P3b and P3f

The components P3b and P3f as ICA decomposition of the P300 ERP evoked in a five location visual 'oddball' paradigm (Townsend et al., 1996) were first described in Makeig et al. (1999b) and later in Makeig et al. (1999a). The latter study focused on the early period and was able to show that the components P3b and P3f appeared only in target trials or when the white circle occurred in the attended location with a green frame (Makeig et al., 1999a, p. 1139). See the task description in chapter 2.2 and 4.2 for details. Unfortunately all twenty participants and all conditions were calculated in one decomposition and so we do not know how many of them showed a P3b and especially a P3f component. The main empirical evidence gained by that paper, regarding the focused components, was that both ICs were two of the six largest ICs contributing most strongly to the ERP also in the time period from -100 ms prestimulus to 400 ms poststimulus. Therefore the P3b and the P3f could be expected within a such small group of largest components, especially if we consider later periods as their main activity. Furthermore the authors summarize their first interpretations about the nature of those two ICs as follows.

P3b [...] might reflect more widespread brain activity involved in the resetting of both stimulus expectancy and response preparation after target events. [...] The target selective nature of P3f, its frontoparietal topography and its close association with response onsets in faster responders all suggest that it might be associated with spatial orientating and motor response engagement.

(Makeig et al., 1999a, p. 1143)

Makeig et al. (1999b) offered the empirical base for that conclusion by focusing on the later period of the same dataset as mentioned above. In addition to the ICA of the concatenated dataset of all subjects, another decomposition of the individual data revealed that seven out of ten subjects had an IC similar to the P3f (Makeig et al., 1999b, p. 2671) and furthermore all of them had a P3b analog. The subjects without a P3f belong to the four with the slowest reaction times and a comparison shows that the P3f begins earlier and grows larger for the fast responders of those seven subjects (figure 18, bottom). Decompositions of subgroups with the five fastest and the five slowest responders led to a P3f component for faster but not for slower participants. As a consequence of that results the relationship of reaction time to the P3f has been an important topic of the whole sequel (see e.g. Delorme et al., 2007).

In fact the ICs P3b and P3f appeared for separate decompositions of the 'discrimination' and the 'detection' task (task explanation above) and the P3f occurs earlier in both conditions (figure 17, top). The onset was at about 140 ms poststimulus and the offset about 60 ms after the median reaction time. The P3b peak latency covaried with the median reaction time of 353 and 455 ms in the 'detection' and 'discrimination' condition, both indicated by vertical lines in figure 17 (top). The comparison of scalp maps in both conditions reveals differences between the P3f distributions but the P3b and the Pmp pairs are highly correlated (figure 17, bottom). The P3f amplitude was larger in the 'discrimination' task, even though the postulated frontoparietal topography with the largest activation in periocular channels and a weak central parietal positivity was visible in both conditions. Please also note the widespread posterior distribution of the P3b component. The root-mean square projected amplitude in the grand mean of the target trials was 1.5 μ V for the IC P3f and 6.1 μ V for the IC P3b and is therefore about four times larger in the latter case.

The other ICs are either limited to the nogo-distractor-trials in the 'discrimination' condition in the case of the Pnt (figure 17, top) or to the trials with button press as one control experiment with one subject shows for the Pmp (figure 18, top). For that control experiment a slow responder was instructed to mentally note targets without pressing a button. In that condition no relevant Pmp appeared. The characteristics of Pmp is described as a positivity with an onset nearly coincided with the median reaction time and a topographic distribution near the central sulcus. Makeig et al. (1999b) found associated components for eight out of ten subjects and the individual maximum was at about 80 ms after movement. The root-mean square projected amplitude in the grand mean of the response trials was 3.09 μ V. The scalp map of seven out of those eight Pmp findings had a contralateral distribution. For the empirical part the 'detection' task with button press is replicated and therefore a Pmp but no Pnt is expected even though not primarily focused.

Jung et al. (2001a) and the corresponding paper Jung et al. (2001b) represent efforts to overcome the approach of decomposing already averaged groups of epochs, by offering an ICA of single trials and individual data also from that 'detection' task experiment. Furthermore IC clustering was implemented to allow further comparison of ICs between subjects by using a modified Mahalanobis distance calculation (Enghoff, 1999; Jung et al. 2001a, p. 185). The last papers (Makeig et al., 2004; Delorme et al., 2007) of that sequel benefited from that work and applied further analysis to a subset of fifteen subjects with following additional insights regarding the ICs P3b and P3f.

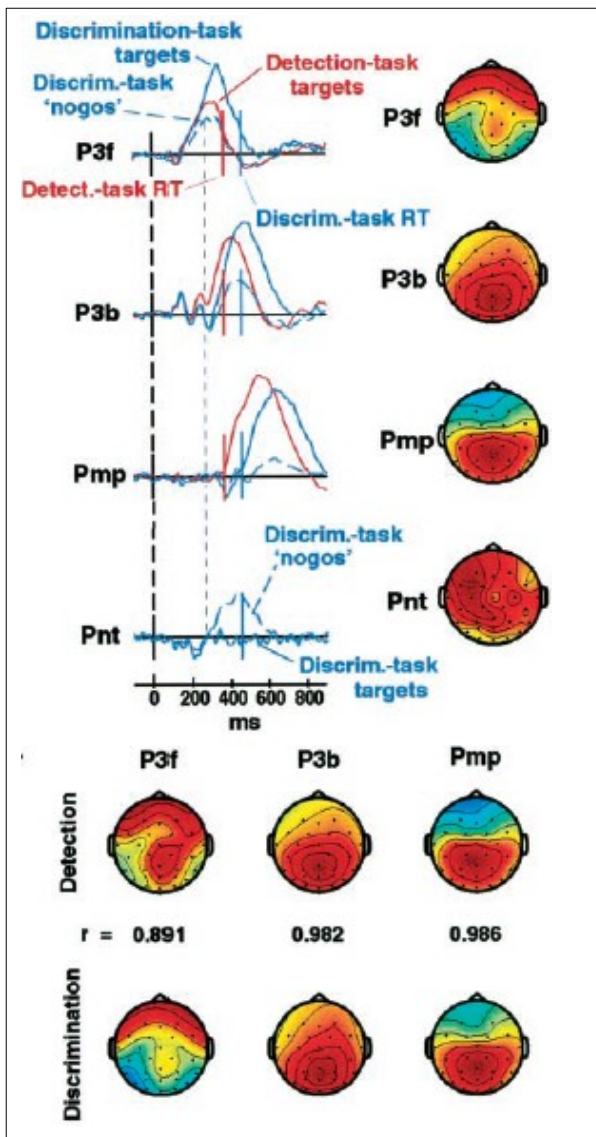


Figure 17: The main ICs decomposed using P300 ERPs evoked in the target trials of the 'detection' condition and in target and nogo-distractor trials of the 'discrimination' condition and ten subjects. The topography and the ERPs of four ICs with the median reaction times indicated by vertical lines (top). The scalp map pairs of three ICs with correlations between both conditions (bottom). See Makeig et al. (1999b, p. 2668) for details.

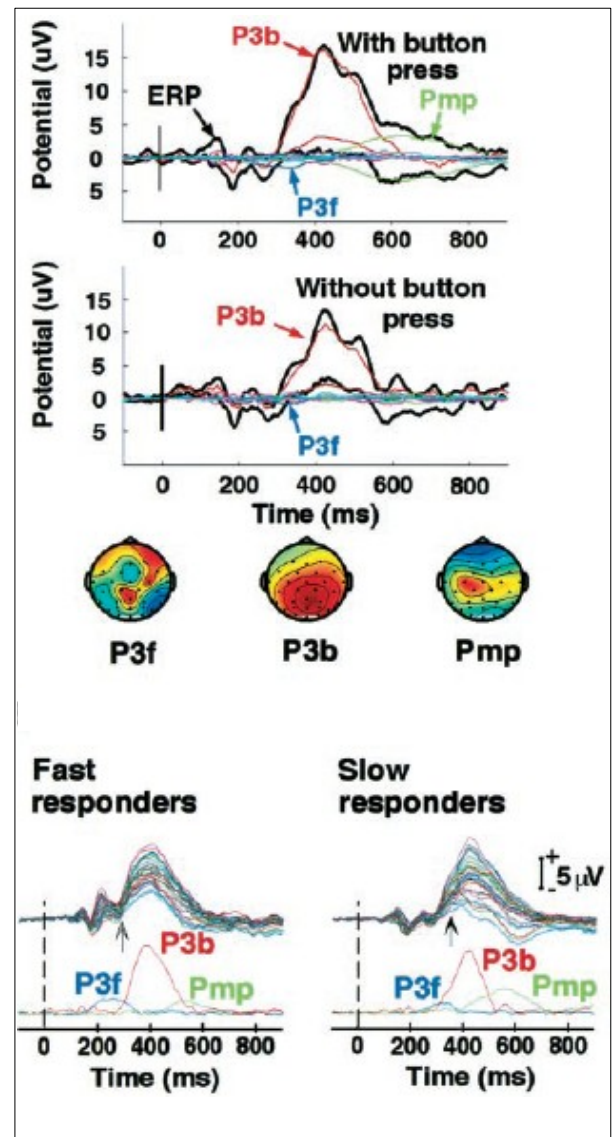


Figure 18: The envelopes of three ICs of one slow responder subject in the 'detection' condition with vs. without a button press instruction (top). For the latter control experiment this subject had to mentally note targets. ICA decomposition was conducted for the concatenated data of both 'instruction-conditions'. Below there are scalp maps of the ICs of this dataset (middle). Next, we have ten subjects separated into groups of fast and slow responders. The plots show the ERPs of all channels and the ERPs of P3f, P3b and Pmp (bottom). All values are normalized. See Makeig et al. (1999b, p. 2670) for details.

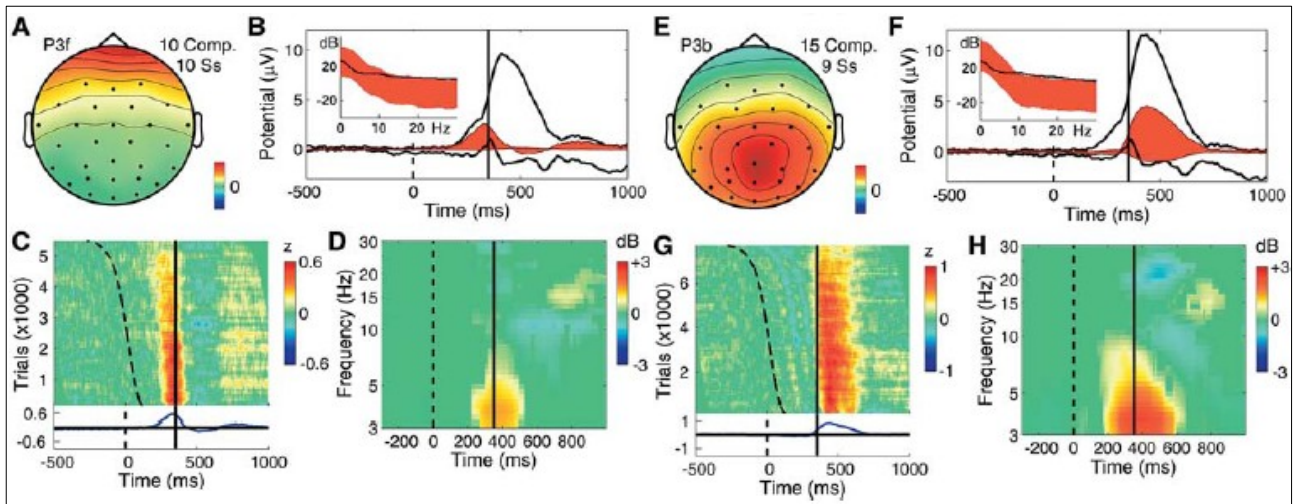


Figure 19: The features of the IC clusters P3f (A-D) and P3b (E-F). The plots show the mean scalp topographies (A and E), the response locked ERPs with envelopes and frequency spectra of the whole data (black line) and the clusters (red fill) (B and F). Below are the response locked ERPs with the normalized single trials (C and G) and the response locked event related spectral perturbation (ERSP). The latter shows the mean event related changes of the spectral power (D and H). See Makeig et al. (2004, p. 752) for details.

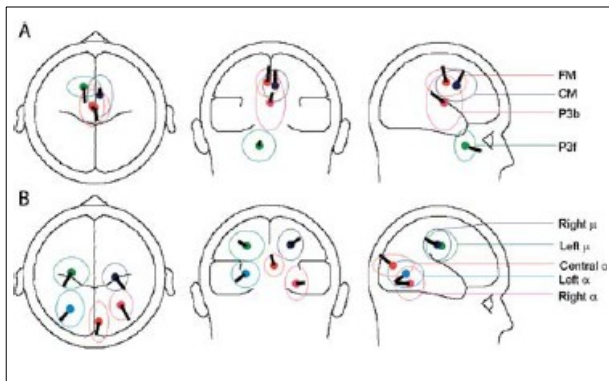


Figure 20: A single dipole solution (BESA) of all the nine IC clusters. Ellipses are the spatial standard deviations depending on the location of individual ICs. See Makeig et al. (2004, p. 757) for details.

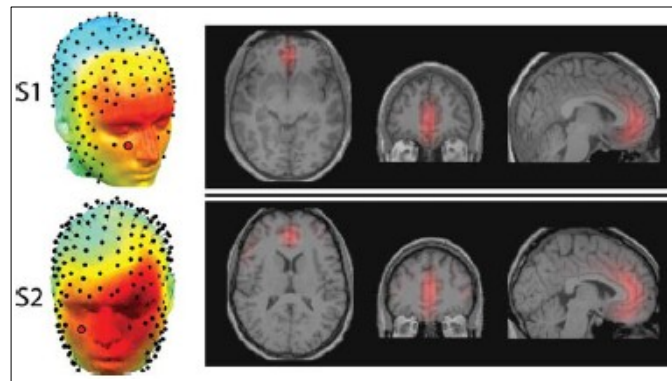


Figure 21: A source density solution (LORETA) of the P3f ICs of two subjects in two additional experiments. The red color indicates the estimated distribution. See Makeig et al. (2007, p. 11955) for details.

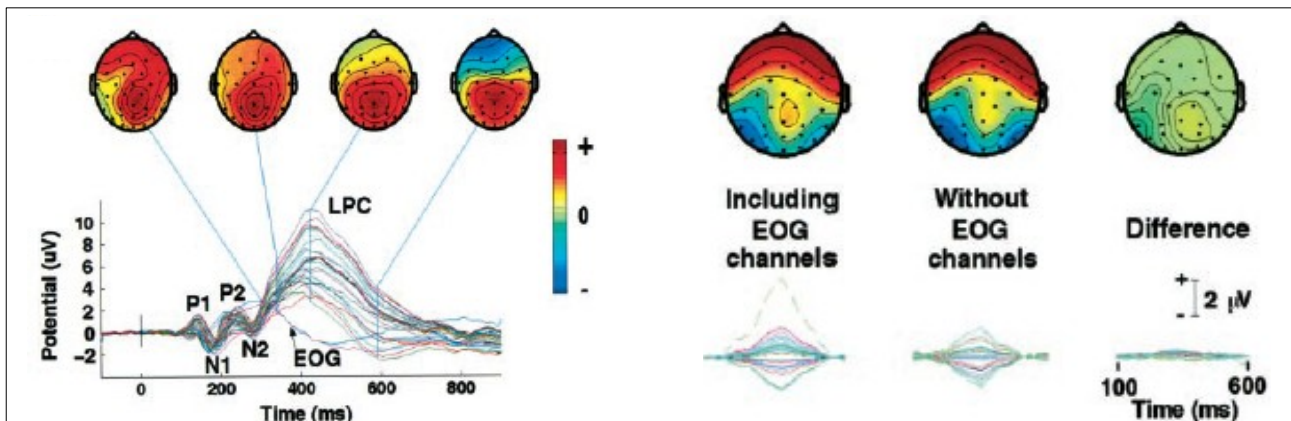


Figure 22: The grand mean of 29 scalp and two periocular channels (EOG) and the scalp maps at significant latencies. Note the early frontal activation. (left). The P3f topography of decompositions with and without the periocular channels showed no big difference (right). See Makeig et al. (1999b, p. 2668) for details.

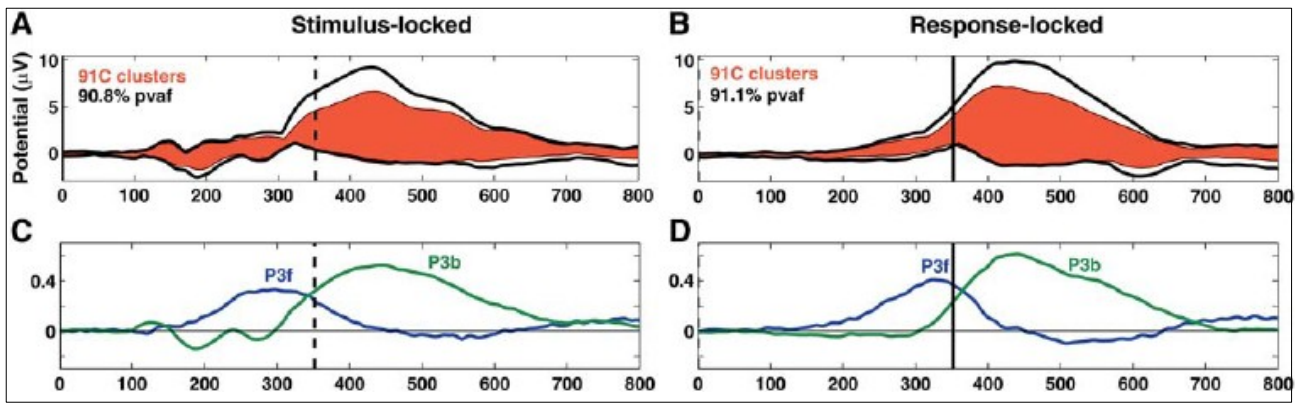


Figure 23: The stimulus-locked (A and C) and the response-locked (B and D) ERP of all nine clusters summed together and implemented into the envelopes of the whole data (A and B). The plots below show the ERP of the IC clusters P3f and P3b (C and D). See Makeig et al. (2004, p. 757) for details.

Makeig et al. (2004) identified 15 clusters by taking the normalized topographies and the power spectra of 465 components into account. Prior to this clustering a PCA reduction to five dimensions was conducted. In the paper of Delorme et al. (2007, p. 11951) the chosen dimension was twelve and 150 for 256 channel recording. Please note that after the clustering many 'outlier' and 'noisy' ICs were not included into any cluster. Six clusters were removed because they are likely related to artifacts. Two out of the remaining nine clusters were labeled as P3b and P3f clusters due to similar features already reported in previous papers. Figures 19 and 23 will support the following description.

The response locked P3f cluster has a mean onset at about 150 ms and peaks 39 ms before button press. Stimulus locked, the mean onset was at about 120 ms. If we consider about 25 ms electromyographically measured button travel time and about 15 ms neuromuscular conduction time, then we are close to the subcortical motor command. The P3b cluster was response locked, followed the motor command and is therefore linked to the also response locked P3f component. Because of the mentioned latencies, the P3b can not be associated with any motor decision or action but the P3f. Please note a small positive activation of the P3b in the stimulus locked plot of figure 23 regarding that information. The main difference to the previous studies is that there were no bilateral parietal features in the P3f cluster and so this single-trial analysis likely separated the parietal from the frontal activity. Please note the larger P3f amplitude for faster respondings indicated by more red color in figure 19 (C). This relationship was already mentioned above. All nine clusters (figure 23, A and B) explain about 91 % of the variance of the ERP (figure 23) and 60 % of the variance of the whole EEG. The P3f was the major prestimulus cluster and the P3b the

major poststimulus cluster. The P3f cluster contained ten ICs from decompositions of ten out of fifteen subjects and for the P3b fifteen ICs from nine subjects were clustered (Makeig et al., 2004).

To complete the description of the ICs P3b and P3f a BESA dipole localization (Scherg, 1990) for all subjects recorded with 31 channels generated some further insights regarding the origin of the corresponding clusters (figure 20, top) (Makeig et al., 2004). To gain better results a second LORETA source-density calculation (Pascual-Marqui, Michel & Lehmann, 1994) was applied to the data of two subjects recorded with 253 channels. The results were two ICs with activation within and near the bilateral frontopolar and ventral cingulate cortex (Delorme et al., 2007) as shown in figure 21.

Further features regarding the P3b and the P3f, for instance the connected event related spectral perturbation (ERSP), are discussed in Makeig et al. (2004) and Delorme et al. (2007). Remarkable for the question of this thesis is that Delorme et al. (2007, p. 11952) calculated a peak intertrial coherence (ITC) to gather information regarding the stimulus vs. response locked character of the P3f. If the ITC is close to one, the phase is locked to the event of interest. For further analysis the authors selected response locked trials only. This result suggests to soften the criterion that the P3f has to be response locked, as it was originally introduced. Additional discussions about IC clustering are available in Onton et al. (2006, p. 817ff.).

Finally the frontal activation of the P3f could be labeled as an eye movement or an eye blink artifact. For the recording of the original experiment the two periocular channels were commonly referenced with the other 29 scalp electrodes. Makeig et al. (1999b, p. 2668) demonstrated that the removal of these two periocular channels did not affect the P3f (figure 22, right). Even though the P3f has a similar phase as the EOG channels in the grand mean plot (figure 22, left; figure 23, bottom), they do not solely determine this IC. According to Makeig et al. (1999b, p. 2669) the P3f is likely no eye artifact because such movements need to be small, slow, diagonal and especially time locked in the most single trials. Furthermore comparing the grand mean at the periocular channels of trials with left, right and center presentation, after removing the six artifact clusters, showed only small differences (figure 22, right). This result indicates a low contamination by eye movement artifacts and suggests mainly cortical sources (Delorme et al., 2007, p. 11950f.).

2.5 P3b and P3f – Other Reports

The relationship between the ERP components P3b and P3a described by Polich & Criado (2006) and the ICs P3b and P3f or the clusters P3b and P3f (e.g. Makeig et al., 1999b; Makeig et al., 2004) needs further considerations. The IC P3b obviously explains a notable part of the variance of the P3b ERP in the 'detection' and the 'discrimination' condition. The task conditions, the corresponding latencies and other features are similar to the description in the 'oddball' and the '3-stimulus' situation in figure 14. According to the introduction of Polich & Criado (2006) the P3a ERP is only evoked in the latter situation in nogo-distractor trials and therefore is similar to the Pnt of Makeig et al. (1999b) shown in figure 17 (top). The IC and the cluster P3f are also decomposed in the 'detection' condition without any nogo-distractor and also in the target trials of the 'discrimination' condition. Even though the P3f and the P3a have similar scalp distributions they are not evoked in the same situations and so we have to assume different phenomena.

Considering the relatively early latency of the P3f component leads us to the frontal selection positivity (FSP), the anterior P2 (P2a) and the frontal polar component (FP) as discussed in Potts (2004). All three ERPs have a frontal topography, latencies between 180 and 300 ms and they are evoked in target trials. Unfortunately no other studies are based on ICA to gain further insights regarding the relationship of these ERP components with the IC P3f. Please note that Makeig et al. (2004, p. 750f.) and Delorme et al. (2007, p. 11956) mentioned these authors and hypothesized that P3f and P2a refer to the same phenomenon. In fact these papers do not include an extensive discussion about this relationship even though they recognize the similar latencies.

3 Research Question

Considering thirty years history of ICA application on neurophysiological data, no accepted guideline for necessary preprocessing steps is available. Groppe et al. (2009, p. 1208) published a greater number of reliable components for when the mean of each epoch is removed versus using the conventional prestimulus baseline correction method. Recent discussions of the same research group favor to skip the baseline correction prior to the ICA without offering any empirical evidence for this recommendation (EEGLABlist: <http://sccn.ucsd.edu/pipermail/eeglablist/>, A quick question about baseline correction after ICA, [05.01.10]). Groppe et al. (2009) presented a solution to estimating the reliability of ICs with moderate computational efforts. This assessment is essential for this thesis due to three topics of interest. First, various preprocessing steps were calculated and are explained in the methodical description below. For each proceeding the impact on the number of reliable ICs is calculated. Second, each reported IC gets such a reliability assessment to support the interpretation and to demonstrate a practical implementation of this algorithm. Assessing the reliability of each IC from individual datasets was a fundamental motivation for Groppe et al. (2009, p. 1199f) to develop that proceeding which is also recognized in this thesis. Third, the assessment in this thesis serves as contribution to the ongoing baseline discussion to overcome a lack of empirical evidence for recommendations, as introduced above. That could also support the development of approved preprocessing guidelines.

The visual attention task described in the historical and the methodical perspective above and in the experiment description below, has a dominant role for ICA research at the Swartz Center / San Diego and accordingly for ICA application on EEG in common. The original experiment was likely conducted with 22 subjects and two additional participants for source localization. Up to now no additional data support the major findings solely reported by this research group in five papers (Makeig et al., 1999a; Makeig et al., 1999b; Jung et al., 2001b; Makeig et al., 2004; Delorme et al., 2007). In addition to the methodical intentions introduced above, basic findings, particularly the postulated ICs P3b and P3f, are focused for replication in this thesis. Please note that the mentioned reports refer to different subsets out of all 24 participants and that not all these subjects showed a P3b and a P3f. Makeig et al. (1999b) found seven P3f ICs but ten P3b ICs in a selection of ten subjects. Makeig et al. (2004) clustered ten P3f ICs from ten subjects and fifteen P3b ICs from nine

out of fifteen subjects. A further description of the attended features is available in the chapters above, and the proceeding of the replication in this thesis is briefly introduced as follows.

At first the conducted visual 'oddball' experiment is expected to evoke P300 ERPs. Next, the result of the ICA-decomposition is a number of ICs which depends on the number of channels, proceedings and subjects. The preprocessing with the best results regarding the mentioned reliability assessment is focused first. The largest components contributing most strongly to the ERP of each subject in the relevant time period are further analyzed as theoretically discussed above. ICs with features associated with the ICs P3b, P3f and Pmp are reported. Finally the reliability assessment is completed with content related reports about the impact of various preprocessing steps on significant components to assess the validity of these ICs.

Empirical Part

4 Materials and Methods

4.1 Subjects

Fifteen right-handed volunteers, seven women and eight men, with normal or corrected to normal vision participated for the experiment. To avoid age-effects on attention and consequently on the outcome of the experiment, no subjects younger than 19 were recruited, corresponding to the original experiment. Therefore the age of the participants at test date ranged from 20 years, 2 months to 34 years, 1 month, with a mean value of 26 years, 4 months and a standard deviation of 3 years, 7 months. The Edinburgh Handedness Inventory (Oldfield, 1971) was used to assess handedness. All volunteers reported no neurological or infectious disease, psychiatric history or skull fracture. All subjects were previously informed about the procedure, the risks and their rights, specifically regarding privacy and the possibility to leave the testing procedure at any time, in the event of discomfort.

4.2 Visual Attention Task

The experiment (figure 25) based on the design of Townsend & Courchesne (1994) and is additionally explained e.g. in Makeig et al. (1999a, p. 1136) and in related chapters above (figure 13). For this procedure filled white circles appeared briefly for 117 ms in one of five possible squares with 16 mm outline. Each lower boundary of the constantly displayed squares was situated 8mm above a central fixation cross at the visual angles of $0^\circ \pm 2.7^\circ$ and $\pm 5.5^\circ$ from the fixation considering a monitor to subject distance of 70cm. One of the five square outlines was green, serving as a rare target location, while the other four were colored blue on a black background. Each of the thirty blocks took 74.2 s and presented 100 stimuli respectively white circles, twenty at each location, with an interstimulus interval of 250, 500, 750 or 1000 ms in a pseudorandom sequence. Each block had one pseudorandomly chosen but fixed target location respectively green square, so overall 600 target and 2400 non-target stimuli were presented on screen. Please note the possibility of allowed responses after the next target had already appeared on screen, in the event

that one white circle in the green square rapidly followed the other. In rare cases the response trigger could be situated within the accepted time window of 150 and 1000 ms for both targets, which requires a decision during preprocessing of the data as described below. Please note that this detail is not discussed in any of the referenced literature (e.g. Makeig et al., 1999b).

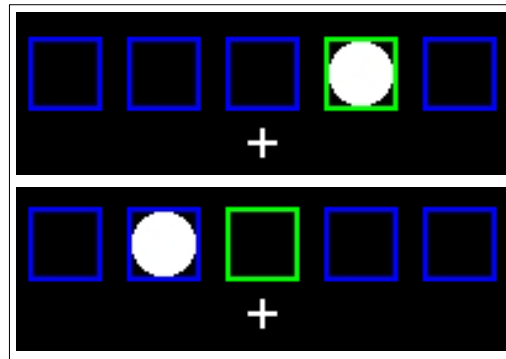


Figure 25: Schematic of a target (above) and non-target (below) trial in two different blocks of the experiment.

The participants were instructed verbally and on screen (see appendix for screenshots) to keep their eyes on the fixation cross in the center of the screen. Furthermore they were requested to respond to each stimulus at a target location or to any white circle in the green square by pressing the space key of a comfortably positioned keyboard with the right hand thumb. The same key was used to go on to the next block because the subjects were instructed to rest and proceed at their own pace (see appendix for pause screenshot).

One difference to the original experiment is that the participants of this experiment did not have to wait exactly one minute, but a minimum of four seconds during each break. This should offer the freedom to work if one feels well and to prolong breaks if a rest is needed. This alternation in procedure is not expected to determine the results of interest.

4.3 EEG-recordings

The experiment was programmed and presented via E-Prime 2.0 (Psychology Software Tools, Inc.: <http://www.pstnet.com/eprime.cfm/>, [last 26.03.10]). This software also provided the trigger synchronization with the EEG recording. Responses to target stimuli were accepted between 150

and 1000 ms after the target onset. The mentioned possibility of overlapping targets, meaning that a response to a target was allowed even after the next target had already appeared, led to a continuous recording of the whole experiment. To collect the EEG data, 61 Ag/AgCl electrodes were equidistantly applied by using an elastic electrode cap (EASYCAP GmbH: <http://www.easycap.de/>, model M10, [last 26.03.10]). Another two electrodes situated on the 7th cervical vertebra and at the right sternoclavicular junction served as a balanced non-cephalic reference with the advantage of minimized cardiac potentials (Stephenson & Gibbs, 1951). The ground electrode was mounted at the forehead. For a bipolar recording of the vertical EOG two electrodes were located above and below the left eye and for the horizontal EOG at the outer canthi of each eye to enable a reduction of artifacts from eye movement and eye blinks via EOG correction as explained below. To improve cephalic skin potentials and to eliminate related artifacts all mentioned electrode sites were carefully scratched by using a sterile single-use needle (Picton & Hillyard, 1972) till a homogeneous and stable input impedance lower than 2 k Ω was achieved, after filling the sites up with degassed electrode gel (Electro-Gel, Electro-Cap International, Inc., Eaton/OH, USA: <http://www.electro-cap.com/>, [last 26.03.10]). Prior to the actual recording 17 predefined electrode locations were measured by a 3D-photogrammetric head digitizer (Bauer, Lamm, Holzreiter, Holländer, Leodolter & Leodolter, 2000). A standard head model and the missing electrodes of the mentioned montage were calculated referring to those 17 positions, including a nasion, an inion and two preauricular electrodes. The EEG signals were recorded using an analog pass band of 0.016 to 100 Hz and a notch filter for elimination of 50Hz line noise. An AD-converter digitized with a sampling frequency of 250 Hz.

5 Analysis

5.1 Behavioral data

Responses to the target stimuli including their latencies were collected while EEG recording. This data led to the number of reactions and missed targets. Furthermore the individual reaction times are described by the values minimum, maximum, mean, standard-deviation and median. The necessary calculations are explained below. All these results calculated for each of fifteen subjects are taken to get the mean and the standard deviation of each value for all participants. The same information was calculated for the data after removing trials with reaction times slower than 800 ms and after the rejection of trials with artifacts. These two datasets for 30 and for 58/59 channels are the basis for all later calculations. Furthermore the remaining sampling points after the preprocessing are calculated considering one second trials with 250 Hz sampling rate.

As described above, the given task implies the possibility that a response to one target stimulus follows the next target. If such a trigger is situated within the accepted time window of 150 to 1000 ms poststimulus of both targets, it was possible to account the response to both stimuli. Even though those cases should be rare, the number of such events are calculated to control the phenomenon. All of these responses are finally moved to the later target. This is done by an own Matlab-script which takes all relevant trigger latencies into account.

5.2 Preprocessing

5.2.1 EOG-correction

In comparison to the original experiment (e.g. Makeig et al., 1999b) two bipolar vertical and two bipolar horizontal eye electrodes were recorded as an electrooculogram (EOG). Before the actual recording started, subjects were asked to perform regular eye movements by following a filled circle (Bauer & Lauber, 1979). These calibration trials were used to get the EOG parameters and the

correction coefficients for each channel. They provided the data to prune artifacts associated with eye movements and blinks from each channel offline and trial by trial. For further information regarding the procedure see Vitouch, Bauer, Gittler, Leodolter and Leodolter (1997), Lamm, Fischmeister and Bauer (2005) and Fischmeister and Bauer (2006). Please note that in comparison to these descriptions no blink correction by a template matching proceeding was conducted.

Skipping this EOG-correction and ignoring the bipolar record would lead to a similar condition as additionally reported in Makeig et al. (1999b). For this analysis the periocular channels were not taken into account, but the authors reported similar P3b and especially P3f components as described in the associated chapters and in figure 22 above. To provide such a proceeding, one additional calculation without any EOG-correction was conducted, even though this step is important to get enough clean epochs. Nonetheless it offers a comparison to control the influence of this correction on the ICA results and especially on the frontal variability. This additional proceeding was applied for the favored epoch mean baseline correction method in the 30 and 60 channels settings because this method had the largest number of reliable components. This and all further analysis steps are described in the following chapters. An overview of all proceedings is provided in chapter 5.4 and figure 30.

5.2.2 Low-pass filtering and epochs

Any further data analysis was conducted using Matlab 7.8.0 and the toolbox EEGLAB 7.2.9.20b (The MathWorks: <http://www.mathworks.com/>, [last 26.03.10]; Delorme & Makeig, 2004). At first a linear finite impulse response (FIR) low-pass filtering with a cut-off frequency of 40 Hz was applied to the continuously recorded data. Next, the epochs were extracted from 100 ms before to 900 ms after the target stimulus onset, according to the original procedure in Makeig et al. (1999b) and in Jung et al. (2001b). For the baseline correction three different proceedings were conducted, as introduced in the next chapter. All non-target events were not considered in the further analysis. The reaction times were calculated as the distance between the target stimulus onset and the corresponding response by using the relevant trigger latencies. Similar to Delorme et al. (2007) all reaction times larger than 800 ms were removed, as already mentioned above.

5.2.3 Baseline Correction

In the most ERP studies the prestimulus baseline is removed prior to any further analysis. In the context of the ICA there is an ongoing discussion regarding this analysis step and particularly about the reliability of the resulting ICs, as mainly discussed in chapter 1.6. Therefore three different proceedings are calculated prior to the ICA decomposition to offer further insights about this topic. First we have the traditional and widely used method of removing the mean of the prestimulus period, which is from -100 to 0 ms in this thesis (e.g. Makeig et al., 1999b; EEGLAB Tutorial: http://scn.ucsd.edu/wiki/eeglab_tutorial_online/, [last 26.03.10]). The second solution uses the mean of the whole period (in this thesis from -100 to 900 ms) as it is recommended by Groppe et al. (2009) due to a higher number of reliable ICs in their calculations. The third possibility is to skip this step prior to ICA calculations, as it is most recently recommended without offering any empirical evidence (EEGLABlist: <http://scn.ucsd.edu/pipermail/eeglablist/>, A quick question about baseline correction after ICA, [05.01.10]). It is important to note that after ICA calculations the prestimulus baseline has to be removed for all three proceedings to enable interpretable scalp map or ERP plots.

5.2.4 30 vs. 59 channels setting

The data for this experiment were recorded by using 61 commonly referenced channels. These electrodes were situated equidistantly by using an elastic electrode cap as shown in figure 26. The two preauricular channels were removed for all subjects for further analysis with 59 channels. Please note that the bipolar recorded EOG electrodes are not mentioned here. The original experiment (e.g. Makeig et al., 1999b) was recorded with 29 scalp electrodes located based on a modified international 10-20 system and two additional periocular electrodes. To provide a similar situation 29 electrodes were removed and the 30 channels left have intended equivalents in an extended 10-20 system (figure 27) as described in table 1. Therefore, a maximally similar location was searched for. Because no commonly referenced periocular recording was done, one extra Afz was kept for this analysis, in order to offer more frontal information. Finally we have two different settings with 59 (figure 28) and 30 (figure 29) channels.

Table 1: Channel-numbers in a 59 and a 30 channels setting and the intended equivalent in a 10-20 system.

Channels 59 (figure 28)	Channels 30 (figure 29)	Equivalent channels in 10-20 (figure 27)	Channels 59 (figure 28)	Channels 30 (figure 29)	Equivalent channel in 10-20 (figure 27)
1	1	FP2	30	16	FP1
2	2	F8	31	17	F7
3	3	FT8	32	18	FT7
4	4	Afz	34	19	F3
6	5	F4	36	20	Fz
9	6	FC4	38	21	FC3
11	7	FCz	41	22	C3
13	8	C4	43	23	T7
15	9	T8	44	24	Cz
17	10	CP4	46	25	CP3
20	11	TP8/TP10	49	26	TP9/TP7
21	12	CPz	52	27	P7/P3
24	13	P4/P8	54	28	Pz
27	14	O2	56	29	O1
29	15	Afz extra	58	30	Oz

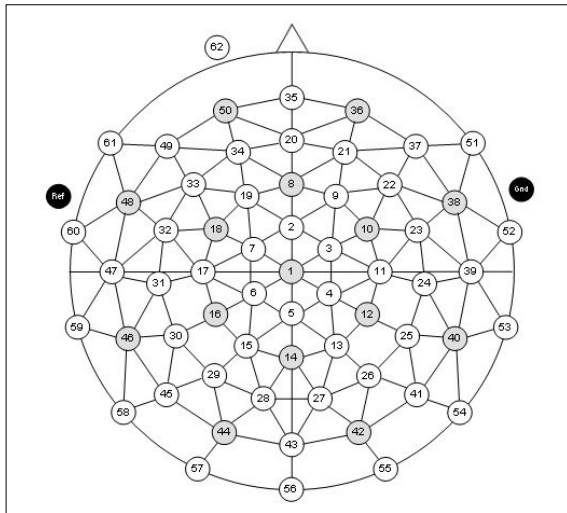


Figure 26: The electrode cap used for this recording with 61 channels. (EASYCAP GmbH: <http://www.easycap.de/>, model M10, [last 26.03.10])

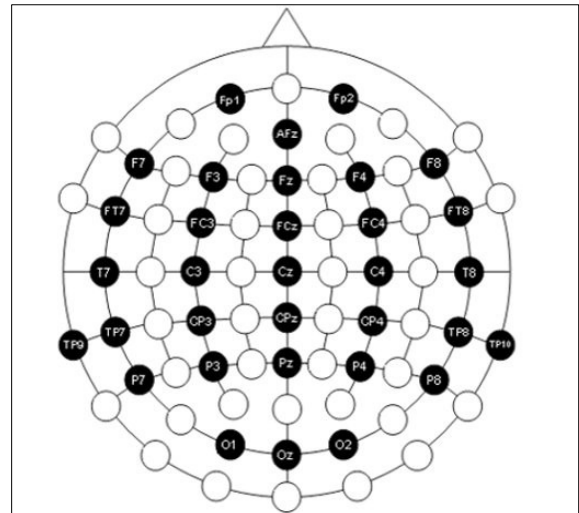


Figure 27: An electrode cap with an extended 10-20 system and 30 + 3 channels. (EASYCAP GmbH: <http://www.easycap.de/>, model M3, [last 26.03.10])

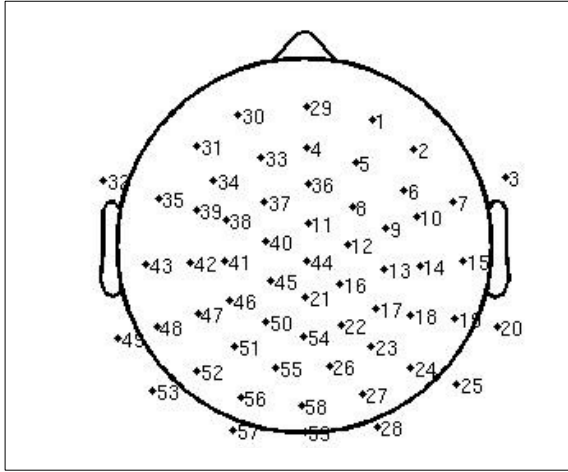


Figure 28: The 59 channels setting pictured with the electrode locations of subject 01.

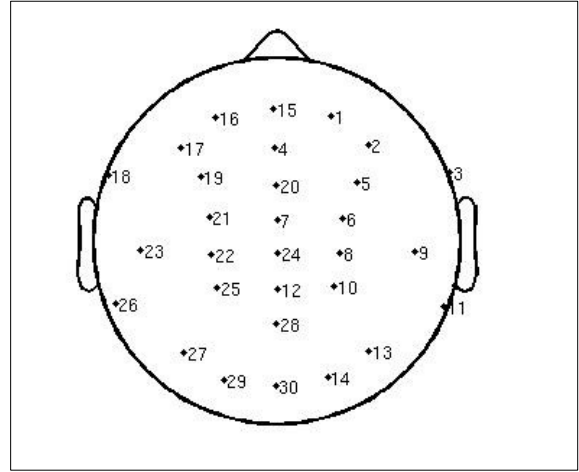


Figure 29: The 30 channels setting pictured with the electrode locations of subject 01.

5.2.5 Artifacts

At first, a semiautomatic inspection of all trials was conducted by using a voltage threshold of ± 70 μV and the datasets with the epoch mean baseline correction method, with all 59 channels after EOG correction, as mentioned above. Larger amplitudes than this threshold, marked in up to three channels but likely caused by stereotyped artifacts, such as eye blinks, were accepted. Non-stereotyped artifacts, as e.g. certain muscle activity or technical problems, were removed even if they were marked in less or no channels. Two subjects had one highly contaminated channel and were further analyzed by using 58 channels to prevent a loss of too much datapoints, as it is recommended by Onton et al. (2006). Theoretical guidelines for this visual inspection are discussed above.

As second step, trials containing larger amplitudes than ± 100 μV in any channel were removed. This automatic rejection was conducted for the 58/59 channels setting and the 30 channels setting separately, to keep marginal more trials. Again the EOG and epoch mean baseline corrected dataset was used. The remaining trials of both settings were also selected for all other proceedings with the same channels setting as the overview in figure 30 shows. This similar artifact treatment of all baseline correction methods allows comparing them to each other. Each subject's number of trials left for these two settings is reported together with the corresponding behavioral results.

For control purpose a similar artifact treatment as in the original experiment (e.g. Makeig et al.,

1999b) was conducted for 30 channels and for the epoch mean baseline correction method with EOG correction. This dataset was pruned again with a relatively strict automatic rejection, determined by a threshold of $\pm 70 \mu\text{V}$ and a maximum voltage drift of $40 \mu\text{V}$ and an R-squared limit of 0.3.

5.3 Reliability and ICA Calculation

The main objective of all above introduced preprocessing proceedings is to offer further insights regarding the influence on the number of reliable components calculated, as introduced by Groppe et al. (2009). In accordance with that guideline two split-half datasets were generated, using the odd and the even trials of each subject's full dataset. After that, an ICA was calculated for the full, the odd and the even dataset, using an Infomax-algorithm (Nadal & Parga, 1994; Bell & Sejnowski, 1995) for the single trials as discussed above. The input values were calculated by the EEGLAB implementation, corresponding to default values depending on the individual dataset. The learning rate was 0.001, the stopping parameters were a weight change of less than 10^{-7} for 59/58 and 10^{-6} for 30 channels. A second stopping parameter of maximum 512 iterations is not crucial because the necessary training steps for decompositions lay between 282 and 362. The batch size was between 53 and 60 and therefore similar to those reported in the original papers, with a value between 50 and 110 (Makeig et al., 1999a, p. 1137; Makeig et al., 1999b, p. 2669; Makeig et al., 2004, p. 760; Delorme et al., 2007, p. 11951). The bipolar EOG channels and the electrocardiac channel were kept out of this analysis. For each decomposition a minimum amount of datapoints is required, these limits were calculated and reported according to Onton et al. (2006). Please note that each baseline correction method has the same number of trials and that both channels settings have a similar number of trials.

The actual calculation of this reliability assessment published by Groppe et al. (2009) was conducted by using Matlab-scripts which are available online (Algorithm Reliability: <http://www.cogsci.ucsd.edu/~dgroppe/eeglab.html/>, [last 26.03.10]). For the preparation and input of each dataset, a customized Matlab-script used the EEGLAB .set file format for all full datasets and generated a winv-matrix out of the ICA-weight data of the odd and the even halves. (EEGLAB: <http://scn.ucsd.edu/eeglab/>, [last 26.03.10]). The main advantage of such an extracted winv-matrix

is the accelerated calculation. The results relevant for this thesis are the IC-numbers of the components assessed as reliable as they are labeled in the full dataset and also the corresponding 'L'-shaped critical region. The latter describes the criteria for the similarity-hypothesis test. The first lead to the total and the relative number of ICs assessed as reliable for each subject. For this data the mean reliability with the standard deviation for each setting and overall subjects was calculated. The reliability plots of all proceedings do show the relative number of ICs with the corresponding standard error of the mean, analogous to Groppe et al. (2009).

5.4 Preprocessing Proceedings - Overview

To summarize all introduced preprocessing steps, a reliability estimation for nine different proceedings is conducted, which requires 27 ICA decompositions. Figure 30 illustrates all variations and the significant steps for each branch. The first junction distinguishes between conducting an EOG correction or not. All proceedings underwent one collective semiautomatic approach to reject the artifact contaminated trials. This step was carried out with the epoch mean baseline corrected epochs after an EOG correction with all available channels. To keep more trials, the automatic artifact rejection with a threshold of $\pm 100 \mu\text{V}$ was conducted for both channels settings separately after an epoch mean correction. These trials were used as references for all other branches with the same channels setting, which allows a real comparison of different proceedings. For the six main baseline correction methods the proportion of reliable components is shown in one plot and the differences are tested using a 2 x 3 repeated measurement analysis of variance with the factors 'channels setting' and 'baseline correction method' (ANOVA). Next, simple contrasts referenced on the 30 channels setting and the prestimulus baseline correction method were calculated. All these effects are reported as significant for $p \leq 0.05$.

One extra control experiment was conducted using an amplitude threshold of $\pm 70 \mu\text{V}$ and a drift limit ($40 \mu\text{V}$ and a R-squared limit of 0.3) to illustrate this influence on the number of reliable ICs, shown in an extra plot. The epoch mean baseline correction method had the largest number of reliable components in Groppe et al. (2009) and therefore was a priori selected for the artifact rejection and first calculations. Due to the results of this thesis presented below, this method was also selected for the extra branches without EOG correction and with extra artifact criteria (figure

30). The reliability for these branches is just calculated for control purpose and therefore not part of further statistical tests. The main focus for this replication was the epoch mean baseline correction method with respect to the content related influence of other conditions further explained in the following chapters.

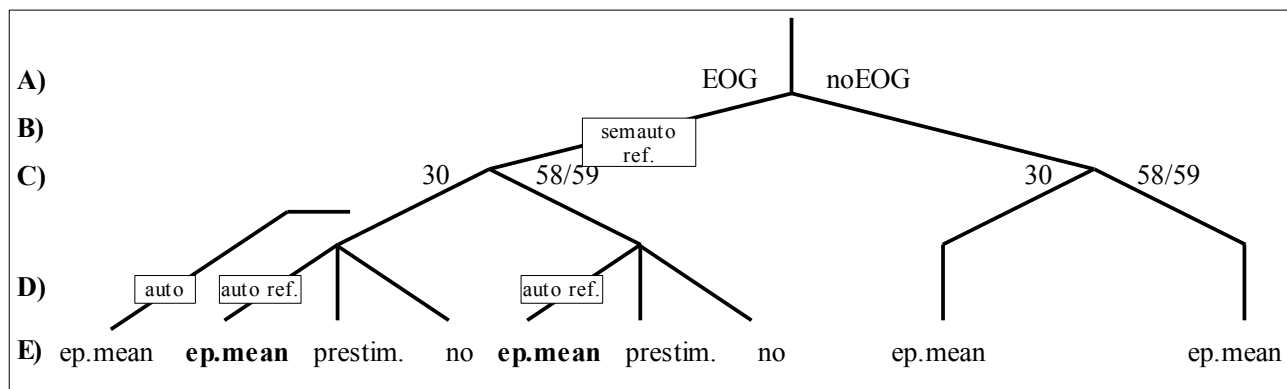


Figure 30: Schematic overview of the significant preprocessing steps including **A)** the EOG correction, **B)** the semiautomatic and visual artifact rejection, **C)** the 30 vs. 58/59 channel settings, **D)** the automatic artifact rejection by using a $\pm 70\mu V$ threshold (auto) or a $\pm 100\mu V$ (auto ref.) threshold and **E)** three different baseline correction methods (epoch mean, prestimulus and no correction). Nine different reliability calculations were conducted. See the description of each step and the text in this overview for details.

5.5 Event Related Potentials

To control the experimental manipulation, the grand mean for all subjects with the standard deviation is calculated stimulus locked for the electrodes Afz and Pz (number 4 and 28 in the 30 channels setting according to table 1). For these plots the 30 channels setting with the EOG correction and the corresponding artifact rejection were shown with the complete epoch from -100 to 900 ms. The chosen epoch mean baseline correction method should be similar to the two other preprocessing datasets because a prestimulus correction is done after the ICA decomposition and prior to this and all other plots. Please note that further information regarding the ERP of each subject is available in figures 36-39.

5.6 Independent Components – Reports and Plots

The result of all nine proceedings for all fifteen participants were 4783 ICs (5 datasets x 15 subjects

x 30 channels + 3 datasets x 13 subjects x 59 channels + 2 datasets x 2 subjects x 58 channels = 2250 + 2533 ICs). Please note further 9566 ICs calculated for the split-half datasets but not relevant for this content related report. A reasonable solution to handle the large amount of information was to focus on the results with the best reliability result as first step. This proceeding used the epoch mean baseline correction method with EOG correction. The alternative artifact approach had no better but a slightly lower reliability for all subjects. This dataset was therefore ignored even though some subjects would have a better result with this artifact rejection. Finally the 30 channels setting offers the possibility to completely report all scalp maps due to less calculated components.

That remaining proceeding of epoch mean baseline correction method with EOG correction used 30 channels and has 15 subjects x 30 channels = 450 ICs left. The first step was to calculate the seven largest components of each subject contributing most strongly to the period from 100 to 600 ms poststimulus. The ICs P3b and P3f are expected within this selection according to the reports of Makeig et al. (1999a). Please note that each plot includes the variance explained by this selection. The mean and the median of the variance of all subjects with the standard deviation has been calculated and reported additionally.

The remaining 105 ICs were inspected concerning the ICs P3b, P3f and Pmp. The P3f components should have a positive deflection in the ERP plots from about 150 ms after stimulus onset and there should be a peak at about 39 ms before button press. The P3b is expected to occur after the response and the P3f. The Pmp should peak at about 80 ms after a button press and the Pnt is not expected in these target trials. Due to slightly slower responses (shown in chapter 6.2) all components are expected accordingly. Furthermore the ICs P3f and Pmp are described with lower amplitudes than the P3b (e.g. Makeig et al., 1999b). See figures 17-23 and the theoretical descriptions for more details. A stimulus locked average for each inspected component with an extra ten trials moving average, sorted by the reaction time as shown e.g. in Makeig et al, (2004) will reveal more information. This plot is based on the projection of the relevant ICs to the electrodes Afz and Pz. ICs associated with a frontal distribution or mixed phenomena are reported at the electrode Afz and parietal distribution is reported at Pz. Due to the fact that the P3f and the P3b are mainly reported as response locked, this plot supports a decision regarding that feature. Finally, the main topographic distribution should be frontal for the P3f, more parietal for the P3b and slightly over the left central sulcus for the Pmp. This information is provided by the corresponding scalp map plots. These ERP

and topography plots are reported for significant Pmp, P3b and P3f candidates. The frequency spectrum from 1 to 30 Hz is also observed to recognize artifacts as introduced above (e.g. Onton et al., 2006). A comparison of trials with targets at the left vs. the right side of the screen is conducted to find a possible influence of eye movements. These results are reported without any plot.

It is important to be aware that the polarization of a scalp map of ICs is not meaningful because no projection to a channel is calculated. All scalp maps of the main proceeding (epoch mean baseline correction method with an EOG correction and a 30 channels setting) including the information about the reliability assessment for each IC are available in the appendix.

5.7 Preprocessing Influence on P3fs

All preprocessing steps are compared regarding the number of ICs assessed as reliable. To offer information regarding the validity and the content of these components, the scalp maps of selected subjects were compared for three proceedings. These participants were selected to illustrate the influence of following preprocessing decisions on significant P3f candidates. The approach without EOG correction serves to ensure that this step does not influence the P3f components due to a possible reduction of the frontal variability. Furthermore the baseline correction method with prestimulus baseline removal and without any correction prior to the ICA should demonstrate the associated influence. For these three proceedings the 30 channels setting was used again. This also offers the possibility to show all scalp maps and to compare them with the results displayed in the previous chapter. The corresponding ICs were sought for these proceedings by using the plot of the largest ICs contributing most strongly to the ERP period from 100 to 600 ms poststimulus. The further analysis was done as described above. ICs identified as corresponding P3f candidates were highlighted in each figure if possible. This analysis is furthermore provided for one subject in the proceeding with the epoch mean baseline correction method, an EOG correction and a 59 channels setting. This participant showed a mixed IC in the main analysis above. This should provide the information whether the limited number of channels led to this contamination.

6 Results

6.1 Behavioral Data and Artifact Rejection

The following data are calculated by using the trigger latencies recorded with the EEG data. Table 2 contains all recorded responses within the accepted time window from 150 to 1000 ms after the stimulus trigger. The number of trials slower than 800 ms is available in the last column of table 2. These trials were removed as one preprocessing step. After that a semiautomatic removal was conducted by taking all channels into account. The automatic artifact rejection with a threshold of $\pm 100\mu\text{V}$ was separately calculated for the 58/59 channels setting (table 3) and the 30 channels setting (table 4) leading to a marginal different behavioral result and a slightly larger number of sampling points for the latter case, as shown in tables 3 and 4.

Table 2: Behavioral data of all 15 subjects for the target trials before preprocessing. Reaction times (RT) in ms.

Subject	Responses	%	Missed Targets	Min. RT	Max. RT	Mean RT	SD. RT	Median RT	RT > 800
1	528	88	72	256	992	426.27	108.01	400	7
2	515	85.83	85	264	992	454.31	107.83	440	10
3	532	88.67	68	256	816	435.46	72.48	424	1
4	512	85.33	88	304	968	438.78	91.15	424	7
5	561	93.5	39	240	876	376.22	74.98	356	1
6	563	93.83	37	252	968	382.94	85.67	368	3
7	529	88.17	71	240	992	420.73	89.94	396	7
8	520	86.67	80	240	920	424.32	99.10	408	8
9	563	93.83	37	244	888	372.73	144.99	356	6
10	529	88.17	71	248	924	420.06	63.37	400	7
11	492	82	108	196	992	485.20	86.94	460	16
12	506	84.33	94	288	988	475.10	91.70	456	14
13	539	89.83	61	268	884	399.81	178.26	384	8
14	555	92.5	45	232	972	386.93	169.93	376	2
15	550	91.67	50	252	868	387.79	100.64	372	4
Mean	532.93	88.82	419.11	252	936	419.11	104.33	401.33	6.73
SD	22.03	3.67	35.02	24.61	57.71	35.02	34.05	33.86	4.33

Table 3: Behavioral data of all 15 subjects after the removal of slow responses (> 800 ms) and the artifact rejection finally conducted for the 58/59 channels setting.. Reaction times (RT) in ms.

Subject	Trials	%	Min. RT	Max. RT	Mean RT	SD. RT	Median RT	Sampling points (250 / trial)
1	499	83.17	292	764	434.93	100.06	412	124750
2	484	80.67	264	724	440.66	101.08	426	121000
3	530	88.33	256	752	43.90	71.27	424	132500
4	436	72.67	348	756	489.61	86.16	476	109000
5	292	48.67	260	460	347.18	45.29	344	73000
6	458	76.33	264	648	369.71	74.41	356	114500
7	463	77.17	284	756	429.17	93.55	412	115750
8	358	59.67	240	588	395.66	76.92	384	89500
9	545	90.83	260	528	359.94	58.57	356	136250
10	326	54.33	284	596	386.94	65.94	380	81500
11	409	68.17	296	756	463.67	169.86	456	102250
12	475	79.17	304	776	458.14	109.58	420	118750
13	522	87	268	704	392.90	66.02	384	130500
14	423	70.5	268	704	372.19	79.65	360	105750
15	546	91	260	588	382.24	63.43	364	136500
Mean	451.07	75.18	276.53	673.33	410.39	84.12	396.93	112766.67
SD	78.21	13.03	26.22	99.18	42.5	29.53	39.21	19552.23

Table 4: Behavioral data of all 15 subjects after the removal of slow responses (> 800 ms) and the artifact rejection finally conducted for the 30 channels setting.. Reaction times (RT) in ms.

Subject	Trials	%	Min. RT	Max. RT	Mean RT	SD. RT	Median RT	Sampling points (250 / trial)
1	499	83,17	292	764	434,93	100.06	412	124750
2	484	80,67	264	724	440,66	101.08	426	121000
3	530	88.33	256	752	432.90	71.27	424	132500
4	436	72.67	348	756	489.61	86.16	476	109000
5	292	48.67	260	460	347.18	45.29	344	73000
6	459	76.5	264	648	369.77	74.34	356	114750
7	463	77.17	284	756	429.17	93.55	412	115750
8	384	64	240	588	398.75	76.33	384	96000
9	545	90.83	260	528	359.94	58.57	356	136250
10	420	70	284	556	388.24	56.72	380	105000
11	409	68.17	296	756	463.67	169.86	456	102250
12	475	79.17	304	776	458.14	109.58	420	118750
13	522	87	268	704	392.90	66.02	384	130500
14	423	70.5	268	704	372.19	79.65	360	105750
15	546	91	260	588	382.24	63.43	364	136500
Mean	459.13	76.52	276.53	670.67	410.69	83.46	396.93	114783.33
SD	68.57	11.43	26.22	101.91	42.38	30.04	39.21	17143.27

Regarding the mentioned possibility that some rare responses could be attributed to two different target stimuli, all relevant trigger latencies for each subject were checked. According to that, no subject had any ambivalent response, because each single reaction was within the accepted time window of just one target stimuli.

6.2 Reliability Results

To provide a reasonable ICA decomposition one needs a minimum number of datapoints calculated according to Onton et al. (2006) by using a highly generous k-value of 20 with respect to 250 Hz and 1 s trials. Therefore the most demanding situation of 59 channels needs a minimum of 69620 sampling points or 279 trials. The 58 channels of the subjects 4 and 5 require 67280 sampling points or 270 trials. For 30 channels with the same but overdimensioned k-value 18000 sampling points or 72 trials are necessary. For all full datasets and for the split half datasets with 30 channels, no subject violates this assumption (tables 3 and 4). For 58 and 59 channels less sampling points are available considering a split half of the whole dataset and a k-value of 20. Subject five has the least amount of available data. A maximum k-value of 10.85 would be the threshold to have enough sampling points for the split-half datasets of this subject. The results of all nine preprocessing proceedings (figure 30) and all fifteen subjects are reported in table 5. The IC numbers of each full dataset with a positive reliability estimation and the corresponding 'L'-shaped critical regions are available in the appendix.

The first six proceedings of all nine calculations (table 5) are focused to decide which baseline correction method offers the best reliability outcome (figure 31). Due to the fact that the epoch mean baseline correction method showed the largest number of reliable components, the three additional proceedings were calculated by using this preprocessing. Considering a given sphericity (Mauchly test), the ANOVA calculation (Wilks-Lambda) showed significant main effects for the factors 'baseline correction method' [$F(2,13) = 50.158, p < 0.001$] and 'channels setting' [$F(1,14) = 4.587, p = 0.050$] and significant interactions [$F(2,13) = 7.908, p = 0.006$]. Simple contrasts showed that the prestimulus correction was different from the epoch mean correction [$F(1,14) = 8.759, p = 0.010$] and the epoch mean correction was different to no correction at all [$F(1,14) = 43.581, p < 0.001$]. The interactions were associated with differences between the prestimulus correction and the epoch mean correction [$F(1,14) = 13.376, p = 0.001$] but not between the epoch mean correction and no correction [$F(1,14) = 0.247, p = 0.627$]. Further information is available in the 95 % confidence interval (CI) for the 30 channels setting [0.202, 0.274], the 58/59 channels setting [0.179, 0.241] and for the prestimulus correction [0.144, 0.230], the epoch mean correction [0.263, 0.348] and no correction [0.146, 0.212].

Figure 32 illustrates the differences regarding an artifact rejection conducted for control purpose. The third bar (epoch mean best, figure 32) is the mean of the relative number of ICs assessed as reliable after taking the better solution for each participant. The two results for preprocessing without an EOG correction are available in figure 33. That value is only mentioned because potential differences are expected regarding the content reported below.

Table 5: The absolute and the relative number of ICs assessed as reliable for all nine proceedings. See the text above and the overview in chapter 5.4 for details. For IC numbers with positive estimation and for critical regions of the similarity-hypothesis see the appendix.

	Prestim.		Ep. mean		No corr.		Prestim.		Ep. mean		No corr.		Ep. mean		Ep. mean		Ep. mean	
	58/59		58/59		58/59		30		30		30		30 extra		58/59		30	
	EOG		EOG		EOG		EOG		EOG		EOG		EOG		no EOG		no EOG	
Subj.	ICs	%	ICs	%	ICs	%	ICs	%	ICs	%	ICs	%	ICs	%	ICs	%	ICs	%
1	7	0.12	13	0.22	10	0.17	10	0.33	15	0.50	6	0.20	14	0.47	25	0.42	13	0.43
2	7	0.12	16	0.27	6	0.10	5	0.17	6	0.20	5	0.17	7	0.23	20	0.34	8	0.27
3	6	0.10	15	0.25	9	0.15	5	0.17	8	0.27	8	0.27	9	0.30	16	0.27	10	0.33
4	12	0.21	16	0.28	6	0.10	10	0.33	8	0.27	2	0.07	7	0.23	17	0.29	7	0.23
5	6	0.10	16	0.28	7	0.12	3	0.10	4	0.13	4	0.13	2	0.07	22	0.38	8	0.27
6	11	0.19	18	0.31	12	0.20	7	0.23	10	0.33	7	0.23	8	0.27	15	0.25	11	0.37
7	16	0.27	23	0.39	13	0.22	8	0.27	10	0.33	7	0.23	10	0.33	23	0.39	8	0.27
8	8	0.14	19	0.32	18	0.31	6	0.20	11	0.37	9	0.30	13	0.43	16	0.27	8	0.27
9	10	0.17	17	0.29	11	0.19	9	0.30	10	0.33	3	0.10	9	0.30	20	0.34	9	0.30
10	15	0.25	26	0.44	14	0.24	12	0.40	13	0.43	7	0.23	14	0.47	21	0.36	14	0.47
11	12	0.20	28	0.47	10	0.17	9	0.30	11	0.37	4	0.13	13	0.43	28	0.47	12	0.40
12	2	0.03	11	0.19	15	0.25	1	0.03	10	0.33	7	0.23	5	0.17	14	0.24	7	0.23
13	8	0.14	16	0.27	7	0.12	5	0.17	9	0.30	3	0.10	12	0.40	19	0.32	11	0.37
14	4	0.07	13	0.22	6	0.10	6	0.20	3	0.10	5	0.17	4	0.13	19	0.32	5	0.17
15	6	0.10	26	0.44	10	0.17	6	0.20	8	0.27	6	0.20	10	0.33	25	0.42	12	0.40
mean	8.67	0.15	18.2	0.31	10.27	0.17	6.8	0.23	9.07	0.3	5.53	0.18	9.13	0.3	20	0.34	9.53	0.32
SD	3.94	0.07	5.2	0.09	3.63	0.06	2.91	0.1	3.13	0.1	2.03	0.07	3.7	0.12	4.07	0.07	2.56	0.09

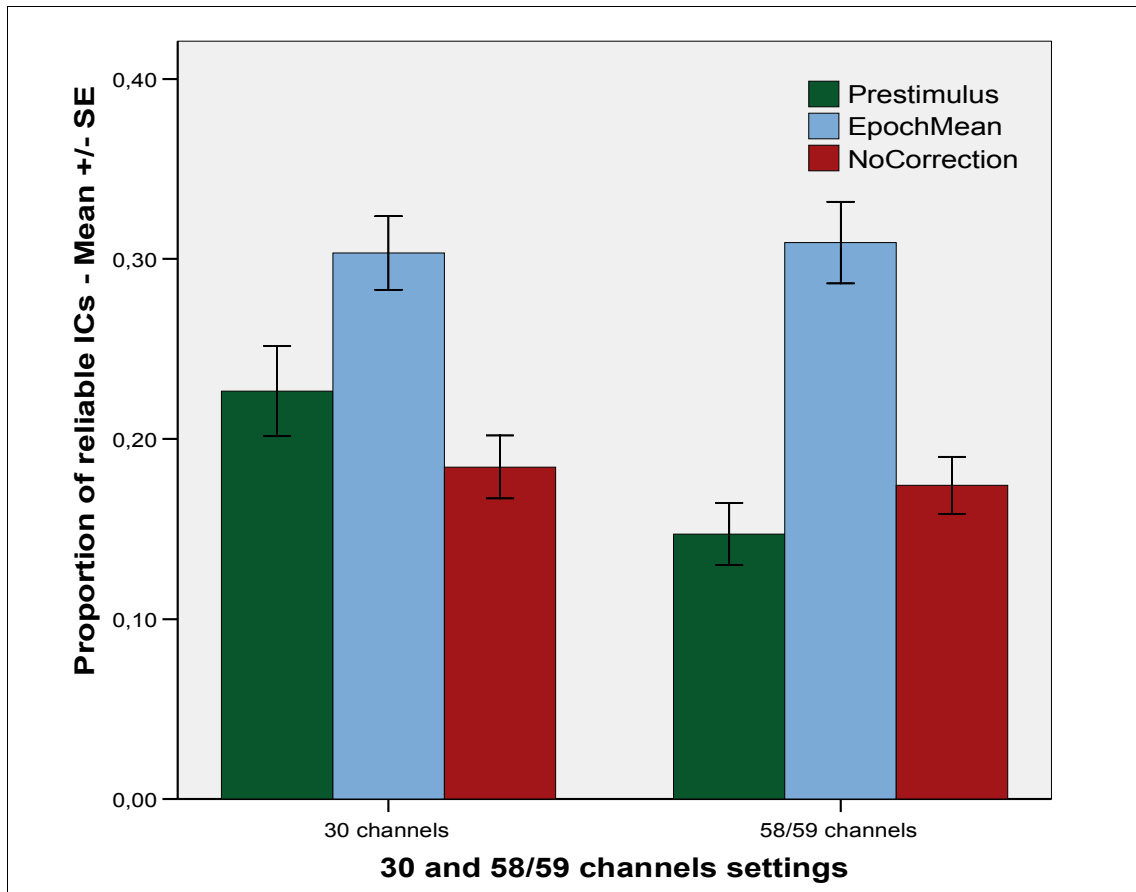


Figure 31: The mean proportion of ICs assessed as reliable and the standard error of the mean for the prestimulus, the epoch mean and no correction baseline correction method with a 30 and a 58/59 channels setting.

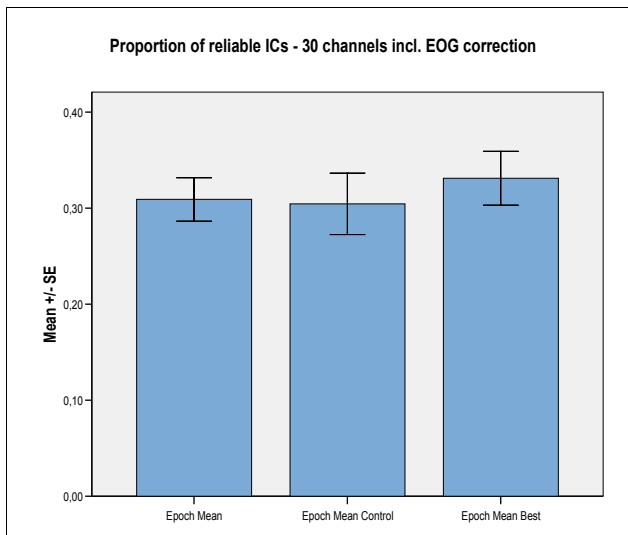


Figure 32: The mean proportion of ICs assessed as reliable and the standard error of the mean for two different artifact approaches and after choosing the most reliable solution for each participant ('epoch mean best').

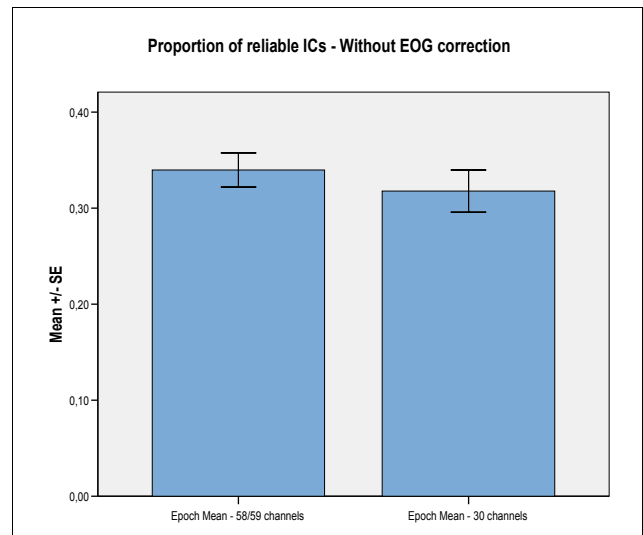


Figure 33: The mean proportion of ICs assessed as reliable and the standard error of the mean for both proceedings without EOG correction.

6.3 Event Related Potential - P300

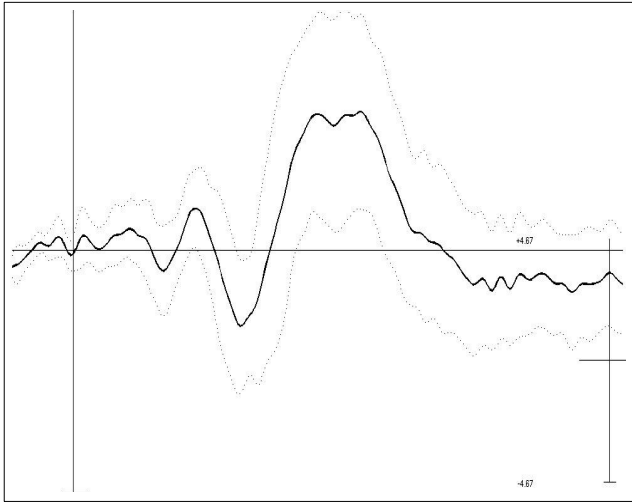


Figure 34: The grand mean at the electrode Afz of all 15 subjects including the standard deviation.

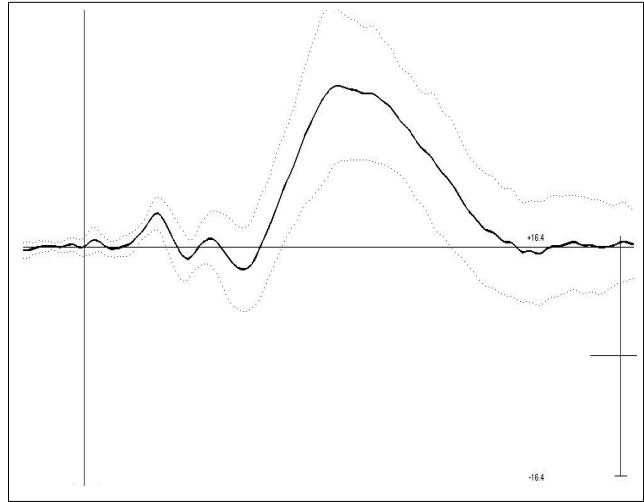


Figure 35: The grand mean at the electrode Pz of all 15 subjects including the standard deviation.

6.4 Independent Components Results – P3b and P3f

The following figures 36-37 are illustrations of the seven largest components contributing most strongly to the ERP period from 100 to 600 ms poststimulus of each participant. The used proceeding was the epoch mean baseline correction method with an EOG correction and the 30 channels setting. All seven components explain between 59 % and 98.59 % (mean = 90.39 %, standard deviation = 9.72 %, median = 93.19 %) of the ERP variance of each subject in this period. Please note that figures 36-37 include artifact and cortical components and therefore the resulting 105 components were inspected regarding P3b, P3f and Pmp characteristics according to the theoretical descriptions above. The figures 38-39 show a selection of associated ICs which explain between 16.24 % and 97.96 % (mean = 70.4 %, standard deviation = 22.87 %, median = 80.75 %) of the ERP variance of each subject in the mentioned period. The overview in table 5 contains all suggested P3b, P3f and Pmp assignments. All results associated with frontal and mixed activity are reported with projection to Afz and for parietal phenomena to Pz. The ICs assessed as reliable are highlighted with green boxes in the figures 36-39. All scalp maps of this proceeding with the highlighted reliability assessment are available in the appendix.

Each subject had one component with a postmotoric positive potential highly correlated with the button press similar to the characteristics of Pmp. Because of a very low intersubjective variability, only two examples of an ERP projection to the Pz are reported (figure 40).

The P3b phenomenon is illustrated by using two regular (figure 41) and two rather irregular examples (figure 42). Please note that the majority of the P3bs listed in table 5 are similar to the examples in figure 41. Nonetheless all the associated ICs are either distinct P3b components or they represent significant variance of this phenomenon. Following that definition all subjects had such a P3b component, even though the components of subjects 12 and 14 are not that sound (figure 43). Please note the relatively low amplitude of the P300 ERPs of these participants as shown in figure 37 and the response locked activity of these ICs contaminated with an early stimulus locked activity not visible at other P3b candidates.

Some more variance of the P3b and also of the P3f could be explained for subjects 1, 9, 11 and 15 because their decomposition led to the mixed components 11, 6, 3 and 4 (figures 44 and 45). Obviously the interpretation of such ICs is difficult. For example the IC11 of subject 9 could be a mixture of a P3f and a later activity but not P3b (figure 44). In case of the IC4 of subject 15 a mixed component containing a P3b and a P3f variance is more likely (figure 45). Please note the results of the next chapter (figure 59) regarding subject 15.

Finally ten components of the table 5 have features of a P3f. The ICs 5 and 13 for subjects 1 and 12 (figure 46) contain response locked variance associated with a P3f but contaminated with a strong stimulus locked early positivity. Please note that a similar phenomena was demonstrated for the P3b components of subjects 12 and 14 (figure 43). The components 5 and 6 of subjects 4 and 12 (figure 47) display a frontal distributed positivity but with a stimulus locked tendency. Therefore these ICs meet all but one criteria of a P3f. The IC of subject 4 is closer to being response locked, but the association with an earlier stimulus locked deflection is still possible. Please note the results in the next chapter with the P3f candidate of subject 4 after a prestimulus correction proceeding (figure 52). The parietal scalp map distribution of ICs 6 and 8 of subjects 8 and 13 (figure 48) is contrary to the description of P3f. That is possibly caused by other parietal variance or due to a parietal projection from a frontal source.

The ICs 4 and 9 of subjects 8 and 5 (figure 49) and the ICs 4 and 2 of subjects 7 and 11 (figure 50) meet all criteria to suggest them as a P3f IC, especially for IC 4 of subject 7. Please note the replication of the P3f of subject 7 after two other proceedings in the next chapter (figure 58). Please also note the reliability information highlighted by using bold numbers in table 5.

Table 5: ICs selected for inspection due to associated characteristics with a P3b, a P3f, a mixture of P3b and P3f or a Pmp. Please note the introduction of significant components in the text. As proceeding an epoch mean baseline with an EOG correction and 30 channels was used. Bold ICs are assessed as reliable.

Subject	P3f		P3b		P3f/P3b		Pmp	
1	5		1		11		2	
2			1	2			3	
3			1				2	
4	5		7				4	
5	9		1				3	
6			2				1	
7	4		2				3	
8	6	4	2				5	
9			1		6		3	
10			6	2			1	
11	2		6	4	3		1	
12	6	13	2				1	
13	8		2	3			1	
14			9				1	
15			3		4		2	1
Total Number	8	2	15	3	5	0	15	1

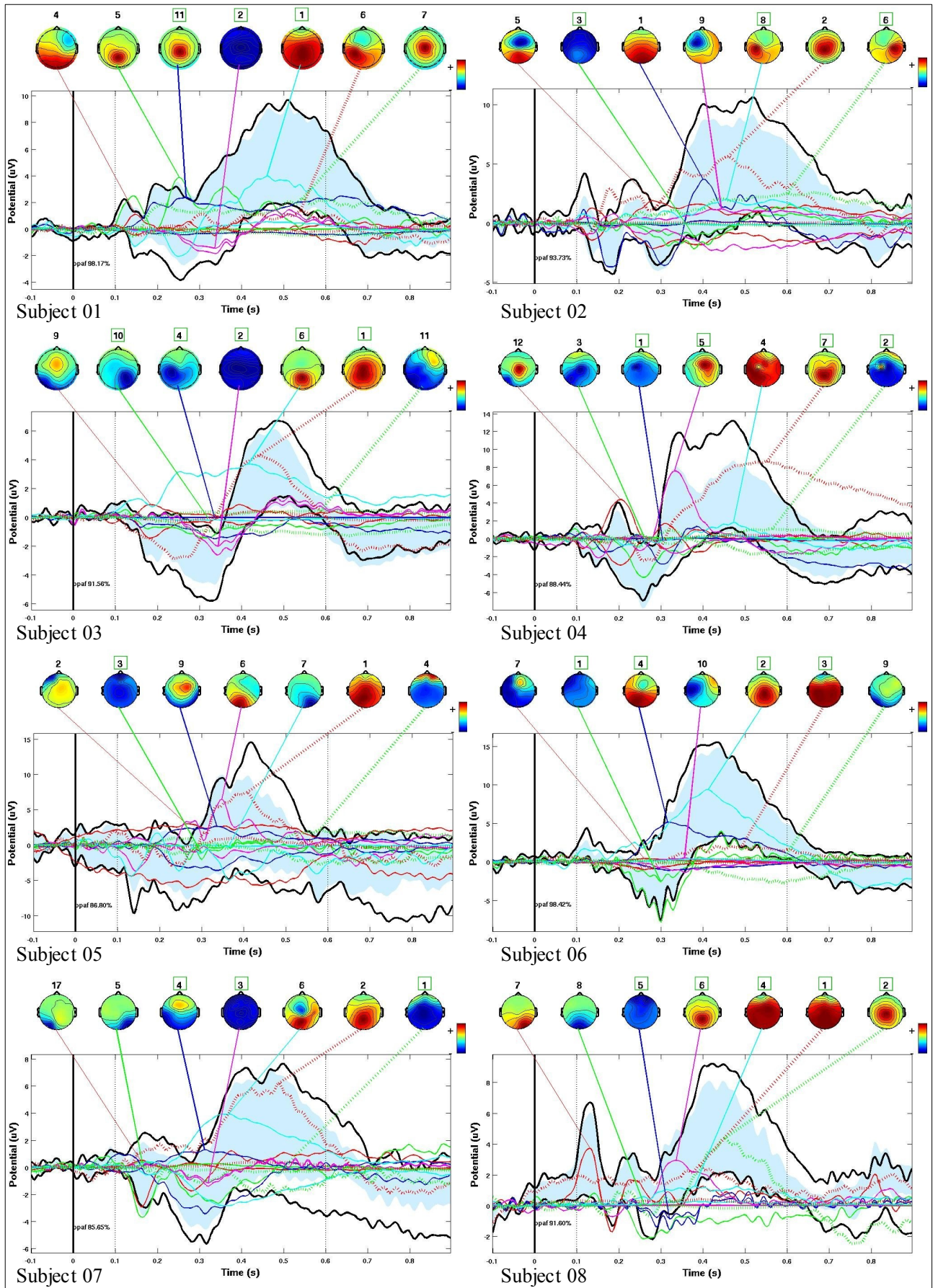


Figure 36: The ICs most strongly contributing to the ERP of subject 01-08 using the epoch mean baseline with an EOG correction and 30 channels. ICs assessed as reliable (green square) are highlighted. See text for details.

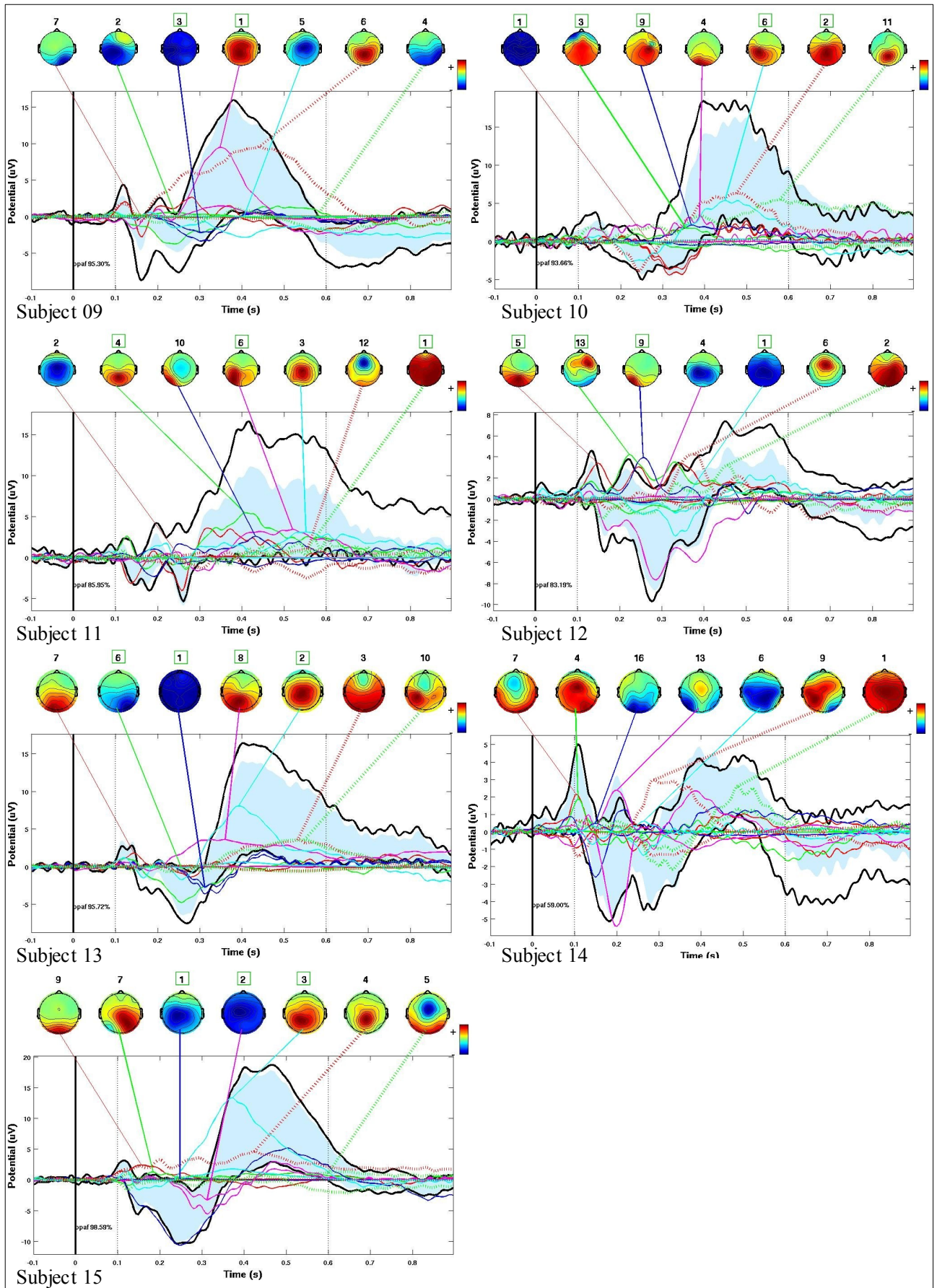


Figure 37: The ICs most strongly contributing to the ERP of subject 09-15 using the epoch mean baseline with an EOG correction and 30 channels. ICs assessed as reliable (green square) are highlighted. See text for details.

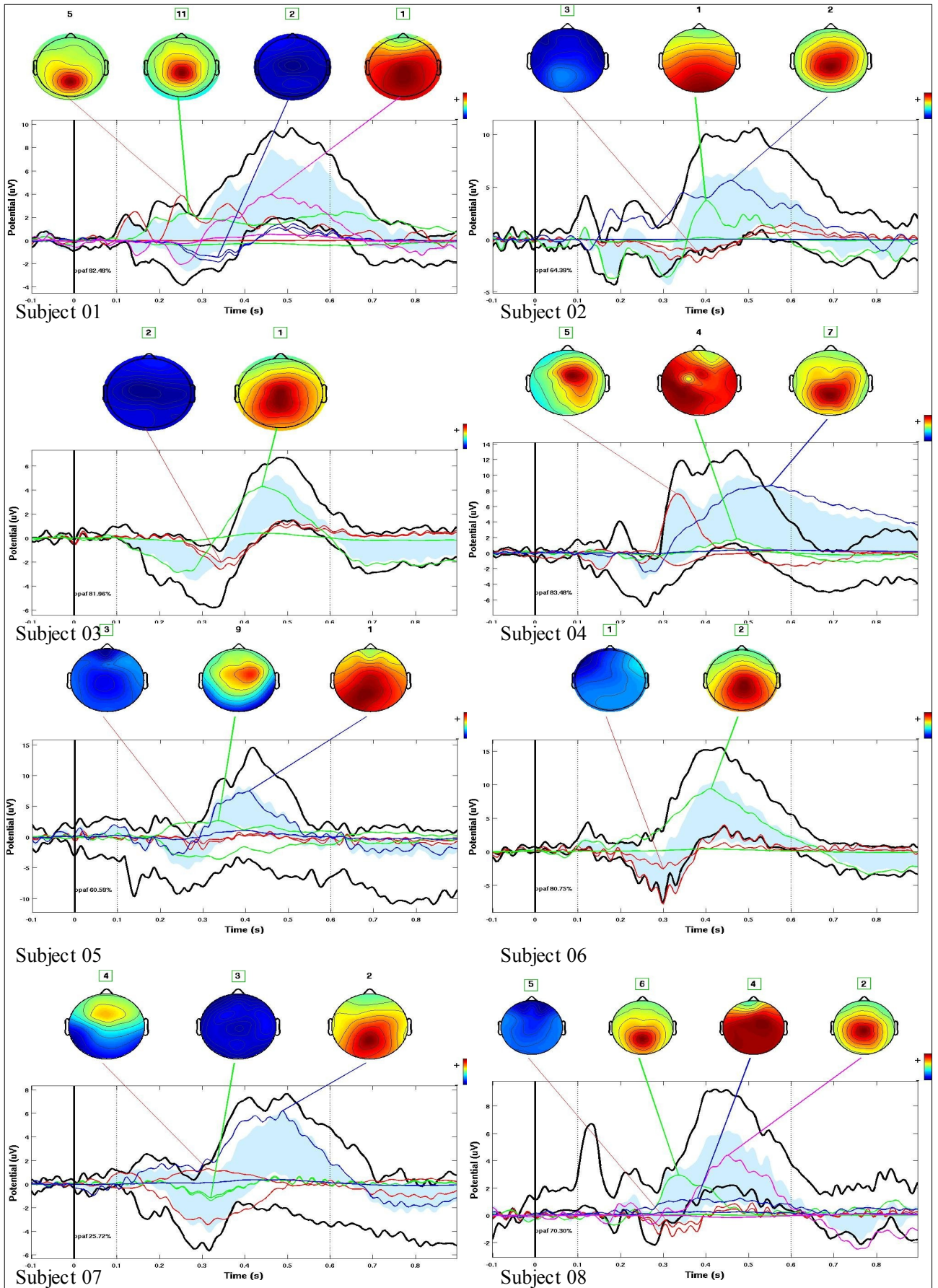


Figure 38: A selection of P3f, P3b and Pmp associated components of subject 01-08 using the epoch mean baseline with an EOG correction and 30 ch. Reliable ICs (green square) are highlighted. See text for details.

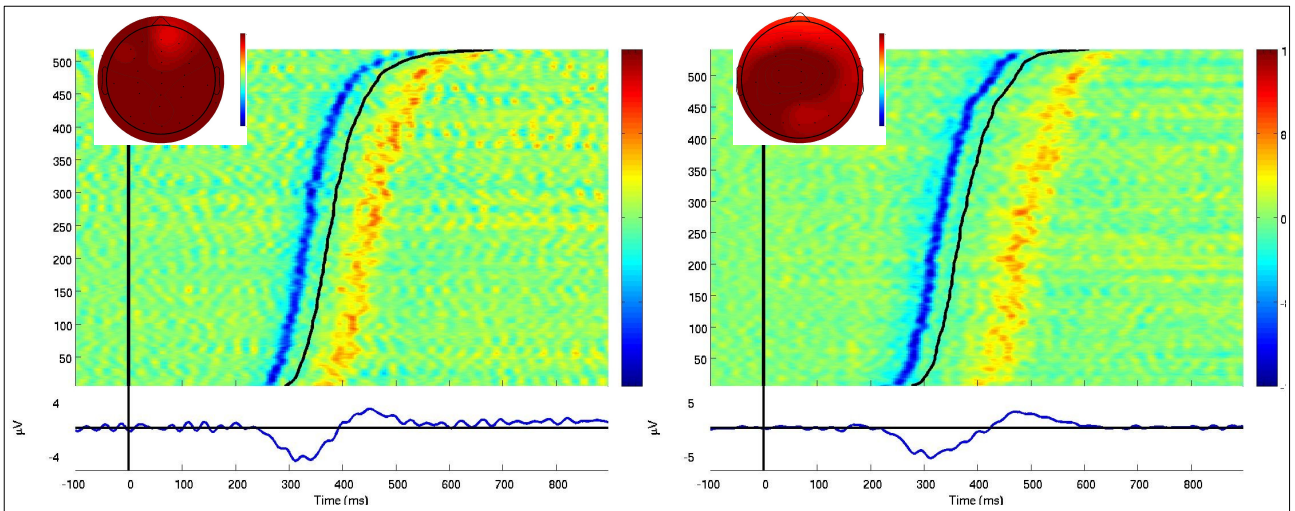


Figure 40: Subject 13, IC1 (left) and subject 15, IC2 (right) are associated with a Pmp: Scalp map and proj. of the IC to Pz with a stimulus locked ERP of all trials and 10 trials vertical smoothing window. See text for details.

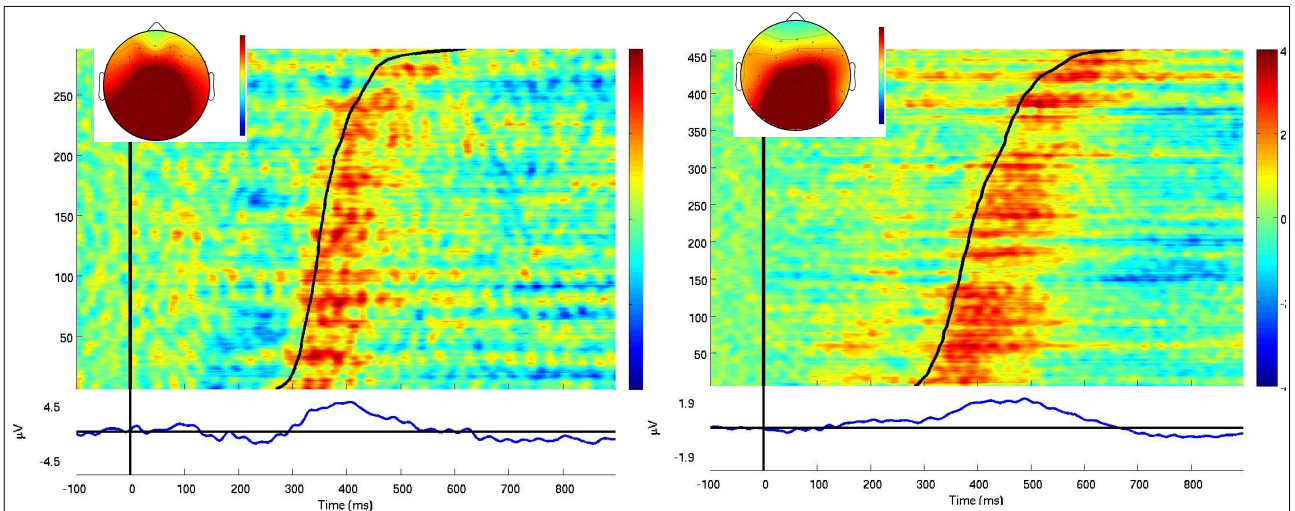


Figure 41: Subject 05, IC1 (left) and subject 07, IC2 (right) are associated with a P3b: Scalp map and proj. of the IC to Pz with a stimulus locked ERP of all trials and 10 trials vertical smoothing window. See text for details.

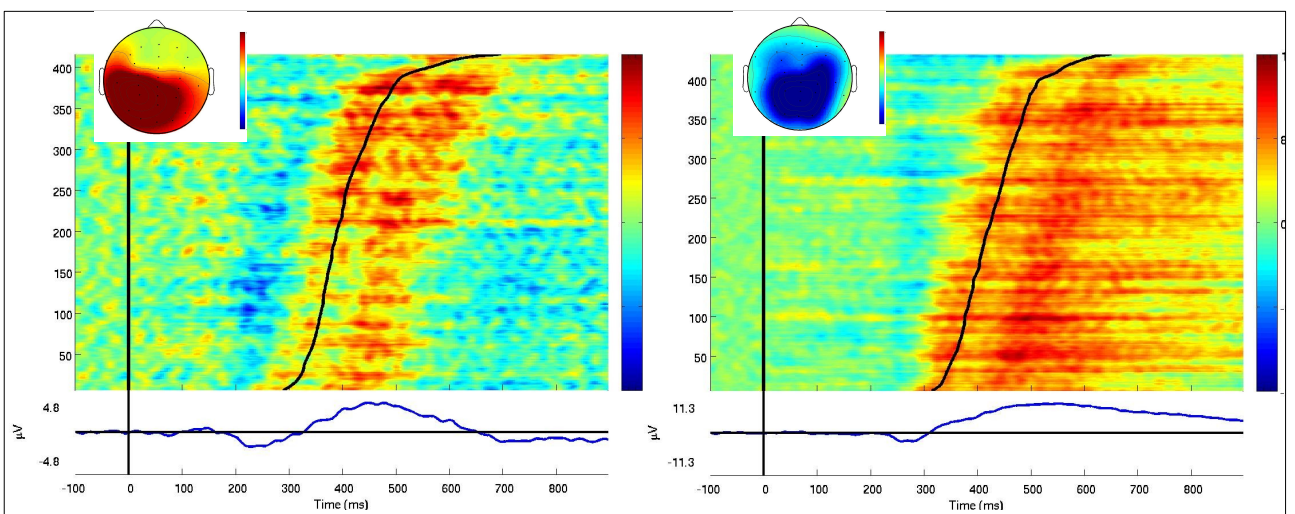


Figure 42: Subject 10, IC6 (left) and subject 04, IC7 (right) are associated with a P3b: Scalp map and proj. of the IC to Pz with a stimulus locked ERP of all trials and 10 trials vertical smoothing window. See text for details.

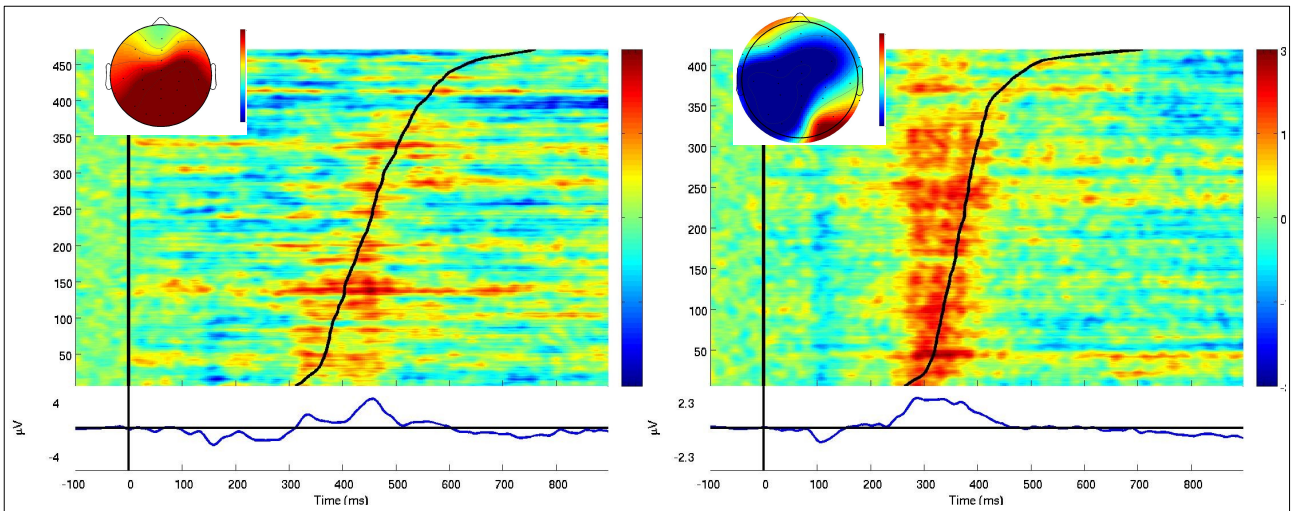


Figure 43: Subject 12, IC2 (left) and subject 14, IC9 (right) are associated with a P3b contaminated with an earlier positivity: Scalp map and proj. of the IC to Pz with a stimulus locked ERP of all trials and 10 trials vertical smoothing window. See text for details.

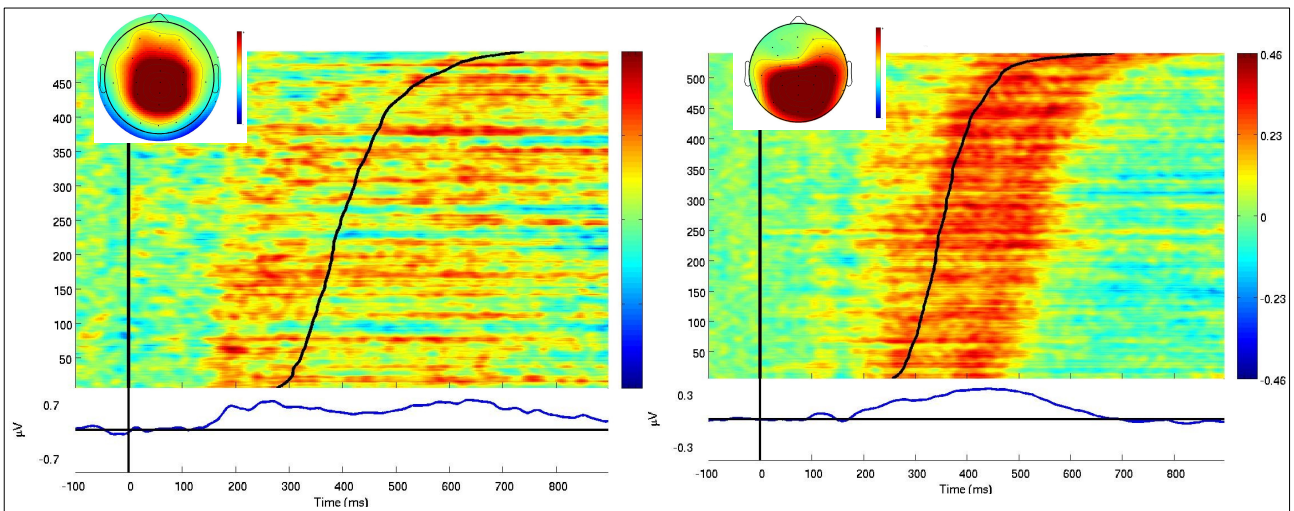


Figure 44: Subj. 01, IC11 (left) and subj. 09, IC6 (right) are associated with a P3b/P3f: Scalp map and proj. of the IC to Afz with a stim. locked ERP of all trials and 10 trials vertical smoothing window. See text for details.

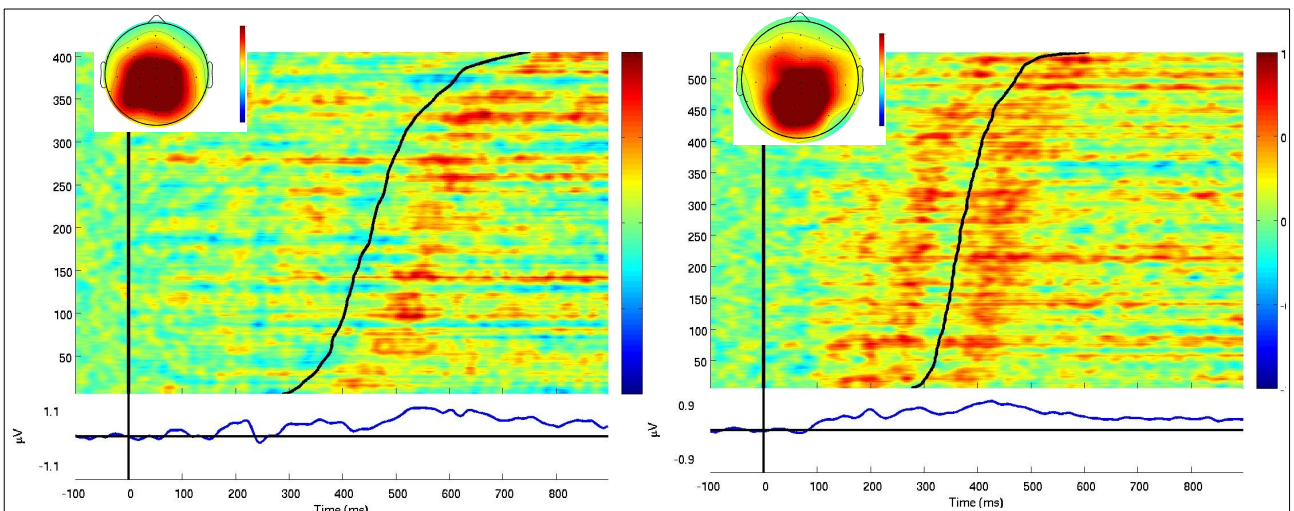


Figure 45: Subj. 11, IC3 (left) and subj. 15, IC4 (right) are associated with a P3b/P3f: Scalp map and proj. of the IC to Afz with a stim. locked ERP of all trials and 10 trials vertical smoothing window. See text for details.

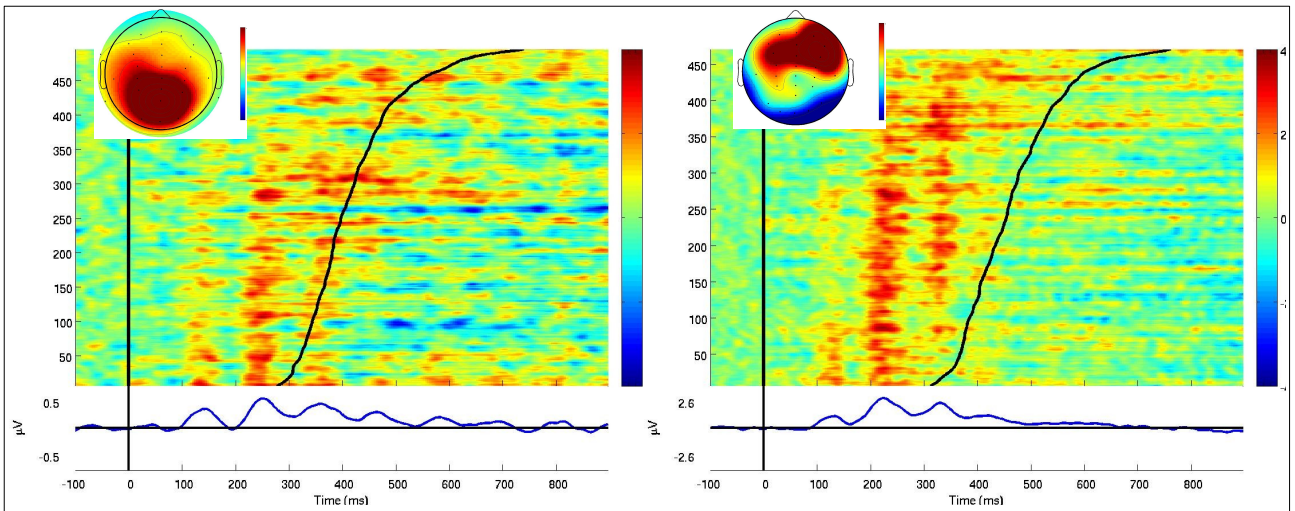


Figure 46: Subject 01, IC5 (left) and subject 12, IC13 (right) are associated with a P3f but contaminated with an earlier positivity: Scalp map and proj. of the IC to Afz with a stimulus locked ERP of all trials and 10 trials vertical smoothing window. See text for details.

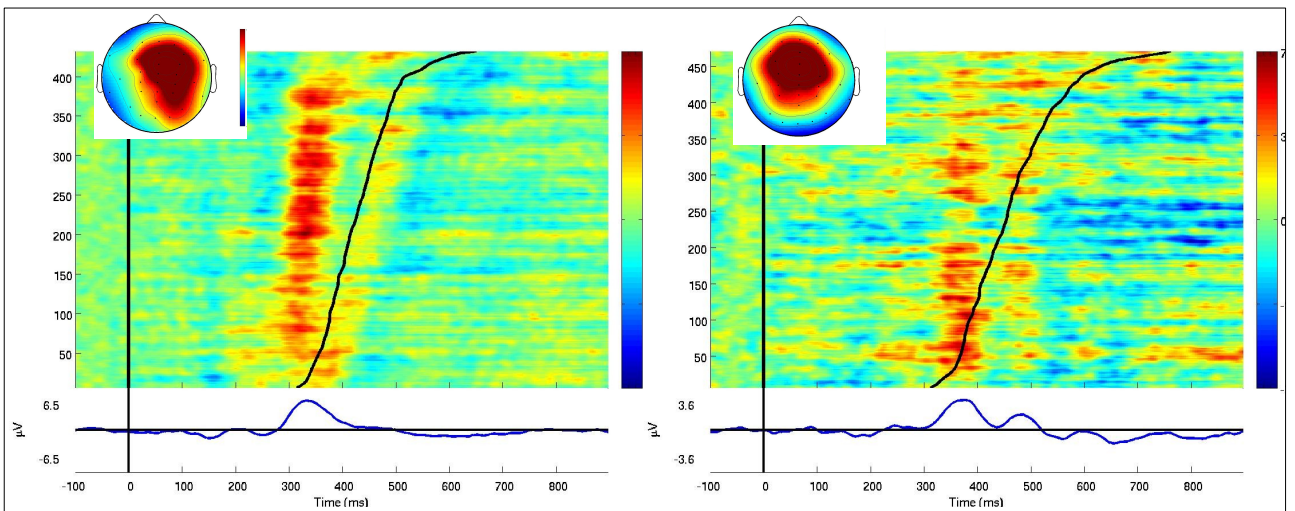


Figure 47: Subject 04, IC5 (left) and subject 12, IC6 (right) are associated with a P3f: Scalp map and proj. of the IC to Afz with a stim. locked ERP of all trials and 10 trials vertical smoothing window. See text for details.

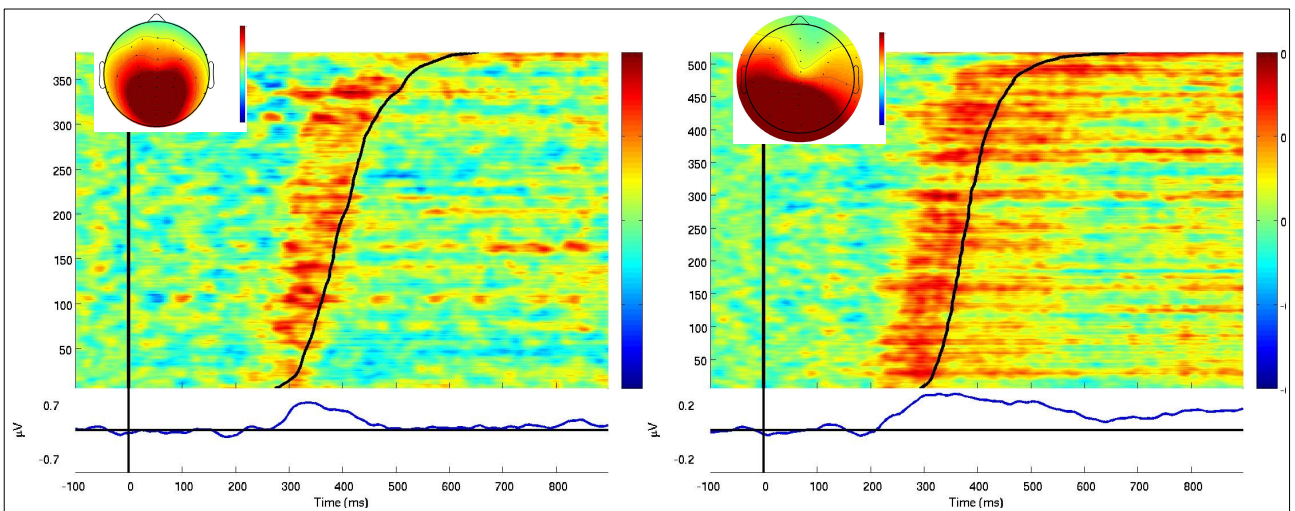


Figure 48: Subject 08, IC6 (left) and subject 13, IC8 (right) are associated with a P3f but with parietal positivity: Scalp map and projection of the IC to Afz with a stimulus locked ERP of all trials and 10 trials vertical smoothing window. See text for details.

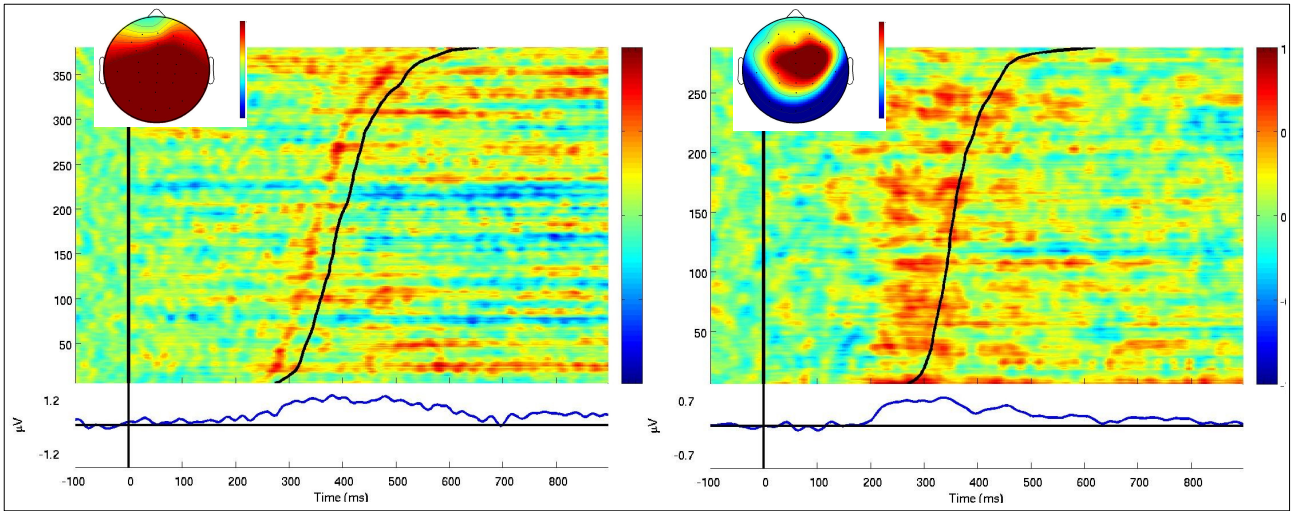


Figure 49: Subject 08, IC4 (left) and subject 5, IC9 (right) are associated with a P3f: Scalp map and projection of the IC to Afz with a stim. locked ERP of all trials and 10 trials vertical smoothing window. See text for details.

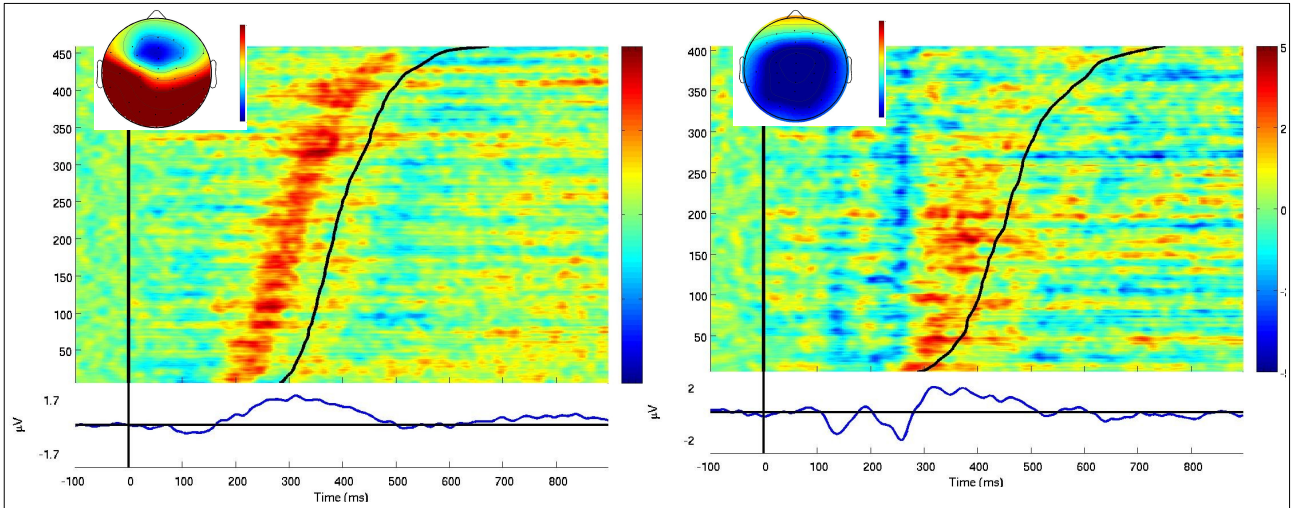


Figure 50: Subject 07, IC4 (left) and subject 11, IC2 (right) are associated with a P3f: Scalp map and projection of the IC to Afz with a stim. locked ERP of all trials and 10 trials vertical smoothing window. See text for details.

6.5 Preprocessing Influence on Components

The following scalp maps of all ICs calculated for subjects 4 (figures 51-53) and 7 (figures 55-57) are suitable to illustrate content related differences due to different proceedings. The first approach skipped the EOG correction and used the epoch mean baseline correction method (figures 51, 55). The next two proceedings illustrate the influence of the prestimulus baseline correction method (figures 52, 56) and of skipping the baseline correction (figures 53, 57). The corresponding P3f candidates to the ICs 5 and 4 after the epoch mean correction method as discussed above are highlighted for all three proceedings when available. That example should demonstrate the

influence of these steps.

The plots related to subject 5 had an equivalent topographic distribution but one remarkable difference (figure 54). Applying the epoch mean baseline without EOG correction method, the same stimulus locked positivity appeared, but using the prestimulus baseline with EOG correction method the corresponding component showed a response locked positivity. For subject 7 also nearly equivalent P3f components were found (figure 58). The differences of the topographic distribution after skipping the EOG correction is possibly related to the more artifact contaminated trials. No equivalent IC was found when no baseline correction was done prior to the ICA calculation. The decomposition of all channels for subject 15 led to two distinct and consecutive components with a parietal topography (figure 59). Please use the appendix and the plots above (particularly figures 45, 47 and 50) as reference plots of the proceeding with 30 channels and an epoch mean with an EOG correction.

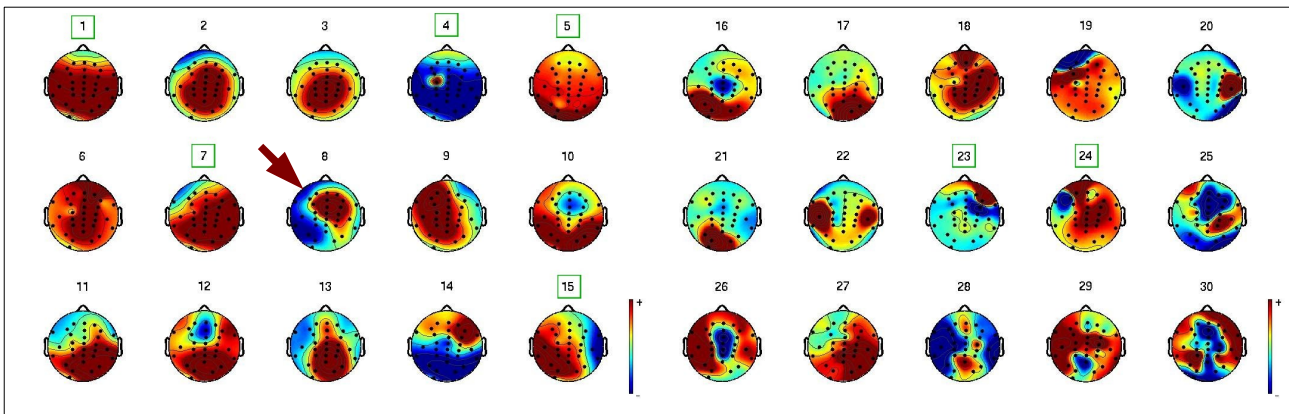


Figure 51: Scalp map of all 30 ICs of subject 04 with epoch mean but without EOG correction and 30 channels. The reliable ICs (green square) and the P3f candidate (red arrow) are highlighted. See text for details.

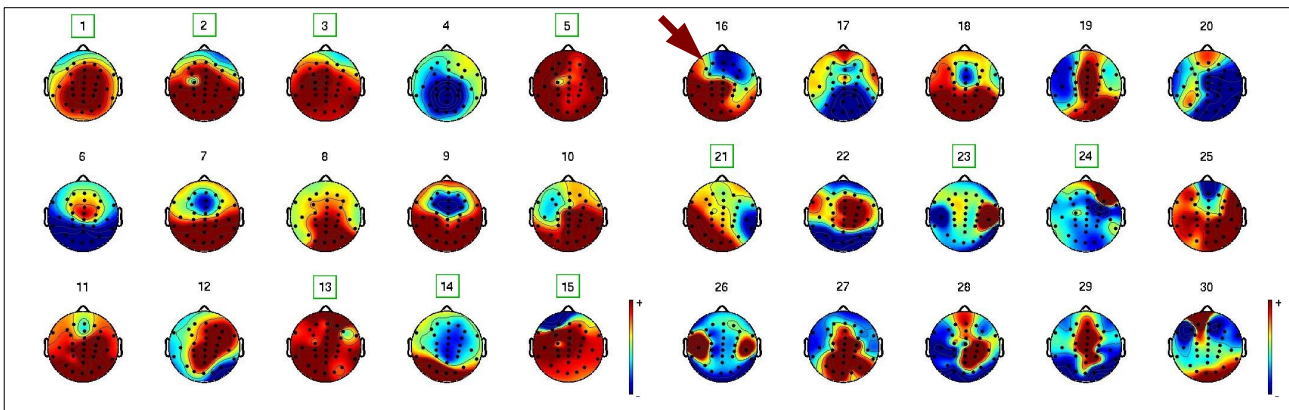


Figure 52: Scalp map of all 30 ICs of subject 04 with prestimulus baseline and EOG correction and 30 channels. The reliable ICs (green square) and the P3f candidate (red arrow) are highlighted. See text for details.

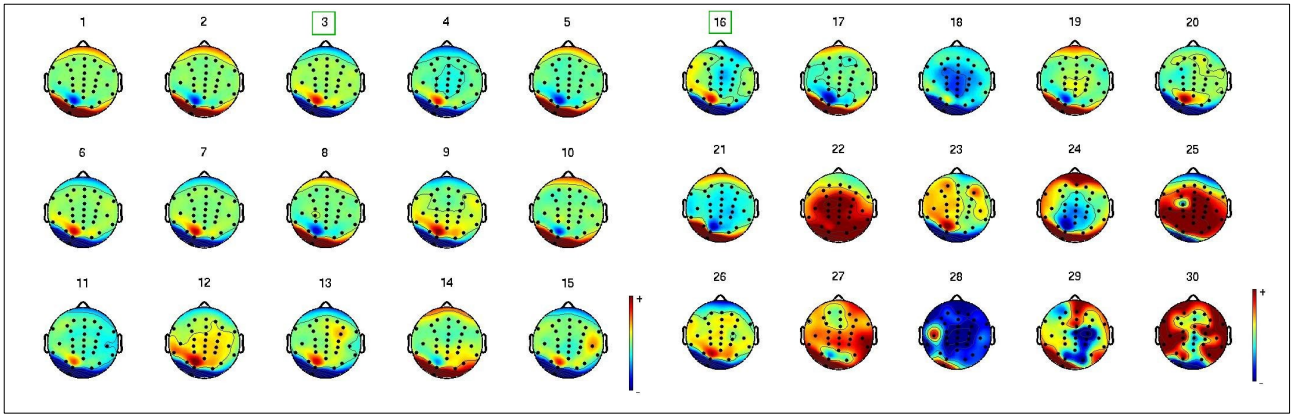


Figure 53: Scalp map of all 30 ICs of subject 04 without baseline but with EOG correction and 30 channels. The reliable ICs (green square) are highlighted. See text for details.

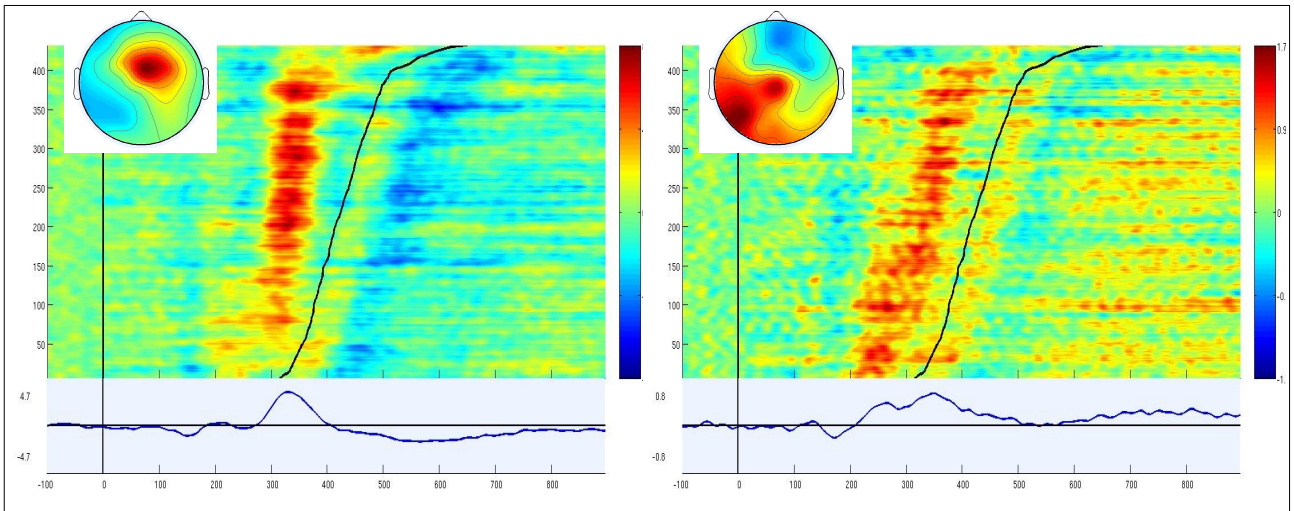


Figure 54: Subject 04, IC8 without EOG but with epoch mean baseline correction (left) and IC16 with EOG and prestimulus baseline correction (right). Both are associated with a P3f: Scalp map and projection of the IC to Afz with a stimulus locked ERP of all trials and 10 trials vertical smoothing window. See text for details.

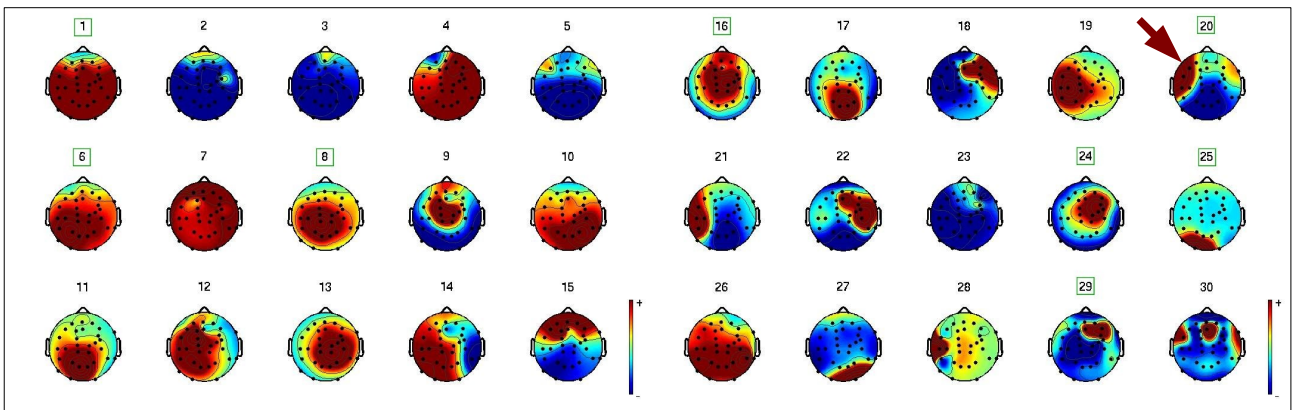


Figure 55: Scalp map of all 30 ICs of subject 07 with epoch mean but without EOG correction and 30 channels. The reliable ICs (green square) and the P3f candidate (red arrow) are highlighted. See text for details.

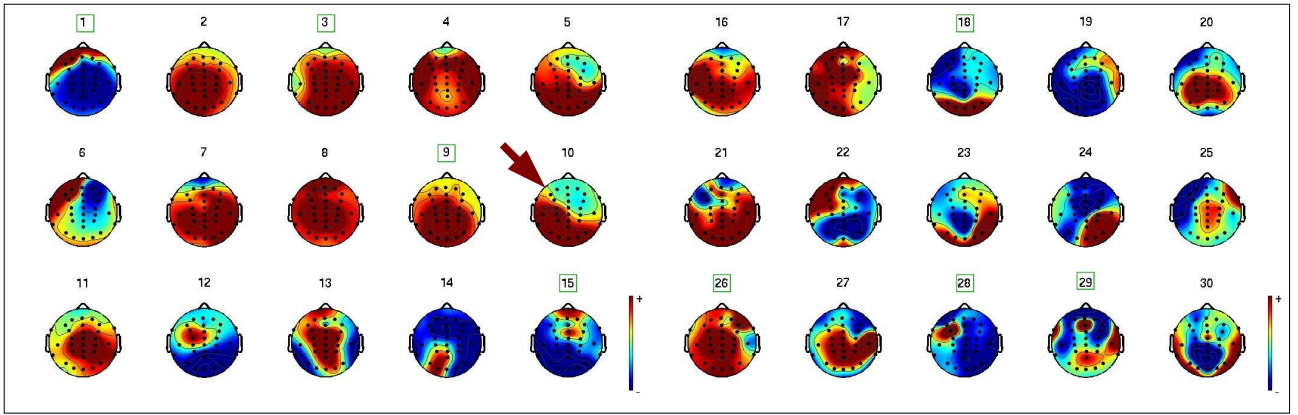


Figure 56: Scalp map of all 30 ICs of subject 07 with prestimulus baseline and EOG correction and 30 channels. The reliable ICs (green square) and the P3f candidate (red arrow) are highlighted. See text for details.

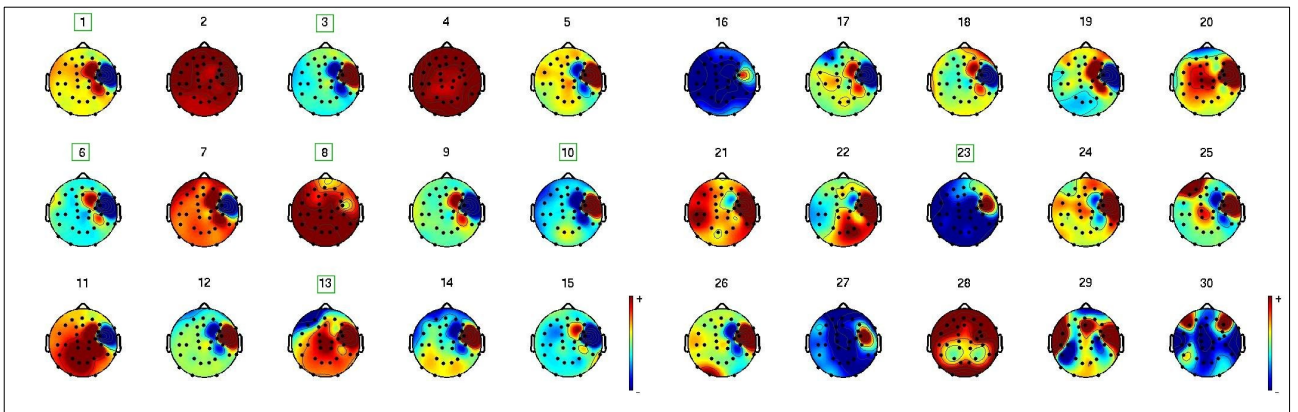


Figure 57: Scalp map of all 30 ICs of subject 07 without baseline but with EOG correction and 30 channels. The reliable ICs (green square) are highlighted. See text for details.

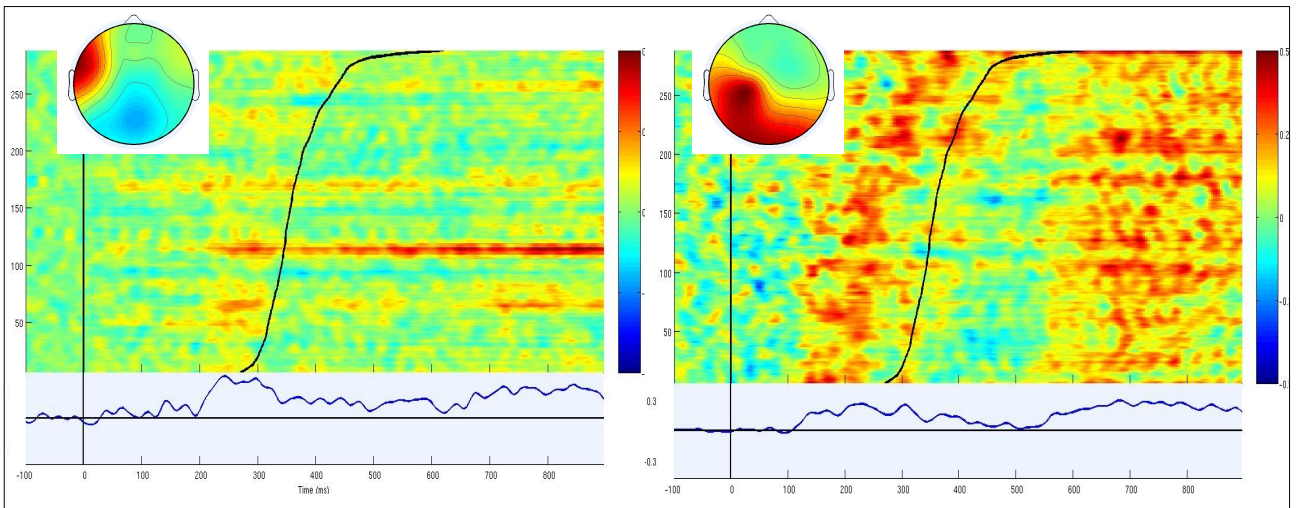


Figure 58: Subject 07, IC20 without EOG but with epoch mean baseline correction (left) and IC10 with EOG and prestimulus baseline correction (right). Both are associated with a P3f: Scalp map and projection of the IC to Afz with a stimulus locked ERP of all trials and 10 trials vertical smoothing window. See text for details.

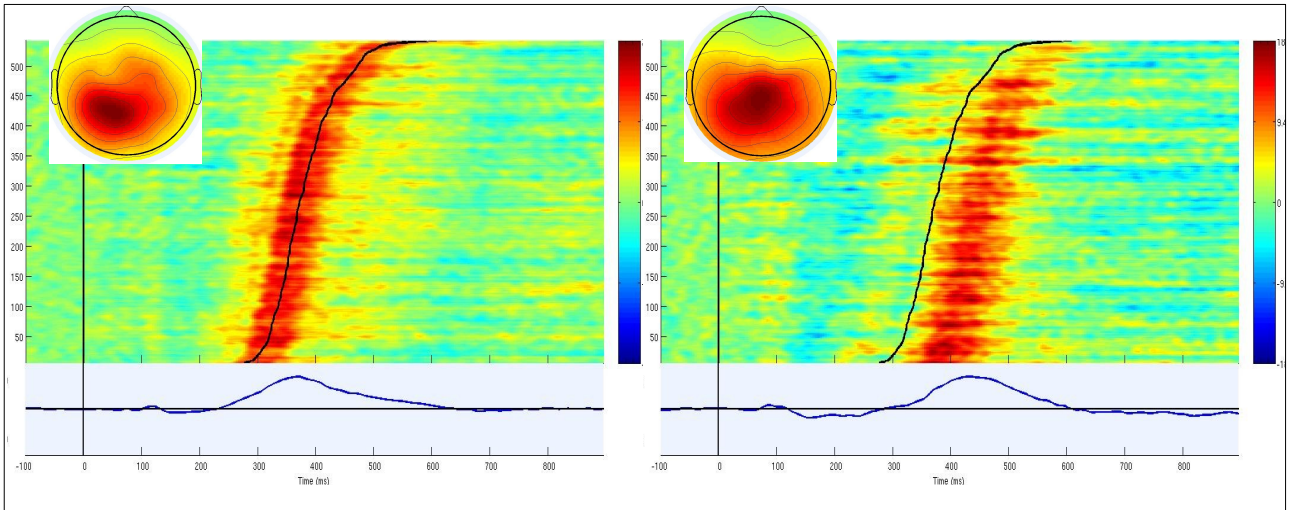


Figure 59: Subject 15, IC03 (left) and IC01 (right) using all 59 channels with an EOG and an epoch mean baseline correction. Both are topographically associated with a P3b: Scalp map and projection of the IC to Afz with a stimulus locked ERP of all trials and 10 trials vertical smoothing window. See text for details.

Discussion

The application of an ICA in the context of EEG research is a promising field not limited to the artifact rejection. Makeig et al. (1999b) successfully demonstrated the usability of this analytical approach on ERP data and confirmed the role of the Swartz Center / San Diego as major player within this field, as first done by Bell & Sejnowski (1995) by presenting the Infomax algorithm. The experiment replicated in this thesis focused on the P300 ERP evoked by a visual 'oddball' paradigm. The major advantages of this decision are the large amplitude of this ERP and the long research tradition on other phenomena also regarding the ICA. The ICs P3b and P3f firstly postulated by Makeig et al. (1999b) were not replicated in other locations with other subjects than the 22 participants of the recordings for the original datasets. To recognize the historical meaning of these findings in the context of the ICA application on ERP data, this experiment and the ICs P3b and P3f were first replicated for the empirical work of this thesis with other fifteen participants. These results will be discussed in the second part of this concluding chapter. To emphasize the methodical character of this thesis the first part is dedicated to the ongoing discussion of different preprocessing steps. Considering thirty years history of ICA application on neurophysiological data, no accepted guideline for necessary preprocessing steps is available. Groppe et al. (2009), also researching at the mentioned center, published an efficient way to assess the reliability of ICs. The results of implementing this algorithm in this thesis demonstrate a quality estimation in the context of ICA.

The initial question addressed to this assessment was which baseline correction method has the best outcome regarding the number of components assessed as reliable. Groppe et al. (2009) could show for data of four different experiments that removing the whole epoch mean led to better results than the traditional approach to remove the mean of the prestimulus baseline. Nonetheless, recent discussions from the protagonists of the same research group favor to skip any baseline correction prior to ICA calculations without offering any empirical evidence (EEGLABlist: <http://scn.ucsd.edu/pipermail/eeglablist/>, A quick question about baseline correction after ICA, [05.01.10]). The results of the same algorithm applied to the datasets of this replication experiment show that the epoch mean is significantly better than both other approaches for the 30 and the 58/59 channels setting (figure 31). That supports the published result to favor an epoch mean correction and provides an empirical evidence against skipping this step as recently recommended. All following calculations took these results into account by conducting an epoch mean correction. The

better results for the epoch mean correction in Groppe et al. (2009) were explained by two different theories. On the one hand, removing the mean of each epoch may work as leaky high-pass filter and the removed low frequency variance lead to more variable ICA solutions. On the other hand, possibly all baseline correction methods do affect ICA decompositions, but the epoch mean approach to a lesser extent. In this thesis no baseline correction was also worse than the epoch mean correction and therefore the latter answer is questionable. The results of this calculation would therefore support the high pass hypothesis. Additional content related comparison do not contradict this explanation as shown below.

According to Onton et al. (2006) a good quality ICA decompositions requires a minimum number of sampling points highly and nonlinearly dependent on the numbers of channels. As we have a similar number of trials for both settings, the reliability was expected to be better for less channels. The results show that these differences are significant but with respect to a significant interaction with the baseline correction method. That is mainly caused by the traditional prestimulus baseline correction method. If the best preprocessing proceeding, which is the epoch mean baseline correction method, is used, such differences disappear. In that case more channels led to a slightly larger proportion of reliable components. That is remarkable especially because conservative calculations regarding the minimum number of trials showed that for the 58/59 channels settings the criteria of minimum sampling points is violated when split half datasets are generated. Even subject five, with the lowest number of trials after artifact rejection, had a slightly larger proportion of reliable ICs. These results lead to the interpretation that this estimation of minimum sampling points could be to conservative. Results published by Groppe et al. (2009) could support the idea that the number of channels has tremendous influence due to the relative numbers of reliable components after the epoch mean correction method (up to more than 90 % for 30 channels; between 40 % and 50 % for 64 channels). A closer view shows that the 64 channels settings had a smaller number of trials (mean 643 and 844) than the 30 channels setting (mean 1641 and 1765). The results in this thesis were gathered with less trials (mean 459 and 451), likely explaining the smaller reliability value of about one third for the main epoch mean proceeding. These relatively low number of reliable ICs support the expectation to deal with a relatively conservative reliability assessment. Taking all this data into account, the proportion of reliable components is likely dependent on the number of sampling points irrespective to the number of channels considering the best baseline correction method. A review of the calculation suggested by Onton et al. (2006) with respect to empirical data considering reliability calculations and other quality criteria would be a contribution

to a reasonable ICA guideline.

The results of three extra proceedings calculated to control the influence of skipping an EOG correction and of an alternative artifact approach revealed that the number of ICs assessed as reliable was not dependent on these variables. This stable proportion of reliable ICs points out the influence of different baseline correction methods. The slightly larger value without EOG correction is possibly caused by more artifacts that are likely easier to recognize in both halves due to a very distinct appearance. This case supports the important role of the validity of resulting components. Even if skipping the EOG correction led to a slightly better reliability outcome, these results are obviously worse considering the content of these ICs as discussed next.

Due to the largest number of components assessed as reliable, the main epoch mean baseline correction was focused to prevent going astray seeing that 4783 full dataset components were calculated. The seven largest components of each subject contributing most strongly to the ERP period from 100 to 600 ms poststimulus were inspected regarding the P3b, P3f and Pmp components by using the theoretical background presented in the identification chapters above and in the five referenced papers (Makeig et al., 1999a; Makeig et al., 1999b; Jung et al., 2001b; Makeig et al., 2004; Delorme et al., 2007). Following Makeig et al. (1999a). The remaining 49 candidates are associated with at least one of these ICs and discussed as follows. Please note that that all P3f and P3b ICs were within the six largest components even for that early period used by Makeig et al. (1999a). Therefore missing one of these ICs is less probable after choosing seven components with respect to the major period. That it is also suggested by the variance information of most participants.

For each subject at least one Pmp equivalent and overall 16 ICs with these highly similar features were identified (figure 40). These components are all highly related to the button press with a negativity at the moment when the motor command is expected, considering a button travel time and a neuromuscular conduction time (Makeig et al., 2004, p. 750). Previous reports were constrained on the positivity posterior to the target response without mentioning the negativity matched with the name 'postmotor potential'.

For the 18 P3b candidates the variability was larger (figures 41-43). Considering the weak ICA solutions of subjects 12 and 14 (figure 43) the decomposition of each participant showed such positivity, explaining at least part of the variance with characteristics of interest. The mentioned topic of irregular P3b components is likely related to a very low amplitude of P300 ERPs for subjects 12 and 14 (figure 37). ICs of these subjects (figure 43) support this hypothesis as it contains some response locked positivity associated with a P3b contaminated with an earlier stimulus locked positivity not recognized in other ICs of this thesis. Please also note that subject 14 has a very low number of components assessed as reliable for the focused proceeding and that the proportion of reliable components of subject 12 is affected especially after a prestimulus baseline correction (table 5).

Some ICs are a composition of P3b and P3f characteristics with different weighting. These mixed components lead to the problem of incomplete decompositions for subjects 1, 9, 11 and 15 (figures 44 and 45). Obviously that is not related to the amount of clean data or to a lack of sampling points because subject 15 has the most data due to a low contamination with artifacts (table 3). Furthermore the number of reliable components was moderate respectively largest (50 %) in case of subject 1. For this subject the later positivity is likely related to another phenomenon than the P3b. This IC still indicates that some P3f activity could be covered by a larger positivity. Even though this P3f variance is quite low for subjects 9 and 11 it supports the possibility of relevant positivity in this time period. In the case of subjects 1 and 15 these activities are more distinct, nonetheless the topographic distribution (figures 44 and 45) would never lead to such findings. Therefore such a moving mean plot of single trials is much more powerful than a simple topographic comparison. Additional plots of candidates in a 58/59 channels setting (figure 59) supports an explanation via a phenomenon called underfitting (Brown et al., 2001) or in other terms overcompleteness (Mouraux & Jannetti, 2008). That means that 30 components are less than the learning algorithm would need to separate all major sources of subject 1. In case of 60 available components the separation was obviously successful even though the scalp map showed no expected frontal distribution. This effect and the opposite phenomenon of overfitting have to be considered for a reasonable interpretation of an ICA solution.

Considering all features of the reported P3f components, four ICs of subjects 5, 7, 8 and 11 (figures

49 and 50) meet these criteria at its best. Subject 8 (figure 48) has one additional component possibly covered by parietal activity. A posterior projection of a frontal source could be possible as well. In the case of subject 13 (figure 48) such an activation is the only P3f candidate. The decompositions of subjects 1 and 12 (figure 46) had one and two components respectively, contaminated with stimulus locked activity which possibly contain P3f variance. To prevent a false positive reporting these components are not further taken into account. In case of the also stimulus locked component of subject 4 (figure 47) a tendency towards being response locked was recognized. A comparison with a prestimulus baseline correction showed that the corresponding IC was clearly response locked (figure 54). The reason for this difference is unknown. Nonetheless we can assume that this component is associated with the P3f phenomenon, especially because reports of Delorme et al. (2007, p. 11952) revealed that P3f trials are not always strictly response locked. For this analysis inter trial coherence calculations were conducted to remove trials with a stimulus locked P3f.

According to the decisions above, P3f components were found for five subjects (4, 5, 7, 8 and 11) with a distinct positivity and for nine subjects if a contamination with P3b or another parietal positivity is accepted (also 1, 9, 13, and 15). Please note that the original papers reported different subsets of experiments with 22 plus two subjects. Makeig et al. (1999b) reported P3b components for all of their ten participants and seven P3f components. Later, Makeig et al. (2004) clustered ten P3f components from fifteen subjects and fifteen P3b components from nine subjects. Due to no information about these selections no comparison regarding the representativeness of both results is possible. Therefore the number of ICs found in the decomposition of this thesis equates to former results also considering all incomplete separations.

Finally the comparison of two subjects (figures 51-58) showed that the conducted EOG correction has no remarkable impact, neither on the proportion of reliable ICs nor on the content, except for the reduction of artifacts. Both P3f components were similar without EOG correction. For the traditional approach of a prestimulus baseline removal both results could be replicated even though the stimulus locked tendency of IC5 for subject 4 changed to a response locked character. The late positive shifting of the ICs of both subjects for this proceeding (figures 54 and 58) compared with the epoch mean correction method (figures 47 and 50) likely demonstrates the high pass filter effect. Maybe the same effect led to the stimulus locked character of the P3f for subject 4 as well.

Calculations without baseline correction lead to a low number of reliable components and a rather low validity. Most related plots were not interpretable as the selected scalp maps show (figures 53 and 57). Furthermore no corresponding ICs could be found after this proceeding. Therefore, this work provides an empirical evidence against skipping this baseline correction and to favor an epoch mean baseline correction considering reliability and also validity of calculated components.

References:

- Anemüller, J., Sejnowski, T. J. & Makeig, S. (2003). Complex independent component analysis of frequency-domain electroencephalographic data. *Neural Networks*, 16, 1311-1323.
- Bauer, H. , Lamm, C., Holzreiter, I., Holländer, U., Leodolter, M. & Leodolter, U. (2000). Measurement of 3D electrode coordinates by means of a 3D photogrammetric head digitizer. *NeuroImage*, 11, 461.
- Bauer, H. & Lauber, W. (1979). Operant conditioning of brain steady potential shifts in man. *Biofeedback and Self Regulation*, 4, 145-154.
- Bell, A. J. & Sejnowski, T. J. (1995). An Information-Maximization Approach to Blind Separation and Blind Deconvolution. *Neural Computation*, 7, 1129-1159.
- Brown, G. D., Yamada, S. & Sejnowski, T. J. (2001). Independent component analysis at the neuronal cocktail party. *TRENDS in Neuroscience*, 24 (1), 54-63.
- Cardoso, J. F. (1989). Blind identification of independent components with higher-order statistics. In Nikias, C. L. & Mendel J. M. (Ed.), *Workshop on Higher-Order Spectral Analysis*. (pp. 157-162). New York: IEEE.
- Cardoso, J. F. & Soudoumiac, A. (1993). Blind beamforming for non-Gaussian signals. *IEEE Proceedings-F*, 140 (7), 362-370.
- Common, P. (1989). Separation of stochastic processes. In Nikias, C. L. & Mendel J. M. (Ed.), *Workshop on Higher-Order Spectral Analysis*. (pp. 174-179). New York: IEEE.
- Delorme, A. & Makeig, S. (2004). EEGLAB: an open source toolbox for analysis of single-trial EEG dynamics including independent component analysis. *Journal of Neuroscience Methods*, 134, 9-21.
- Delorme, A., Westerfield, M. & Makeig, S. (2007). Medial Prefrontal Theta Bursts Precede Rapid Motor Responses during Visual Selective Attention. *The Journal of Neuroscience*, 27 (44), 11949-11959.
- Engeloff, S. (1999). Moving ICA and Time-Frequency Analysis in Event-Related EEG Studies of Selective Attention. Unpubl. thesis, Technical University of Denmark & Salk Institute for Biological Studies.
- Fischmeister, F. P. & Bauer, H. (2006). Neural correlates of monocular and binocular depth cues based on natural images: a LORETA analysis. *Vision Research*, 46, 3373-3380.
- Gao, J. F., Yang, Y., Lin, P., Wang, P. & Zheng, Ch.X. (2010). Automatic Removal of Eye-Movement and Blink Artifacts from EEG Signals. *Brain Topography*, 23, (1), 105-114.
- Groppe, D. M., Makeig, S., & Kutas, K. (2009). Identifying reliable independent components via split-half comparisons. *NeuroImage*, 45, 1199-1211.
- Harmeling, S., Meinecke, F. & Müller, K-R. (2004). Injecting for analysing the stability of ICA components. *Signal Processing*, 84, 255-266.

- Himberg, J., Hyvärinen, A. & Esposito, F. (2004). Validating the independent components of neuroimaging time series via clustering and visualization. *NeuroImage*, 22, 1214-1222.
- Hyvärinen, A. & Oja, E. (2000). Independent Component Analysis: Algorithms and Applications. *Neural Networks*, 13 (4-5), 411-430.
- Hyvärinen, A., Karhunen, J. & Oja, E. (2001). *Independent Component Analysis*. New York: John Wiley & Sons.
- Jung, T-P., Humphries, C., Lee, T-W., Makeig, S., McKeown, M. J., Iragui, V. & Sejnowski, T. J. (1998). Extended ICA Removes Artifacts from Electroencephalographic Recordings. *Advances in Neural Information Processing Systems*, 10, 894-900.
- Jung, T-P., Makeig, S., Westerfield, M., Townsend, J., Courchesne, E. & Sejnowski, T. J. (2000a). Removal of eye artifacts from visual event-related potentials in normal and clinical subjects. *Clinical Neurophysiology*, 111, 1745-1758.
- Jung, T-P., Makeig, S., Humphries, C., Lee, T-W., McKeown, M. J., Iragui, V. & Sejnowski, T. J. (2000b). Removing electroencephalographic artifacts by blind source separation. *Psychophysiology*, 37, 163-178.
- Jung, T-P., Makeig, S., McKeown, M. J., Bell, A. J., Lee, T-W. & Sejnowski, T. J. (2001a) Imaging Brain Dynamics Using Independent Component Analysis. *Proceedings of the IEEE*, 89 (7), 1107-1122.
- Jung, T-P., Makeig, S., Westerfield, M., Townsend, J., Courchesne, E. & Sejnowski, T. J. (2001b). Analysis and Visualization of Single-Trial Event-Related Potentials. *Human Brain Mapping*, 14, 166-185.
- Kubinger, K. D. (2006). *Psychologische Diagnostik. Theorie und Praxis psychologischen Diagnostizierens*. Göttingen: Hogrefe.
- Lamm, C., Fischmeister, F. P. & Bauer, H. (2005). Individual differences in brain activity during visuo-spatial processing assessed by slow cortical potentials and LORETA. *Cognitive Brain Research*, 25, 900-912.
- Li, R. & Principe, J. C. (2006). Blinking Artifact Removal in Cognitive EEG Data Using ICA. *Conference Proceedings Eng. IEEE Med. Biol. Soc.*, 28, 5273-5276.
- Makeig, S., Bell, A. J., Jung, T-P. & Sejnowski, T. J. (1996). Independent Component Analysis of Electroencephalographic Data. In D. Touretzky, M. Mozer & M. Hasselmo (Eds.), *Advances in Neural Information Processing Systems* (Vol. 8) (p. 145-151). Cambridge: MIT Press.
- Makeig, S., Delorme, A., Westerfield, M., Jung, T-P., Townsend, J. Courchesne, E. & Sejnowski, T. J. (2004). Electroencephalographic Brain Dynamics Following Manually Responded Visual Targets. *PloS Biology*, 2, 747-762.
- Makeig, S., Jung, T-P., Bell, A. J., Ghahremani, D. & Sejnowski, T. J. (1997). Blind separation of auditory event-related brain responses into independent components. *Proc. Natl. Acad. Sci. USA*, 94, 10979-10984.

- Makeig, S., Westerfield, M., Townsend, J., Jung, T-P., Courchesne, E. & Sejnowski, T. J. (1999a). Functionally independent components of early event-related potentials in a visual spatial attention task. *Philos Trans Royal Society Lond. B*, 354, 1135-1144.,
- Makeig, S., Westerfield, M., Jung, T-P., Convington, J., Townsend, J., Sejnowski, T. J. & Courchesne, E. (1999b). Functionally Independent Components of the Late Positive Event-Related Potential during Visual Spatial Attention. *The Journal of Neuroscience*, 19 (7), 2665-2680.
- Makeig, S., Westerfield, M., Jung, T-P., Enghoff, S., Townsend, J., Courchesne, E. & Sejnowski, T. J. (2002). Dynamic Brain Sources of Visual Evoked Responses. *Science*, 295, 690-694.
- Meinecke, F., Ziehe, A., Kawanabe, M. & Müller, K-R. (2002). A Resampling Approach to Estimate the Stability of One-Dimensional of Multidimensional Independent Components. *IEEE Transactions on Biomedical Engineering*, 49, 1514-1525.
- Mouraux, A. & Iannetti, G. D. (2008). Accross-trial averaging of event-related EEG responses and beyond. *Magnetic Resonance Imaging*, 26, 1046-1054.
- Nadal, J-P. & Parga, N. (1994). Non linear neurons in the low noise limit: a factorial code maximizes information transfer. *Network*, 5, 565-581.
- Oldfield, R. C. (1971). The assessmend and analysis of handedness: the Edinburgh Inventory. *Neuropsychologia*, 9, 97-113
- Onton, J., Westerfield, M., Townsend, J. & Makeig, S. (2006). Imaging human EEG dynamics using independent component analysis. *Neuroscience and Biobehavioral Reviews*, 30, 808-822.
- Pascual-Marqui, R. D., Michel, Ch. M. & Lehmann, D. (1994). Low Resolution Electromagnetic Tomography: A New Method for Localizing Electrical Activity in the Brain. *International Journal of Psychophysiology*, 18, 49-65.
- Picton, T. W. & Hillyard, S. A. (1972). Cephalic skin potentials in electroencephalography. *Electroencephalography and Clinical Neurophysiology*, 33, 419-424.
- Polich, J. (2007). Updating P300: An Integrative Theory of P3a and P3b. *Clinical Neurophysiology*, 118 (10), 2128-2148.
- Polich, J. & Criado, J. R. (2006). Neuropsychology and neuropharmacology of P3a and P3b. *International Journal of Psychophysiology*. 60, 172-185.
- Potts, G. F. (2004). An ERP index of task relevance evaluation of visual stimuli. *Brain and Cognition*, 56, 5-13.
- Scherg, M. (1990). Brain electric source analysis: the importance of physiological constraints. *Brain Topography*, 3, 268 – 269.

- Stephenson, W. & Gibbs, F. A. (1951). A balanced non-cephalic reference electrode. *Electroencephalography and Clinical Neurophysiology*, 3, 237-240. John Wiley & Sons.
- Stone, J. V. (2005). Independent Component Analysis. In B. S. Everitt & D. C. Howell (Eds.), *Encyclopedia of Statistics in Behavioral Science*. (Vol. 2) (p. 907-912). Chichester: MIT Press.
- Townsend, J. & Courchesne, E. (1994). Parietal damage and narrow „spotlight“ spatial attention. *Journal of Cognitive Neuroscience*, 6, 220-232.
- Townsend, J., Harris, N. S. & Courchesne, E. (1996). Visual attention abnormalities in autism: delayed orienting to location. *Journal of the International Neuropsychological Society*, 2, 541-550.
- Viola, F. C., Thorne, J., Edmonds, B., Schneider, T., Eichele, T. & Debener, S. (2009). Semi-automatic identification of independent components representing EEG artifact. *Clinical Neurophysiology*, 120 (5), 868-877.
- Vitouch, O., Bauer, H., Gittler, G., Leodolter, M. & Leodolter, U. (1997). Cortical activity of good and poor spatial test performers during spatial and verbal processing studied with Slow Potential Topography. *International Journal Psychophysiology*, 27, 183-199.
- Volpe, U., Mucci, A., Bucci, P., Merlotti, E., Galderisi, S. & Maj, M. (2007). The cortical generators of P3a and P3b: A LORETA study. *Brain Research Bulletin*, 73, 220-230.

References Online:

- EASYCAP GmbH: <http://www.easycap.de/>, [last 26.03.10]
- EEGLAB: <http://scn.ucsd.edu/eeglab/>, [last 26.03.10]
- EEGLAB Toolbox Download: <http://scn.ucsd.edu/eeglab/downloadtoolbox.html/>, [last 26.03.10]
- EEGLAB Tutorial: http://scn.ucsd.edu/wiki/EEGLAB_TUTORIAL_OUTLINE/, [last 26.03.10]
- EEGLABlist: <http://scn.ucsd.edu/pipermail/eeglablist/>, Interpolation and ICA, [04.-05.01.10]
- EEGLABlist: <http://scn.ucsd.edu/pipermail/eeglablist/>, A quick question about baseline correction after ICA, [05.01.10]
- Electro-Cap International, Inc., Eaton/OH, USA: <http://www.electro-cap.com/>, [last 26.03.10]
- Psychology Software Tools, Inc.: <http://www.pstnet.com/eprime.cfm/>, [last 26.03.10]
- The MathWorks: <http://www.mathworks.com/>, [last 26.03.10]

Appendix

Screenshots of Instruction



Figure A1: Screenshot of the instruction on page one explaining the general setting (first example), to rapidly respond in target trials (second example) and to skip answers in non-target trials (third example).

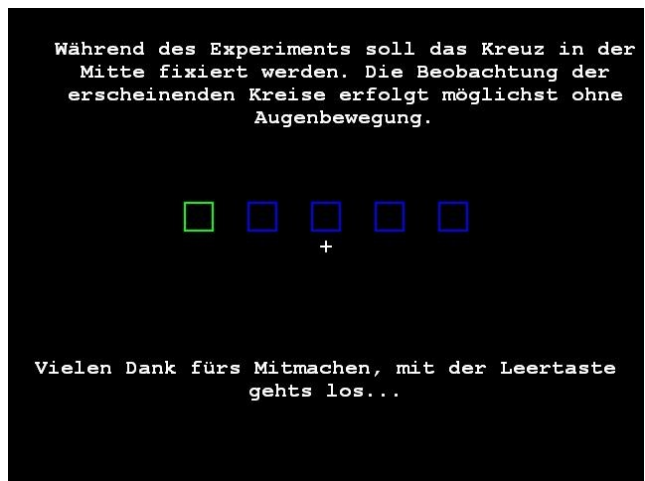


Figure A2: Screenshot of the instruction on page two explaining the fixation cross and the setting of all five boxes as they are on screen during the experiment.

Screenshot of Pause between Blocks

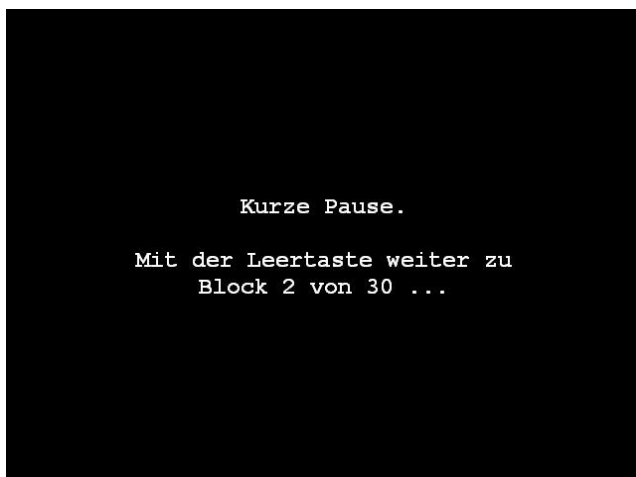


Figure A3: Screenshot of the pause including a status information and additionally offering the self paced proceeding.

Scalp Maps of all Components and Reliability Information

(following pages ...)

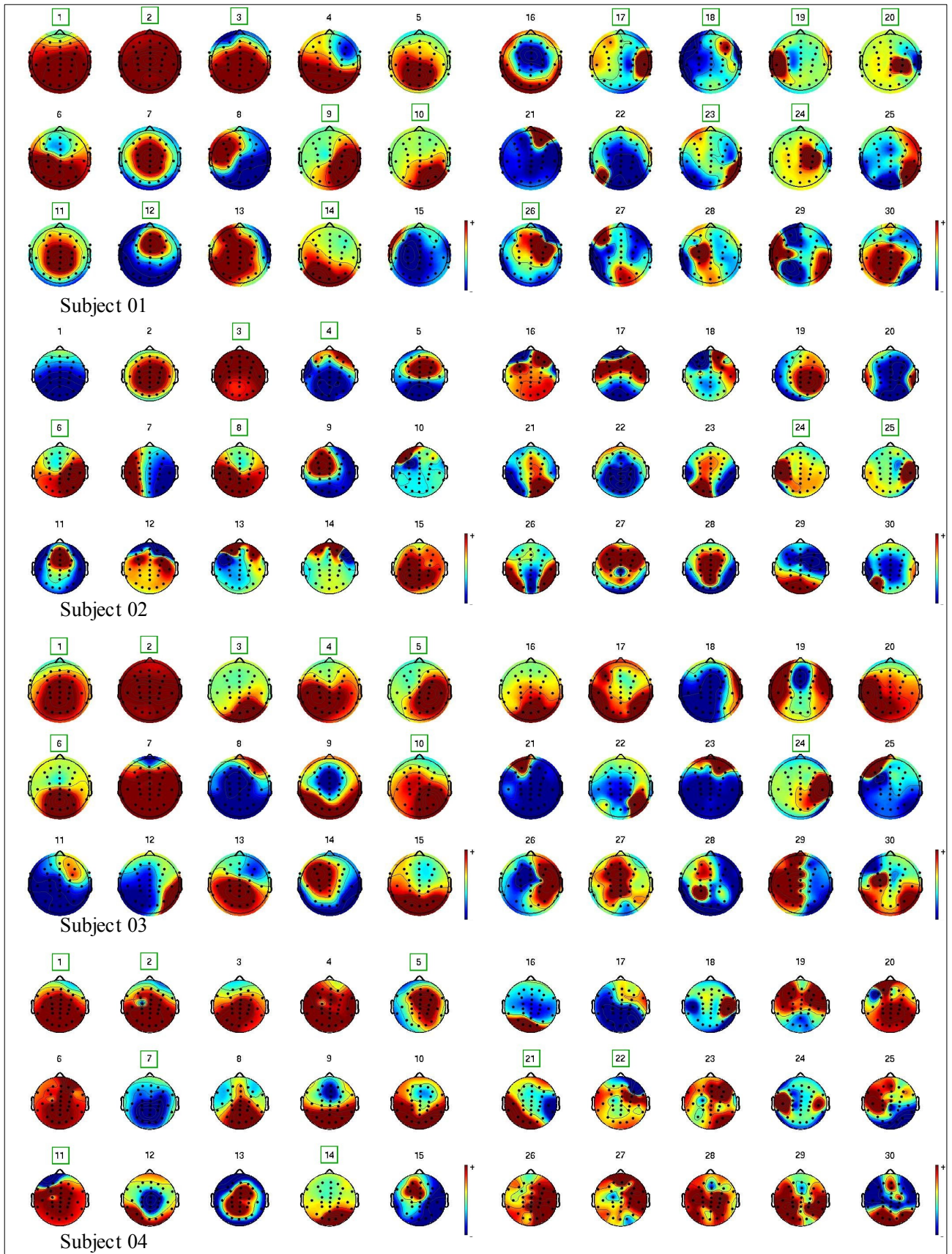


Figure A4: The scalp map of all 30 components of subject 01-05 after using the epoch mean with EOG correction and 30 channels. ICs assessed as reliable are highlighted (green square). See text for details.

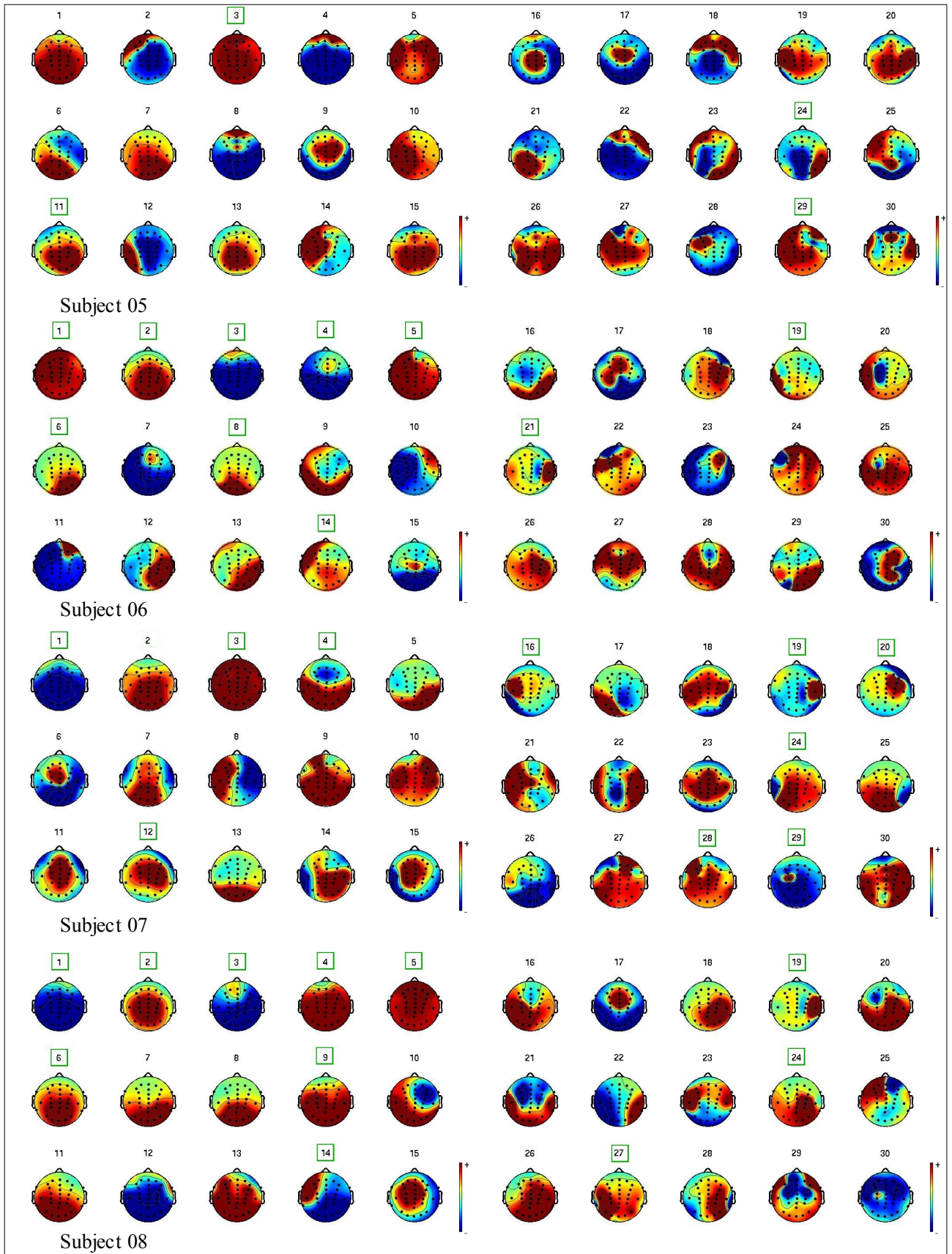


Figure A5: The scalp map of all 30 components of subject 05-08 after using the epoch mean with EOG correction and 30 channels. ICs assessed as reliable are highlighted (green square). See text for details.

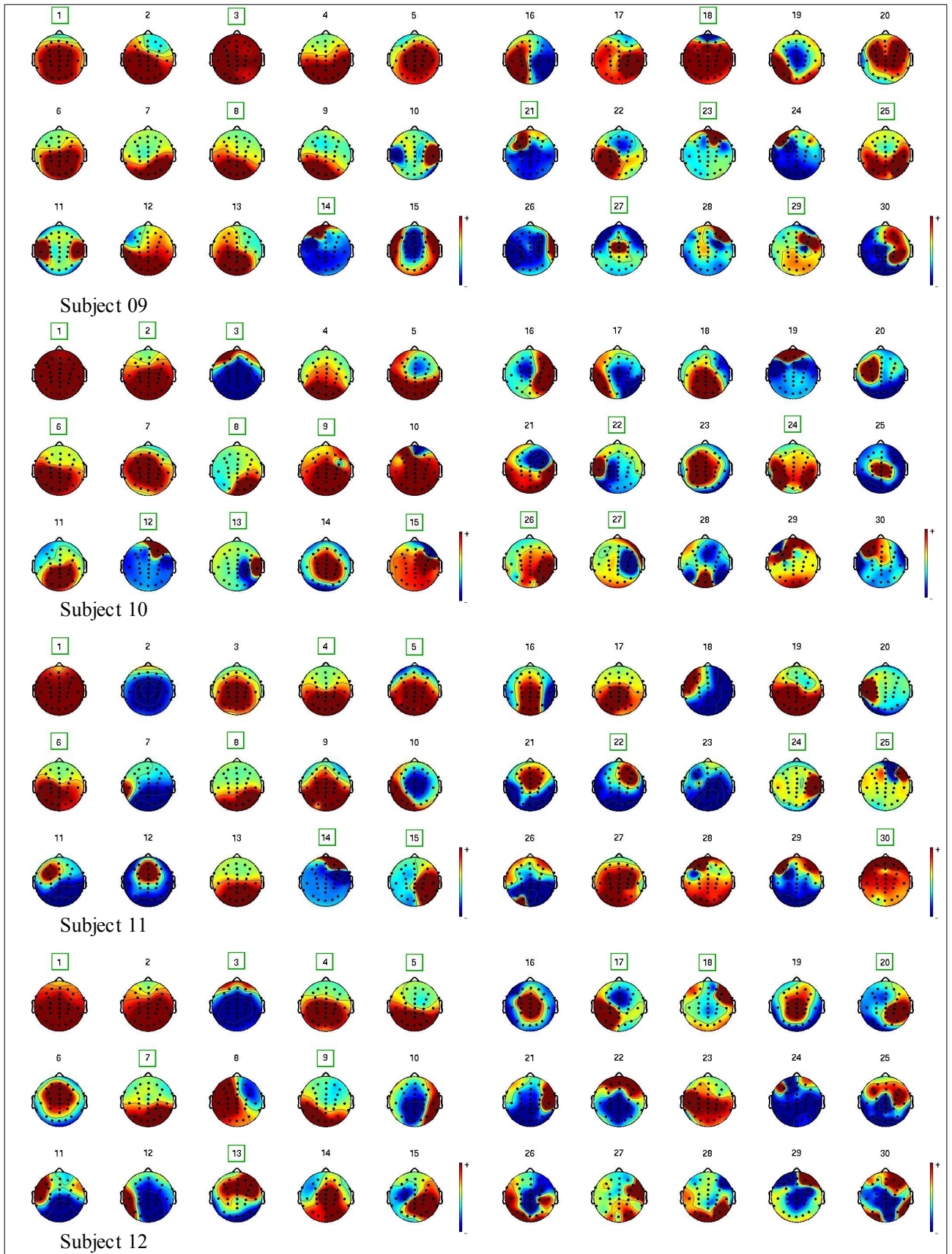


Figure A6: The scalp map of all 30 components of subject 09-12 after using the epoch mean with EOG correction and 30 channels. ICs assessed as reliable are highlighted (green square). See text for details.

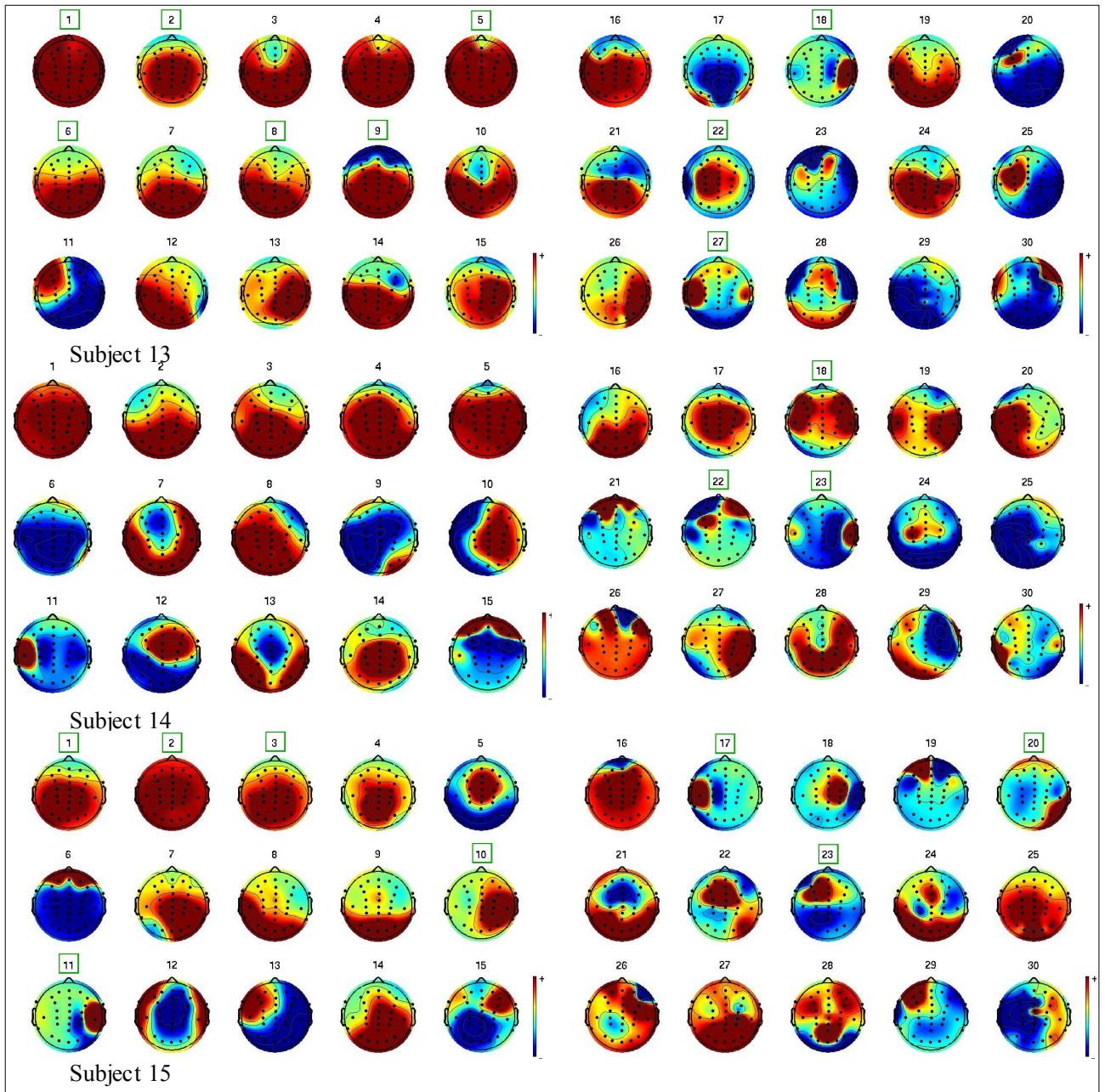


Figure A7: The scalp map of all 30 components of subject 13-15 after using the epoch mean with EOG correction and 30 channels. ICs assessed as reliable are highlighted (green square). See text for details.

'L'-shaped Critical Regions for nine Proceedings

All 'L'-shaped critical regions contain 1 / components of the total sample and reflects the distribution of calculated distances using topography and activity information. ICs with distances between each full dataset and both paired halves within that area are assessed as reliable. See text above for details especially the introduction of this algorithm. Regarding all nine proceedings see the overview in chapter 5.4.

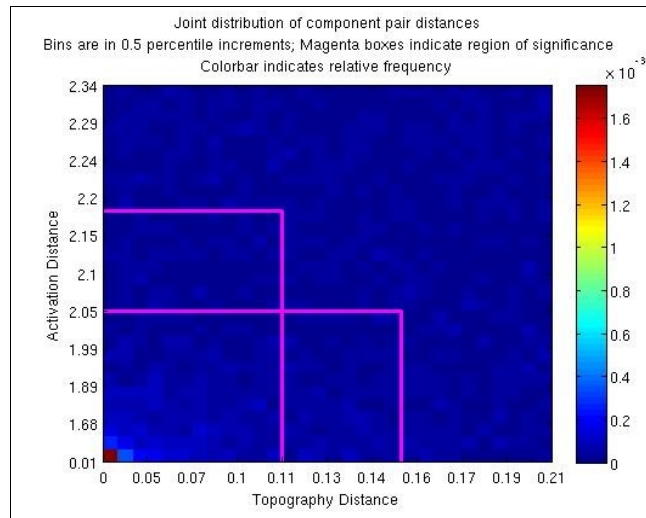


Figure A8: L-shaped critical region for 58/59 channels and prestimulus baseline condition with EOG correction

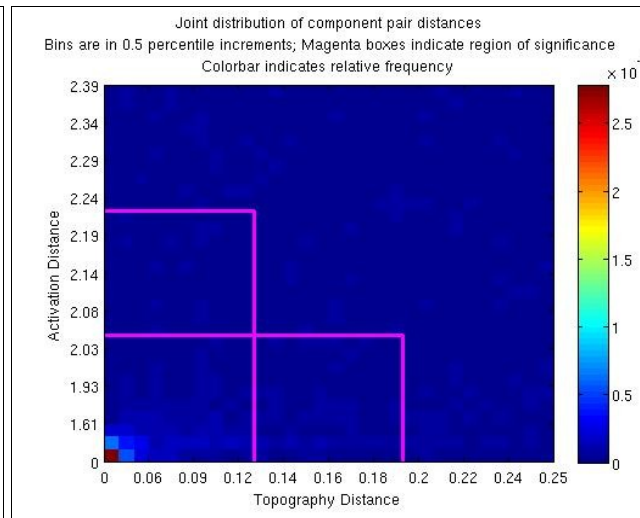


Figure A9: L-shaped critical region for 58/59 channels and epoch mean baseline condition with EOG correction

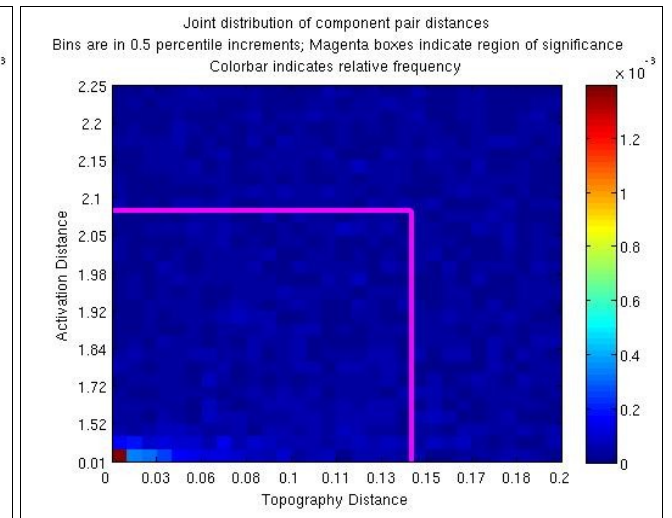


Figure A10: L-shaped critical region for 58/59 channels and no correction condition with EOG correction

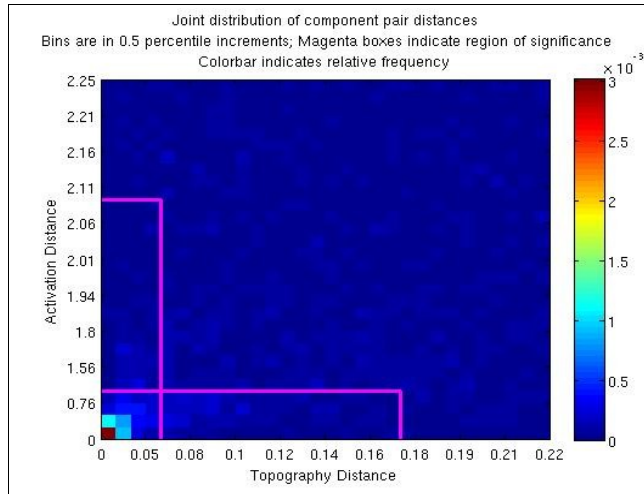


Figure A11: L-shaped critical region for 30 channels and prestimulus baseline condition with EOG correction

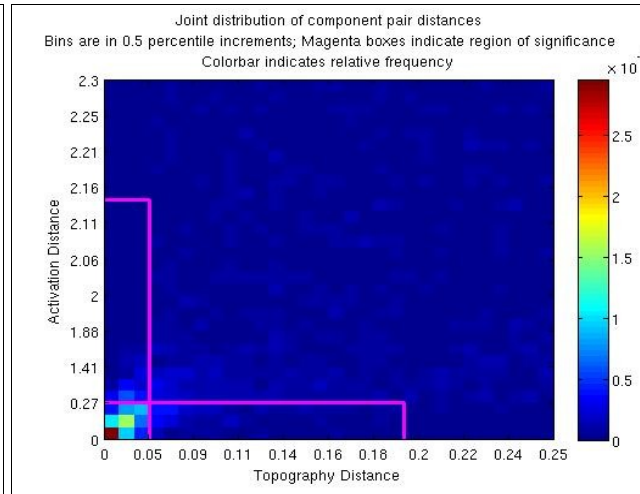


Figure A12: L-shaped critical region for 30 channels and epoch mean baseline condition with EOG correction

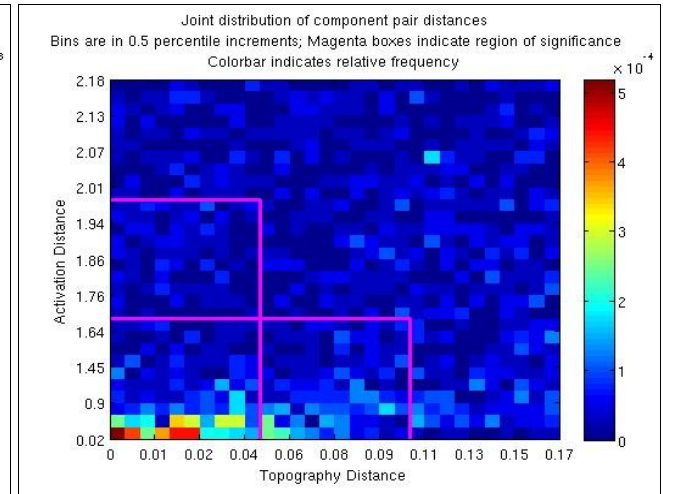


Figure A13: L-shaped critical region for 30 channels and no correction condition with EOG correction

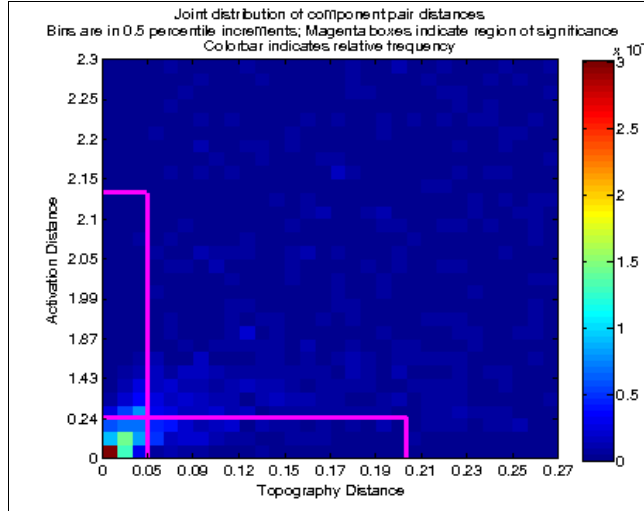


Figure A14: L-shaped critical region for 30 channels and epoch mean baseline with EOG correction calculated using other artifact criteria.

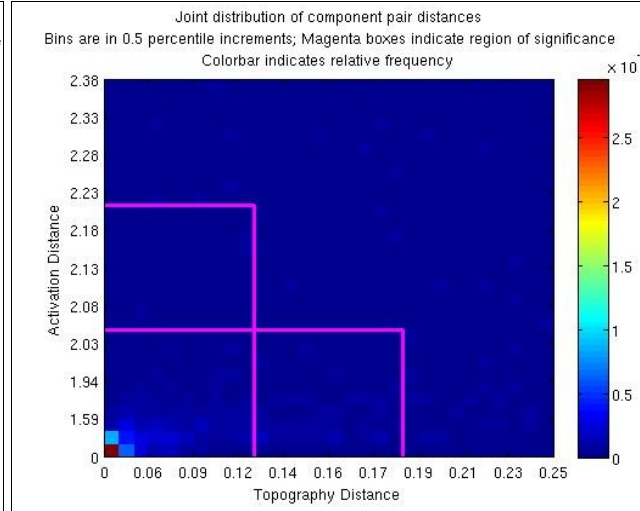


Figure A15: L-shaped critical region for 58/59 channels and epoch mean baseline condition without EOG correction

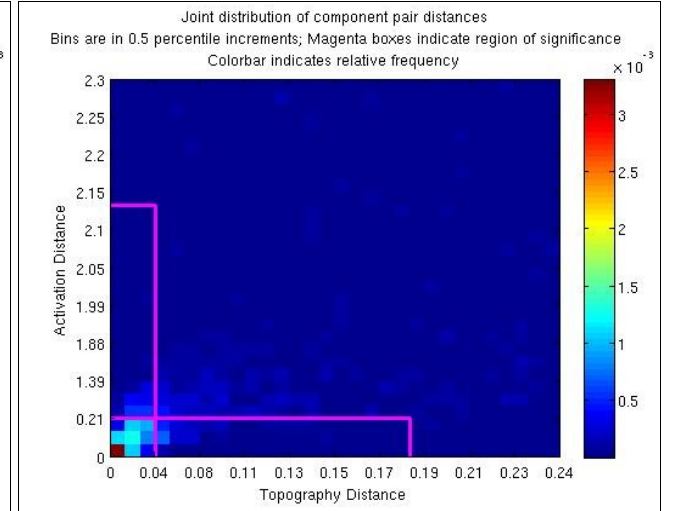


Figure A16: L-shaped critical region for 30 channels and epoche mean baseline condition without EOG correction

Reliable Components

Table A17: The absolute and relative number of ICs assessed as reliable. The column 'Reliable ICs' contains components with a positive estimation. The numbers are according to full datasets for the three main 58/59 channels settings. See text above and overview in chapter 5.4 for details.

	Prestimulus correction - 58/59 EOG			Epoch mean correction - 58/59 EOG			No correction- 58/59 EOG		
Subj.	Reliable ICs	ICs	%	Reliable ICs	ICs	%	Reliable ICs	ICs	%
1	3 4 7 22 29 50 57	7	0.12	1 2 4 6 7 9 10 21 22 36 40 43 44	13	0.22	1 2 6 8 11 13 14 15 18 20	10	0.17
2	6 7 39 43 50 52 55	7	0.12	2 5 7 8 10 11 13 19 32 34 40 41 42 43 49 57	16	0.27	1 2 3 6 16 17	6	0.10
3	3 6 11 13 15 16	6	0.10	2 3 4 6 7 9 12 20 23 25 29 32 39 40 44	15	0.25	2 3 4 8 9 11 12 23 33	9	0.15
4	1 4 11 19 21 24 25 26 29 40 48 49	12	0.21	1 2 9 10 11 13 18 19 21 26 27 30 33 37 40 42	16	0.28	1 6 7 9 16 29	6	0.10
5	1 2 7 11 49 55	6	0.10	1 2 5 6 10 12 16 18 19 23 24 34 35 45 48 49	16	0.28	1 2 7 8 10 13 21	7	0.12
6	1 5 7 13 16 17 23 25 36 38 56	11	0.19	1 2 3 5 7 9 11 12 13 14 15 23 25 28 38 41 43 53	18	0.31	1 3 4 7 8 10 12 13 16 17 20 37	12	0.20
7	1 3 4 16 18 19 22 31 33 37 4 42 43 51 53 55	16	0.27	1 2 8 11 12 15 17 18 22 24 25 29 34 35 36 37 38 40 41 46 52 53 56	23	0.39	1 2 3 4 5 7 8 11 12 25 26 35 37	13	0.22
8	1 4 5 9 13 18 38 40	8	0.14	1 2 3 4 5 6 7 11 12 13 15 21 27 31 37 38 50 52 57	19	0.32	1 2 4 8 11 13 16 17 19 22 23 24 26 31 38 44 45 46	18	0.31
9	1 3 4 7 8 18 28 32 42 52	10	0.17	1 2 3 4 5 6 9 11 13 15 18 21 24 30 35 36 40	17	0.29	1 2 7 8 22 23 32 33 40 41 49	11	0.19
10	1 2 4 5 7 9 20 23 36 42 44 48 50 53 56	15	0.25	1 2 3 4 5 6 9 11 13 14 17 21 22 27 28 30 33 37 40 45 46 47 49 50 53 59	26	0.44	1 2 5 9 12 15 18 19 20 21 23 33 34 39	14	0.24
11	2 5 7 10 15 26 44 45 47 50 51 56	12	0.20	1 2 3 4 5 6 7 8 9 10 11 12 13 17 19 21 30 33 34 37 40 41 43 45 52 53 54 58	28	0.47	1 2 3 6 7 8 10 12 13 29	10	0.17
12	1 27	2	0.03	1 2 3 4 10 13 15 17 26 45 58	11	0.19	1 2 5 8 10 11 13 15 18 20 23 28 30 33 37	15	0.25
13	1 10 11 14 18 20 46 56	8	0.14	1 2 3 5 6 10 11 13 14 22 24 35 45 52 56 57	16	0.27	1 7 9 12 30 31 37	7	0.12
14	11 28 39 42	4	0.07	1 3 5 13 18 20 21 28 30 33 39 51 54	13	0.22	5 6 7 10 11 15	6	0.10
15	1 2 22 30 34 35	6	0.10	1 2 3 4 5 6 7 12 14 19 20 22 24 25 26 28 29 30 31 33 34 36 38 43 46 48	26	0.44	1 4 6 9 10 12 13 14 20 25	10	0.17
mean		8.67	0.15		18.2	0.31		10.27	0.17
SD		3.94	0.07		5.2	0.09		3.63	0.06

Table A18: The absolute and relative number of ICs assessed as reliable. The column 'Reliable ICs' contains components with a positive estimation. The numbers are according to full datasets for the three main 30 channels settings. See text above and overview in chapter 5.4 for details.

	Prestimulus correction - 30 EOG			Epoch mean correction - 30 EOG			No correction - 30 EOG		
Subj.	Reliable ICs	ICs	%	Reliable ICs	ICs	%	Reliable ICs	ICs	%
1	3 4 7 12 16 21 22 23 26 27	10	0.33	1 2 3 9 10 11 12 14 17 18 19 20 23 24 26	15	0.50	1 2 4 10 16 17	6	0.20
2	1 4 7 14 29	5	0.17	3 4 6 8 24 25	6	0.20	1 8 11 13 16	5	0.17
3	1 7 12 15 24	5	0.17	1 2 3 4 5 6 10 24	8	0.27	1 2 3 6 7 8 11 15	8	0.27
4	1 2 3 5 13 14 15 21 23 24	10	0.33	1 2 5 7 11 14 21 22	8	0.27	3 16	2	0.07
5	1 2 4	3	0.10	3 11 24 29	4	0.13	1 13 15 20	4	0.13
6	1 2 9 10 12 13 28	7	0.23	1 2 3 4 5 6 8 14 19 21	10	0.33	1 3 8 9 10 11 23	7	0.23
7	1 3 9 15 18 26 28 29	8	0.27	1 3 4 12 16 19 20 24 28 29	10	0.33	1 3 6 8 10 13 23	7	0.23
8	1 3 5 9 21 28	6	0.20	1 2 3 4 5 6 9 14 19 24 27	11	0.37	1 2 3 4 8 11 12 17 19	9	0.30
9	1 3 5 12 14 15 20 22 27	9	0.30	1 3 8 14 18 21 23 25 27 29	10	0.33	2 5 6	3	0.10
10	1 3 9 10 12 14 16 18 19 22 24 27	12	0.40	1 2 3 6 8 9 12 13 15 22 24 26 27	13	0.43	1 2 3 9 14 19 21	7	0.23
11	1 3 4 6 8 11 13 18 27	9	0.30	1 4 5 6 8 14 15 22 24 25 30	11	0.37	1 2 8 11	4	0.13
12	2	1	0.03	1 3 4 5 7 9 13 17 18 20	10	0.33	1 2 3 4 8 9 10	7	0.23
13	1 2 4 11 21	5	0.17	1 2 5 6 8 9 18 22 27	9	0.30	1 4 8	3	0.10
14	1 3 10 11 18 19	6	0.20	18 22 23	3	0.10	1 3 4 5 8	5	0.17
15	1 2 3 13 19 20	6	0.20	1 2 3 10 11 17 20 23	8	0.27	1 2 3 4 6 15	6	0.20
mean		6.8	0.23		9.07	0.3		5.53	0.18
SD		2.91	0.1		3.13	0.1		2.03	0.07

Table A19: The absolute and relative number of ICs assessed as reliable. The column 'Reliable ICs' contains components with a positive estimation. The numbers are according to full datasets for the three additionally calculated proceedings.

	Epoch mean corr.– extra art. 30 EOG			Epoch mean correction - 58/59 no EOG			Epoch mean correction - 30 no EOG		
Subj.	Reliable ICs	ICs	%	Reliable ICs	ICs	%	Reliable ICs	ICs	%
1	1 2 4 5 9 11 12 13 16 17 18 20 22 25	14	0.47	1 2 3 5 6 9 11 12 13 14 17 19 21 23 24 25 26 32 33 38 40 43 48 49 50	25	0.42	1 5 6 8 9 11 13 17 20 22 23 26 28	13	0.43
2	2 4 7 8 24 25 30	7	0.23	1 2 6 9 10 11 12 13 18 21 29 30 34 39 41 42 43 49 51 54	20	0.34	1 2 7 10 11 12 23 25	8	0.27
3	1 2 3 5 6 8 20 21 24	9	0.30	1 2 6 7 8 10 13 14 23 25 29 30 34 36 39 57	16	0.27	1 2 3 4 5 6 7 10 21 23	10	0.33
4	1 3 4 12 13 20 23	7	0.23	1 3 5 7 8 11 12 14 15 16 33 34 36 39 44 45 55	17	0.29	1 4 5 7 15 23 24	7	0.23
5	2 4	2	0.07	1 2 4 5 6 7 10 11 12 14 15 19 20 25 28 29 30 36 37 42 44 48	22	0.38	1 2 3 8 17 25 27 28	8	0.27
6	1 2 4 5 7 10 19 22	8	0.27	1 2 4 7 10 12 14 16 17 20 26 38 40 42 46	15	0.25	1 2 3 4 5 7 9 18 21 22 23	11	0.37
7	1 2 12 13 16 19 23 26 27 29	10	0.33	1 2 3 4 7 13 14 17 18 19 20 21 23 31 33 34 38 39 45 46 50 53 54	23	0.39	1 6 8 16 20 24 25 29	8	0.27
8	1 3 5 7 9 10 13 18 19 23 24 25 26	13	0.43	1 2 3 5 8 9 10 13 23 29 31 38 43 48 50 58	16	0.27	1 2 3 4 6 7 19 29	8	0.27
9	1 3 4 7 9 14 18 28 29	9	0.30	1 2 3 4 6 8 9 11 12 13 14 15 20 26 33 37 39 55 58 59	20	0.34	1 2 6 9 10 11 12 24 27	9	0.30
10	1 3 6 7 8 12 13 16 19 20 21 26 27 28	14	0.47	1 3 4 5 8 9 13 14 15 16 19 22 23 26 28 34 37 41 46 54 58	21	0.36	1 3 5 7 10 12 13 15 18 20 24 25 27 30	14	0.47
11	1 2 3 4 6 11 14 15 17 18 23 24 29	13	0.43	1 3 4 6 7 10 12 14 16 18 19 21 22 23 26 27 28 29 30 35 36 37 38 40 43 50 53 57	28	0.47	1 2 4 5 6 7 11 19 20 24 25 28	12	0.40
12	2 3 6 9 10	5	0.17	1 2 4 6 8 13 14 20 25 33 37 38 39 54	14	0.24	1 2 3 12 15 18 22	7	0.23
13	1 2 3 5 6 10 13 15 18 19 20 25	12	0.40	1 2 3 4 6 7 10 11 12 24 25 30 37 40 42 45 48 50 57	19	0.32	1 2 3 4 5 6 7 8 9 19 20	11	0.37
14	1 15 24 25	4	0.13	1 3 4 5 6 7 9 11 17 24 29 30 36 38 42 44 50 53 56	19	0.32	1 8 14 20 26	5	0.17
15	1 2 3 6 9 15 17 18 23 30	10	0.33	1 2 3 4 5 6 8 11 16 18 20 21 22 26 27 28 32 34 35 38 41 45 49 50 51	25	0.42	1 2 3 5 7 8 9 15 16 21 28 29	12	0.40
mean		9.13	0.3		20	0.34		9.53	0.32
SD		3.7	0.12		4.07	0.07		2.56	0.0

Lebenslauf

Name: Meyer
Vorname: Bernhard
Geburtsdatum: 20. Juli 1982
Geburtsort: Feldkirch / Vorarlberg
Staatsbürgerschaft: Österreich

Bildungsweg:

Volksschule - Nenzing bis 1992
Hauptschule - Nenzing bis 1996
HTL für Telekommunikation - Rankweil bis Juni 2001

Matura mit Ingenieurprojekt USIC - Universal System Input Control: Tastatur- und Mauseinsatz für Cerebralparetiker (spastische Lähmung) - Jugend Innovativ Finalteilnahme - Wien, 3. Platz

Zivildienst abgeleistet im Landeskrankenhaus Feldkirch (12 Monate) bis Februar 2003

Kurse: CISCO – Netzwerkkurs (2 Semester / HTL-Ausbildung) & IT-Security – Manager (3 Monate)

Universität:

Studium der Psychologie an der Universität Wien ab Oktober 2003

Schwerpunkte: Biologische und Klinische Psychologie, Bildung und Evaluation

Berufserfahrung:

Praxis Allgemein: Elektronik- und Elektroinstallationsbetriebe, Netzwerktechnik und TQM/Qualitätssicherung, Meinungsumfragen und IT-Helpdesk

in Schulzeit: E-Werk Frastanz (1 Monat), Liebherr Nenzing (3 Wochen), Tridonic Dornbirn (1 Monat)

vor Zivildienst: ACP Feldkirch (1 Monat), Liebherr Nenzing (4 Monate)

in Studienzeit: Karmasin, Gemeinde Nenzing (2 x 1 Monat), Thyssen Krupp Presta Liechtenstein (1 Monat)

in Studienzeit: Soziales Kompetenztraining in KMS / Wien (WS 08/09)

6-Wochen Praktikum: TU-Wien - Studie am Institut für Gestaltungs- und Wirkungsforschung (2006)

Praxis Aktuell: Nachtassistent im Schlaflabor Rudolfinerhaus

Vorbereitung und Beobachtung der Polysomnographie und Vorgabe der psychometrischen Testbatterie.